INDUCTIVELY COUPLED PLASMA-OPTICAL EMISSION SPECTROMETRY FOR FORENSIC ANALYSIS

A thesis presented by

Robert Christopher Carpenter, L.R.S.C.

in partial fulfilment of the requirements for the degree of

DOCTOR OF PHILOSOPHY

of the

COUNCIL FOR NATIONAL ACADEMIC AWARDS

Department of Environmental Sciences,
Plymouth Polytechnic,
Drake Circus,
Plymouth,
Devon.
PL4 8AA

Central Research Establishment,
Home Office Forensic Science Service,
Aldermaston,
Berkshire.
RG7 4PN

September 1985

CONTENTS

ABSTRACT

ACKNOWLEDGEMENTS

1 INTRODUCTION 1

1.1 Forensic Science Investigations 1

1.2 Forensic Science Analysis 2

1.3 Inductively Coupled Plasma-Optical Emission Spectrometry 7

1.4 The Aims of This Investigation 8

2 INDUCTIVELY COUPLED PLASMA-OPTICAL EMISSION SPECTROMETRY 10

2.1 Introduction 10

2.2 The Inductively Coupled Plasma 11

2.3 Instrumentation Used in This Study 13

2.3.1 Radio Frequency Generator 13

2.3.2 Sample Introduction and Excitation 13

2.3.3 Light Detection and Data Acquisition 15

2.4 Preliminary Evaluation of Instrumental Characteristics 20

2.4.1 Operating Conditions 20

2.4.2 Stability 23

2.4.3 Limits of Detection 26

2.4.4 Calibrations 30

2.4.5 Interferences 31

2.5 Preliminary Applications Studies 36

2.5.1 Certified Reference Materials 36

2.5.2 Human Tissues and Body Fluids 39

2.5.3 Metal Borides 41

2.6 Conclusions and Recommendations 41

3 SIMPLEX OPTIMISATION OF PLASMA PERFORMANCE 43

3.1 Introduction 43

3.2 The Simplex Method 44

3.3 Preliminary Experiments 52
3.4 Comparison of Sample Introduction - Plasma Torch Configuration 62
3.5 Multielement Optimisation 73
3.5.1 Introduction 73
3.5.2 Preliminary Studies 74
3.5.3 Multielement Simplex Optimisation 77
3.6 Simplex Optimisation for Interference Reduction 84
3.6.1 Introduction 84
3.6.2 Preliminary Studies 85
3.6.3 Multielement Simplex Optimisation for Interference Minimisation 91
3.7 Conclusions 98
4 FORENSIC SAMPLE INTRODUCTION STUDIES 100
4.1 Introduction 100
4.2 Discrete Nebulisation 102
4.2.1 Introduction 102
4.2.2 Experimental 103
4.2.2.1 Instrumentation and Operating Conditions 103
4.2.2.2 Discrete Nebulisation 103
4.2.2.3 Sample and Standards Preparation 105
4.2.2.4 Cutting Experiments 106
4.2.3 Results and Discussion 106
4.2.3.1 Discrete Nebulisation 106
4.2.3.2 Fragment Generation and Analysis 107
4.2.4 Conclusions 110
4.3 Recirculating Nebuliser 111

4.3.1 Introduction 111
4.3.2 Experiments with the Initial Modified Laskin Nebuliser 112
4.3.2.1 Nebuliser Construction and Preliminary Experiments 112
4.3.3 Results and Discussion 114
4.3.4 Experiments with the Improved Modified Laskin Nebuliser 119
4.3.4.1 The Operational Nebuliser 119
4.3.5 Results and Discussion 121
4.3.6 Mode of Operation of the Laskin Nebuliser 123
4.3.7 Nebulisation Effects with Acid Solutions 124
4.3.8 Analysis of Shotgun Steels 129
4.3.8.1 Introduction 129
4.3.8.2 Sample and Standards Preparation 129
4.3.8.3 Analytical Procedure 130
4.3.8.4 Results and Discussion 131
4.3.9 Conclusions 132
5 APPLICATIONS STUDIES WITH INDUCTIVELY COUPLED PLASMA - OPTICAL EMISSION SPECTROMETRY IN FORENSIC SCIENCE 133
5.1 Introduction 133
5.2 The Analysis of Small Samples of Brasses and their Classification by Two Pattern-Recognition Techniques 133
5.2.1 Introduction 133
5.2.2 Composition of Brasses 134
5.2.3 Experimental 135
5.2.3.1 Sample Preparation 135
5.2.3.2 Choice of Elements and Standard Preparation 136

5.2.3.3 Interferences 136
5.2.3.4 Calculation of Results 137
5.2.4 Results and Discussion 137
5.2.4.1 Accuracy and Precision of Analysis 137
5.2.4.2 Analysis and Classification of Sample Set 138
5.2.4.3 Pattern-Recognition 141
5.2.5 Conclusions 143
5.3 The Analysis of Small Fragments of Sheet Glasses 146
5.3.1 Introduction 146
5.3.2 Composition of Glass 149
5.3.3 Experimental 152
5.3.3.1 Preparation of Standards and Preliminary Samples 152
5.3.3.2 Analysis and Computation 152
5.3.3.3 Preparation of Casework Size Glass Fragments 153
5.3.4 Results and Discussion 154
5.3.4.1 Method Performance 154
5.3.4.2 Discrimination of Sheet Glasses 159
5.3.4.3 Forensic Glass Standards 161
5.3.5 Conclusions 162
5.4 The Determination of Metals on Hands 166
5.4.1 Introduction 166
5.4.2 Experimental 166
5.4.2.1 Preparation of Swabs 166
5.4.2.2 Sampling and Analysis 167
5.4.3 Results and Discussion 167
5.4.4 Conclusions 169

5.5 A Proposed Method for the Quantitative Multielement Analysis of White Household Gloss Paints 170

5.5.1 Introduction 170

5.5.2 Experimental 171

5.5.2.1 Preparation of Dry Paint Films 171

5.5.2.2 Dissolution of Paint Samples 171

5.5.3 Results and Discussion 171

5.5.4 Conclusions 174

5.6 Overall Conclusions 174

6 CONCLUSIONS AND RECOMMENDATIONS 176

APPENDICES

A Radio Frequency Generator HFP 2500D 179

B Scanning Monochromator and Computer Control 180

C Polychromator Details 181

D Presentations and Publications 182

E Programme of Related Studies 184

REFERENCES 186

ABSTRACT

Inductively Coupled Plasma - Optical Emission Spectrometry for Forensic Analysis

Robert C. Carpenter

The fundamental characteristics and applications of inductively coupled plasma - optical emission spectrometry (ICP-OES) for forensic science purposes have been evaluated.

Optimisation of ICP-OES for single elements using simplex techniques identified an ICP torch fitted with a wide bore injector tube as most suitable for multielement analysis because of a compact analytical region in the plasma. A suitable objective function has been proposed for multielement simplex optimisation of ICP-OES and its effectiveness has been demonstrated. The effects of easily ionisable element (EIE) interferences have been studied and an interference minimisation simplex optimisation shown to be appropriate for the location of an interference free zone. Routine, interference free determinations (<2% for 0.5% Na) have been shown to be critically dependant on the stability of the injector gas flowrate and nebuliser derived pressure pulses.

Discrete nebulisation has been investigated for the analysis of small fragments of a variety of metal alloys which could be encountered in casework investigations. External contamination together with alloy inhomogeneity have been shown to present some problems in the interpretation of the data.

A compact, corrosion resistant recirculating nebuliser has been constructed and evaluated for the analysis of small fragments of shotgun steels. The stable aerosol production from this nebuliser allowed a set of element lines, free from iron interferences, to be monitored with a scanning monochromator.

The analysis, classification and discrimination of casework sized fragments of brasses and sheet glasses have been performed and a method has been proposed for the analysis of white household gloss paints. The determination of metal traces on hands following the handling of a variety of metal alloys has been reported. The significance of the results from these evidential materials has been assessed for forensic science purposes.

The British Library LENDING DIVISION
Boston Spa, Wetherby, West Yorks LS23 7BQ

PLYMOUTH POLY

PhD Thesis by CARPENTER R.C.

We have given the above thesis the Lending Division identification number:

D 66078/86

In your notification to Aslib please show this number, so that it can be included in their published 'Index to Theses...' and 'Abstracts of Theses', respectively.

J P CHILLAG
Theses Officer

ACKNOWLEDGEMENTS

I wish to express my gratitude to Dr.L, Ebdon and Dr.G. Sanger for their wisdom, sustained interest and guidance throughout this work. In addition, thanks are due to the Controller of the Forensic Science Service and the Director of the Central Research Establishment for granting permission for the research to be performed, also to the Home Office for financial support.

I am grateful to Dr.J. Locke for many helpful discussions on all aspects of the work. I also acknowledge the assistance of Miss C. Till and Miss K. Shah with some of the brass and paint analyses respectively, while working under my direct supervision. I am grateful to the Operational Services Division of the Central Research Establishment for their support in a variety of ways and to Mr.M. Swain, in particular, for the acquisition of many of the references.

To my wife, Valerie, I extend special thanks for her help, support and patience over the last few years.

1 INTRODUCTION

Forensic science can be defined as the investigation and evaluation of scientific evidence and its presentation to the courts of law.

The Home Office Forensic Science Service (HOFSS) consists of six operational laboratories and the Central Research Establishment (CRE). The operational laboratories are directly concerned with casework examinations and the CRE provides information, specialist services and research and development support to these and other associated laboratories in the United Kingdom.

1.1 Forensic Science Investigations

Forensic science investigations can take three basic forms:

(a) Evidential material may be examined to establish whether or not a crime has been committed. Fire investigations are a good example, as most fires are accidental and only infrequently is arson involved. If suspicious circumstances exist at a fire scene, the forensic scientist will remove debris for further examination. At the laboratory the material will be analysed for the presence of accelerants i.e. materials such as petrol, paraffin etc. which may have been used to initiate or propagate the fire.

(b) Scientific examinations may provide information on how and when a crime was committed. For example, in a murder case it is often vital to identify a weapon and this may involve the

examination of a bullet, fragment of a knife blade or the size and shape of a wound. In addition, it is important for the pathologist to establish the time of death so that the movements of suspects can be related to the crime scene.

(c) The most demanding task is that of attempting to link a suspect with a crime, or, of greater importance, to eliminate them from further investigations. This can involve the careful searching of clothing, hair, shoes, vehicles or tools to detect transferred microscopic evidence. The evidential materials which can be recovered include, fibres, wood chips, vegetation, pollens, hair, body fluids, soil and fragments of glass, paint and metal. The majority of developments in forensic science are aimed at increasing the quality, quantity and value of scientific evidence which can be obtained from these materials.

1.2 Forensic Science Analysis

For the purposes of these studies only metallic or inorganic materials or constituents are considered. The analysis and evaluation of this trace evidence is very demanding as a result of the small size of recovered fragments (typically 100μg or less). In addition, the analyst has no control over how the samples were taken and the degree of contamination to which they have been exposed.

Elemental analysis has always made a valuable contribution to forensic investigations and a summary of techniques and applications is shown in Table 1. Conventional analytical instrumentation has generally been used but specialised sample handling and presentation techniques have often been developed for the very small samples.

Table 1

Summary of Forensic Elemental Analysis Techniques and Applications

Technique	Applications	Reference
Emission Spectroscopy (Arc and Spark)	Smears, paint and metal powders	1
	Steel vehicle sections	2
	Paint and glass fragments	3
	Silver theft	4
	Heavy Metals in tissue	5
	Glass fragments	6
Atomic Absorption Spectrometry (Flame)	Lead in paint chips	7
	Lead and cadmium in paint	8
	Trace elements in hair	9
	Trace metal content of papers	10
	Quantitative analysis of glass	11
	Rapid analysis of small glass fragments	12
	Soils, comparison with NAA	13
	Lead content of soils	14
	Lead in acid solubilised tissue	15
	Elements in human liver tissue	16,17
	Heavy metals in enzymic digested tissue	18
	Shot-gun pellet identification	19
	Arsenic murder	20
	Gunshot residues	21

Table 1 (cont'd)

Technique	Applications	Reference
Atomic Absorption Spectrometry (Flame)	Speciation of lead compounds	22
Atomic Absorption Spectrometry (Electrothermal)	Gunshot residues	23-26
	Trace elements in hair	27,28
	Copper conductors	29
	Toxic metals in urine and tissue	30-33
	Glass fragments	34,35
	Lead in soils	36
Laser Microprobe	Paint examinations	37
	General forensic	38
	Textiles defects	39
Spark Source Mass Spectrometry	Bullet lead	40
	Glass examination	41-44
	Soils and rocks	45
	Human liver tissue	46
	Copper conductors	47
	Applications review	48
Neutron Activation Analysis	Trace elements in hair	49,50

Table 1 (cont'd)

Techniques	Applications	Reference
Neutron Activation Analysis	Silverware	51
	Copper conductors	52-55
	Blood and body tissues	56-58
	Glass examination	59,60
	Bullet hole examination	61
	Bullet analysis	62,63
	Gunshot residues	64,65
X-ray Methods	Glass examination	66,67
	Auto, household paint and smears	68-71
	Body fluid stains	72
	Arson residues	73
	Metals	74
	Gunshot residues	75
	Precious metals	76
	Paper and coatings	77
	Documents examination	78
	Bullet fragments	79
	Trace elements in hair	80,81
	Wear metals in oils	82
	Trace elements in soils	83

The majority of early analyses were performed by emission spectroscopy (ES) with arc or spark excitation and the multielement, qualitative data used for identification and comparison purposes. Quantitative determinations have been carried out for specific purposes but these were too time consuming for routine use. Laser microprobe analysis offered the potential for virtually non-destructive analysis of evidential materials. The analysis of inclusions, paint layers and metal smears has been shown to be valuable. However, the technique was less stable and more difficult to quantify than conventional emission spectroscopy.

Atomic absorption spectrometry (AAS) revolutionised analytical spectroscopy following its introduction by Walsh (84) in 1955. Accurate and precise analytical data could now be obtained reasonably rapidly and routinely. However, the available size and variety of forensic samples has led to infrequent use of this technique in casework. Similarly, although valuable trace element determinations have been performed by electrothermal atomisation AAS; the single element nature of this technique restricts the evidential value of analyses for routine casework.

Spark source mass spectrometry was evaluated at the CRE and shown to be a sensitive, multielement technique for small samples. The analyses were, however, very time consuming particularly if quantitative data was required.

Neutron activation analysis (NAA) is a powerful technique as quantitative, multielement data can be obtained following minimal sample preparation. Although useful work has been reported, the lack of availability and high cost preclude the routine use of this technique.

The ideal technique for forensic analysis would be rapid, automated, non-destructive and capable of accurate and precise multielement determinations from trace elements to major constituents. At present, the scanning electron microscope with energy dispersive x-ray analysis (SEM-EDXA) and x-ray fluorescence (XRF) are used extensively in the Home Office forensic science laboratories. Although not ideal, they do offer a non-destructive, multielement capability and precise analyses can be rapidly performed. Good accuracy generally requires matrix matched standards and, as discussed earlier, the matrices encountered in forensic analyses are varied and thus quantitative determinations can be difficult.

1.3 Inductively Coupled Plasma - Optical Emission Spectrometry

The inductively coupled plasma (ICP) was developed as an excitation source for atomic spectroscopy about 20 years ago (85,86). However, it was not until compact, high frequency, low power sources were developed in the mid 1970's that the ICP became widely accepted as an analytical tool. The subsequent rapid growth in commercial plasma systems results from the high quality quantitative, multielement analyses which they can perform. This increasing usage is reflected by the publication of reviews (87,88), conference proceedings (89,90), fundamental studies (91,92,93) and numerous applications (94,95,96). Quantitative data are of increasing forensic interest because they can be used in data bases which are technique independant; inter and intra laboratory comparisons can be readily performed as can comparisons with manufacturers' data and identification of manufacturing sources.

Few applications utilising ICP-optical emission spectrometry

(OES) have so far been reported by forensic scientists. Locke (97) has reported on evaluation of manufacturers' instruments for glass, steel and liver tissue analyses. At the Metropolitan Police Forensic Science Laboratory, Catterick and Hickman (98) have developed a technique for the determination of 5 elements in small glass fragments. Their method has been applied to casework samples and data reported for 350 glass samples (99) has been used to formulate a glass classification scheme (100). A modification of the analytical procedure has recently been reported (101). The instrumentation at the CRE has been evaluated for the analysis of some evidential materials (102) and a detailed study carried out on the analysis and classification of a collection of 37 brass items (103). Discrete nebulisation has been used for the analysis of metal fragments and problems with the interpretation of the data have been discussed (104).

1.4 The Aims of This Investigation

The overall aim of this investigation is the study and evaluation of ICP-OES for forensic analysis with particular reference to instrumental developments and characteristics, fundamental studies and applications.

Quantitative determinations by ICP-OES are routinely performed but the analysis of small sample fragments is a unique and demanding task. A discrete nebulisation technique and a novel recirculating nebuliser were selected for development and study.

True optimisation of plasma performance is rarely performed by spectroscopists and the variable step-size simplex optimisation was considered appropriate for the investigation of optimum, multielement analysis conditions. In addition, this optimisation has been studied

for the objective comparison of alternative sample introduction techniques and for the investigation and elimination of ionisation interferences in argon plasmas.

Included in this study are the development and evaluation of techniques for the analysis of a wide variety of evidential materials.

2 INDUCTIVELY COUPLED PLASMA-OPTICAL EMISSION SPECTROMETRY

2.1 Introduction

In 1947 Babat (105) published the results of his research into the properties of capacitively and inductively coupled discharges. However, it was not until 1961 that Reed (106) described an atmospheric pressure ICP and introduced the principle of vortex stabilisation and isolation of a plasma. Reed then described a plasma torch consisting of three concentric tubes which was used for crystal growing (107) and followed this by describing the physical properties of these plasmas and suggesting their application as spectral emission sources (108).

The analytical potential of plasmas was quickly recognised and research studies initiated at the laboratories of Albright and Wilson (Oldbury, UK) and Ames Laboratory (Iowa State University, USA). In 1964 Greenfield et al. (109) published details of a torch consisting of three concentric tubes with tangential argon introduction. The sample aerosol punched a hole through the plasma fireball, producing an annular plasma, and the spectral emission was recorded from the plasma tail-flame. Wendt and Fassel (110) published an account of a laminar flow plasma torch claiming higher stability than the turbulent, tangential flow system. In their system, the sample aerosol flowed round the outside of a solid plasma and the emission was viewed through a quartz side tube.

Following this pioneering work, ICP-OES entered a period of experimental verification and growth with significant contributions appearing from the USA (111), France (112), and the Netherlands (113). However, it was not until 1974 that details of a system were reported

which used a compact, high frequency, low power radiofrequency generator (114). This paper probably marks the introduction of commercial instrument development and the recognition of the potential of the ICP as a powerful analytical tool.

Inductively coupled plasma - optical emission spectrometry instrumentation was installed at the CRE in 1980 and a programme of research and development initiated with particular reference to forensic science. The aims of this early part of the project were to investigate some of the instrumental characteristics and perform preliminary applications studies to assess the potential of the technique for forensic science purposes.

2.2 The Inductively Coupled Plasma

A plasma can be defined as a gas in which a significant proportion of its atoms or molecules is ionised. Magnetic fields can readily interact with plasmas; of particular interest to spectroscopists is the inductive coupling of an alternating magnetic field with a plasma which is analogous to the inductive heating of a metal conductor.

A diagrammatic representation of an ICP torch is shown in Figure 2.1. This consists of three concentric silica tubes with associated gas supplies (normally argon) to sustain the plasma, cool the silica tubing and enable analyte to be introduced. The top of the torch is surrounded by the radiofrequency (RF) work coil. The sample, normally in the form of a fine aerosol, passes up the central injector tube and punches a hole through the plasma core, forming an annular shaped plasma. Atomic emission is observed in the tail-flame region thus reducing the background signal from the intense argon continuum at the plasma core.

Figure 2.1

Diagrammatic Representation of an ICP Torch

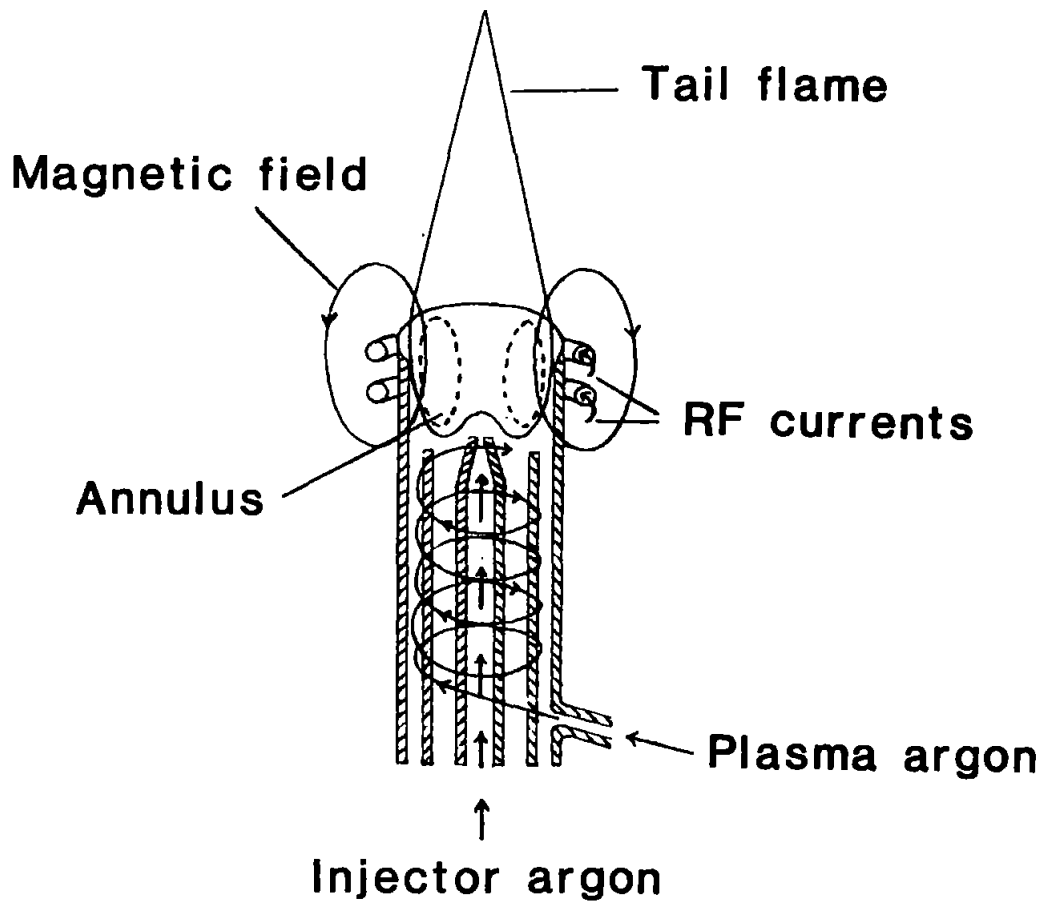

When RF power is applied, the high frequency currents flowing in the work coil generate oscillating magnetic fields whose lines of force are axially orientated inside the coil. These induced magnetic fields cause electrons and ions within the coil to flow in closed, circular, horizontal paths around the field lines, so producing eddy currents. To initiate the plasma the argon has to be "seeded" with electrons; this is normally accomplished with a Tesla coil. The free electrons are then accelerated by the field and Joule or Ohmic heating results in additional ionisation. A stable, argon plasma of extended dimensions is produced almost immediately. Figure 2.2 shows a photograph of such a plasma, the analytically useful region is clearly shown by the blue yttrium II emission.

2.3 Instrumentation Used in This Study

2.3.1 Radio Frequency Generator

This is a crystal controlled generator operating at 27.12 MHz and with a maximum power output of 2.5 kW (Plasma Therm Inc., Kresson, N.J., USA). The system is equipped with automatic power control and impedance matching. Full details are given in Appendix A.

2.3.2 Sample Introduction and Excitation

For the majority of studies and applications, two basic introduction systems have been used since installation. System 1 was supplied with the generator and consisted of a glass, concentric nebuliser (TR-30-A3; J.E. Meinhard Associates Inc., Santa Ana, California, USA), a glass, barrel-shaped spray chamber (SC-5037; Plasma

Figure 2.2

Argon Plasma with Yttrium Solution Spraying

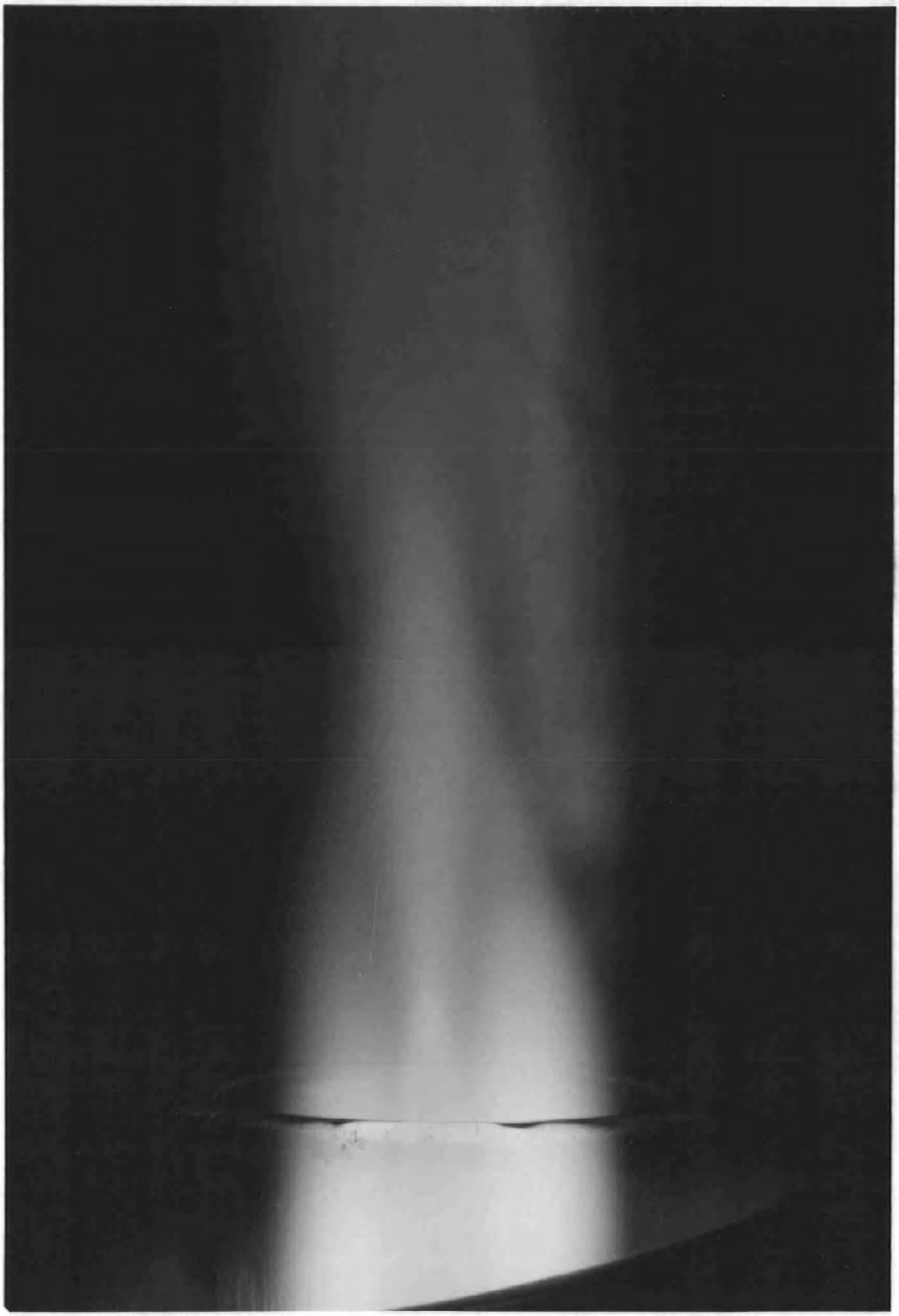

Therm Inc., Kresson, N.J., USA) and a fused silica plasma torch (T1.0; Plasma Therm Inc., Kresson, N.J., USA). A diagram of these components is shown in Figure 2.3.

System 2 was hydrofluoric acid resistant and consisted of a graphite loaded plastic cross-flow nebuliser and barrel-shaped spray chamber (Perkin Elmer Ltd., Beaconsfield, Bucks). The torch was demountable and fitted with quartz outer and intermediate tubes and an alumina injector tube. This system was designed to replace directly the previous one and required only minor modifications to the torch mount. A diagram is shown in Figure 2.4.

Both spray chambers were fitted with a glass drain tube to facilitate the even run-off of waste solution droplets. In addition, the outlet of each spray chamber was fitted with a glass wool plug to reduce pressure fluctuations during liquid draining.

2.3.3 Light Detection and Data Acquisition

The original spectrometer consisted of a 1 metre scanning monochromator fitted with a holographic grating (Bentham Instruments, Reading, UK). This was interfaced to a Commodore PET computer (Santa Clara, Calif., USA) for data acquisition and control of the stepping motor drive.

This system was only suitable for limited performance and applications studies. The optical quality of the monochromator was very poor, the specification not being achieved by the manufacturer until two years after delivery. In addition, the supplied software for the PET was relatively simple and it soon became apparent that the computing power of the PET would be inadequate for a comprehensive sequential analysis system. A photograph of this system is shown in

Figure 2.3

Diagram of Glass - Silica Sample Introduction System

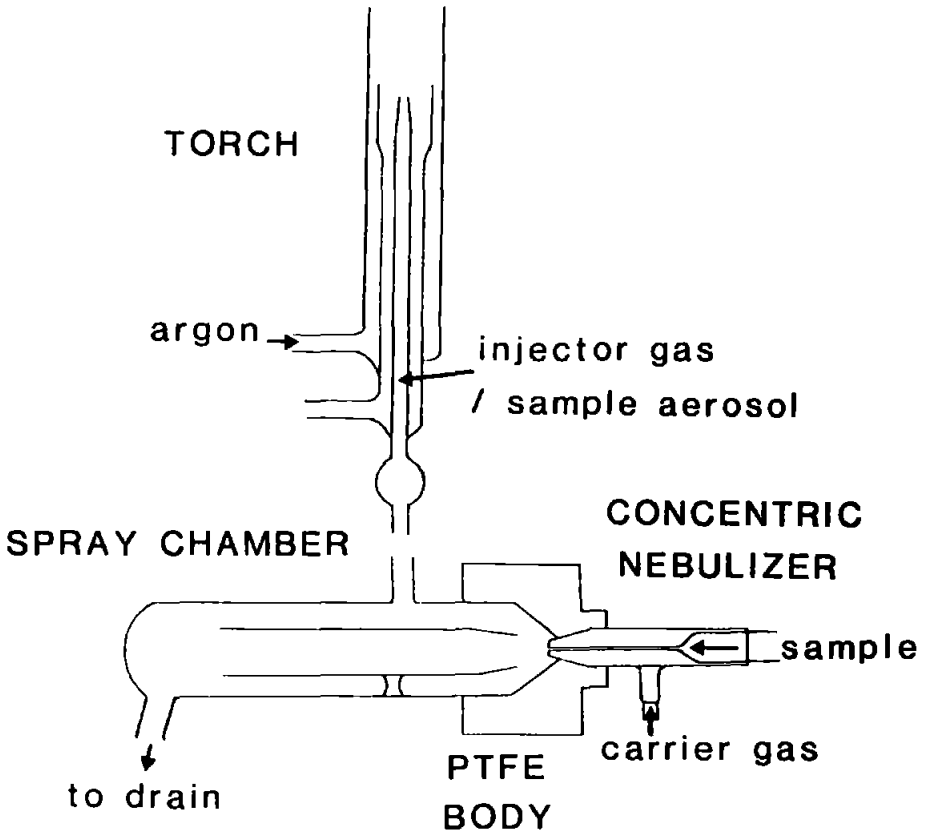

Figure 2.4

Diagram of Hydrofluoric Acid Resistant

Sample Introduction System

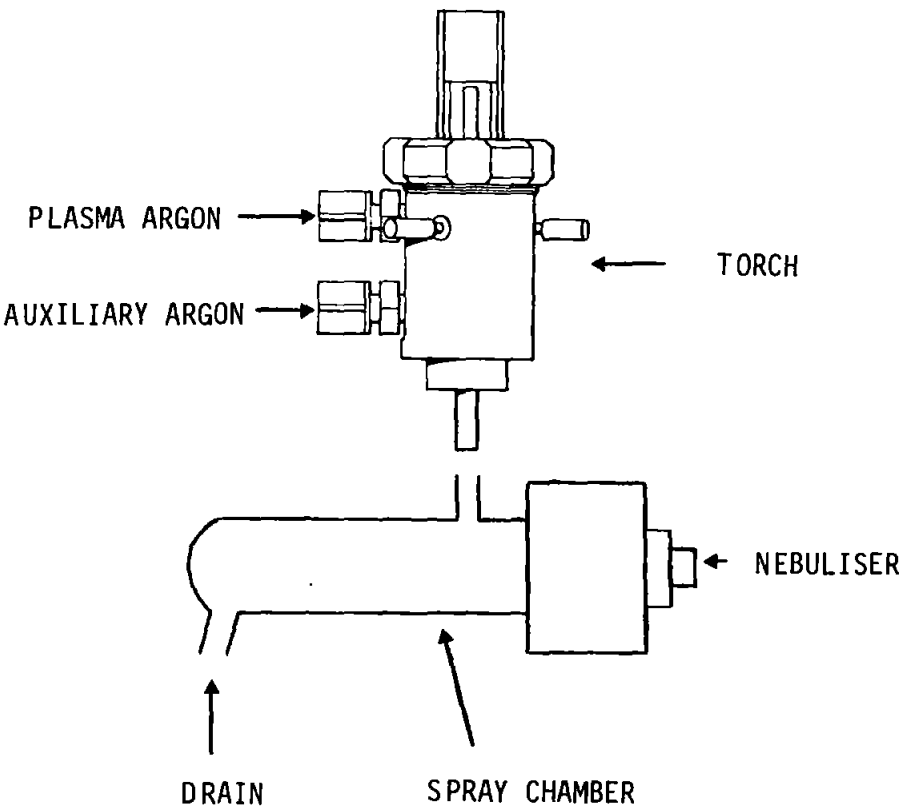

Figure 2.5.

In mid-1982 a MINC 11 computer (Digital Equipment Corporation, Maynard, Mass., USA) was acquired following the completion of another project. Software in both Basic and Fortran was written at CRE to control the spectrometer stepping motor drive and acquire spectral data via IEEE 488c interfaces. The more rapid and comprehensive Fortran program, running under the RT-11 operating system, allows spectral regions to be scanned at pre-selected wavelength steps and integration times. The digitised spectral data are displayed on the VDU together with calculated wavelengths, peak heights and peak areas from the Digital peak processing sub-routine (115). Results are stored on floppy discs and can be printed when required. System details are shown in Appendix B.

A 1 metre polychromator (Optical Emission Services, Milton Keynes, UK) was installed at the end of 1981. This was originally equipped with 12 element channels but has been uprated to a present capacity of 32 element channels. This instrument is fitted with a concave holographic grating and a stepping motor controlled entrance slit. The spectrometer, electronics, power supplies etc. are all housed in a temperature controlled environment. An S100 single board microcomputer containing a Z80 microprocessor (SD Systems, Dallas, Texas, USA) is programed in Fortran and uses the CP/M operating system to control the instrument.

The software acquires and displays intensity data on a VDU from pre-selected analytical channels. Calibrations and inter-element corrections can be calculated with a polynomial expression and sample concentrations can be obtained. The results can be stored on floppy discs or printed out. Analytical line profiles can be displayed on the VDU by keyboard instructions to the stepping motor controlled

Figure 2.5

Original ICP-OES System

entrance slit. These are required for profiling element channels and permit spectral background and line interferences to be determined. System details are shown in Appendix C.

Spectral emission from the plasma is monitored simultaneously by both spectrometers, each can be used as an independant analytical system. A photograph of the complete instrument is shown in Figure 2.6 and a diagrammatic representation given in Figure 2.7.

2.4 Preliminary Evaluation of Instrumental Characteristics

2.4.1 Operating Conditions

All preliminary studies were performed with the sample introduction system 1 (glass - silica) using the conditions shown in Table 2.1. These conditions were established by optimisation of the injector gas flow and observation height for Mn at a power of 1 kW (generator output). The criterion of maximum signal to background ratio was selected for the optimisation.

Nebuliser back pressure, set by the Plasma Therm reducing valve, is the operational parameter for the pneumatic nebulisers used in this work. For each nebuliser used, the pressure gauge was calibrated for argon flow through the torch injector tube.

These operating conditions were established relatively crudely considering ICP-OES is a multielement analytical technique. However, the investigation of a true multielement optimisation by the variable step-size simplex optimisation was not considered appropriate for a preliminary investigation and was studied later (see Chapter 3).

Figure 2.6

Final ICP-OES System

Figure 2.7

Diagrammatic Representation of ICP-OES System

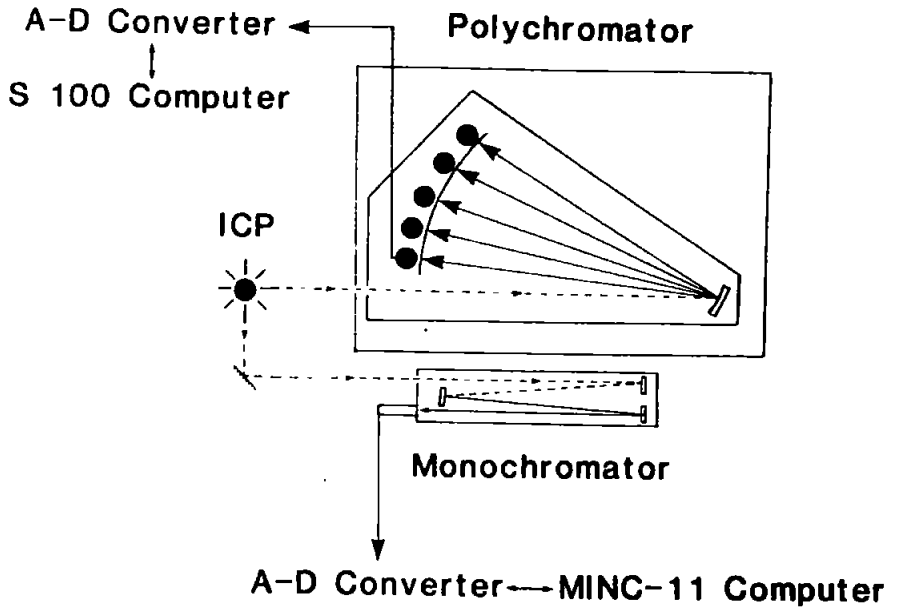

Table 2.1

Operating Conditions for Preliminary Evaluations and Applications

Forward RF power	1.0 kW (Generator output)
Reflected RF power	< 5 W
Argon Plasma Gas	16 l min^{-1}
Argon Auxiliary Gas	0 l min^{-1}
Argon Injector Gas	0.87 l min^{-1}
Nebuliser Back Pressure	20 psi
Solution Uptake	1.5 ml min^{-1}
Observation Height	15-20 mm (above work coil)

2.4.2 Stability

The ICP is regarded as a stable source for emission spectroscopy but its ultimate stability is limited by the fluctuation noise of the source/nebuliser combination. Previous work has shown the nebulisation process to be the major source of instability (116).

Short and long term precisions are important variables as they affect the performance of analytical methods. Figure 2.8 shows the effect of varying integration times on the precision of background measurements at 300 nm using the monochromator. The best relative standard deviation (RSD) obtained was 0.003 for a 10 second integration. However, this only degrades to 0.0035 for a 5 second integration and a significant reduction in analysis time is achieved. A 5 second integration period was thus chosen as standard for all analyses in this work.

Following the introduction of the sample introduction system 2 (corrosion resistant) the precisions of background measurements for 4

Figure 2.8

Variation in Relative Standard Deviation (RSD) of

Background Measurements with Integration Time

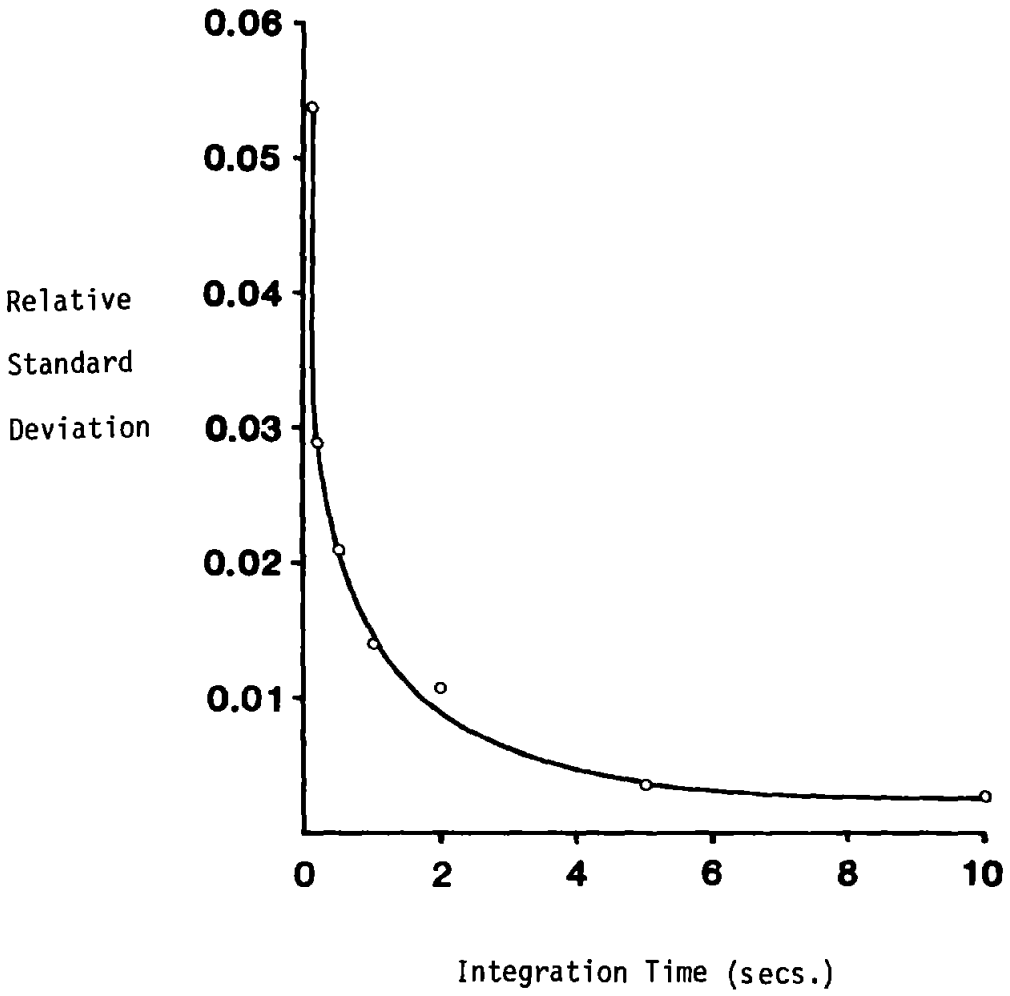

elements were determined on the polychromator. The results obtained over a 6 month period are shown in Table 2.2 and demonstrate the excellent stability obtainable with this system.

Table 2.2

Precision+ of Polychromator Background Determinations

Date	Zn I 213.86 nm	Mn II 257.61 nm	Mg I 285.21 nm	Ba II 455.40 nm
6/83	0.0033	0.0020	0.0020	0.0021
8/83	0.0034	0.0033	0.0041	0.0033
9/83	0.0036	0.0028	0.0025	0.0026
10/83	0.0024	0.0033	0.0020	0.0024
12/83	0.0028	0.0023	0.0021	0.0017

+ Expressed as RSD for 21 integrations of 5 seconds, the background intensity was nominally 1000.

Finally, it was considered appropriate to determine the variation in precision with concentration. This was achieved by repeating measurements on a multielement test solution over a period of 4 weeks. The test solution, which contained six elements at varying concentrations, was analysed 7 times using a 3 point calibration in each case. Table 2.3 shows the results of these determinations together with the concentration of the test solution expressed as multiples of the limit of detection (obtained from Table 2.4).

Table 2.3

Details of Test Solution and Results

Element	Concentration $\mu g\ ml^{-1}$	Detection Limit Multiples*	Relative Standard Deviation+ (RSD)
Pb	0.2	3	0.215
Ni	0.75	30	0.037
Fe	1.0	170	0.026
Mn	1.3	850	0.013
Zn	35.0	5000	0.011
Cu	30.0	10000	0.005

+ Mean of duplicate determinations.

* Multiples of 3s detection limits.

A plot of this data is shown in Figure 2.9 and is typical of the precision - concentration graphs previously reported by Butler (117). It can be seen that the precision obtained at a 3s limit of detection (LOD) is of the order of 40% which, considering this data was obtained over 4 weeks, agrees well with the calculated value of 33% (118).

2.4.3 Limits of Detection

The limit of detection (LOD) is determined from the smallest signal that can confidently be accepted as genuine and not derived from an accidently high blank determination. All LOD's reported in this dissertation have been calculated using the following equation (118):

$$x_{LOD} = \bar{x}_{BL} + 3s_{BL}$$

Figure 2.9

Precision - Concentration Graph for Test Solution

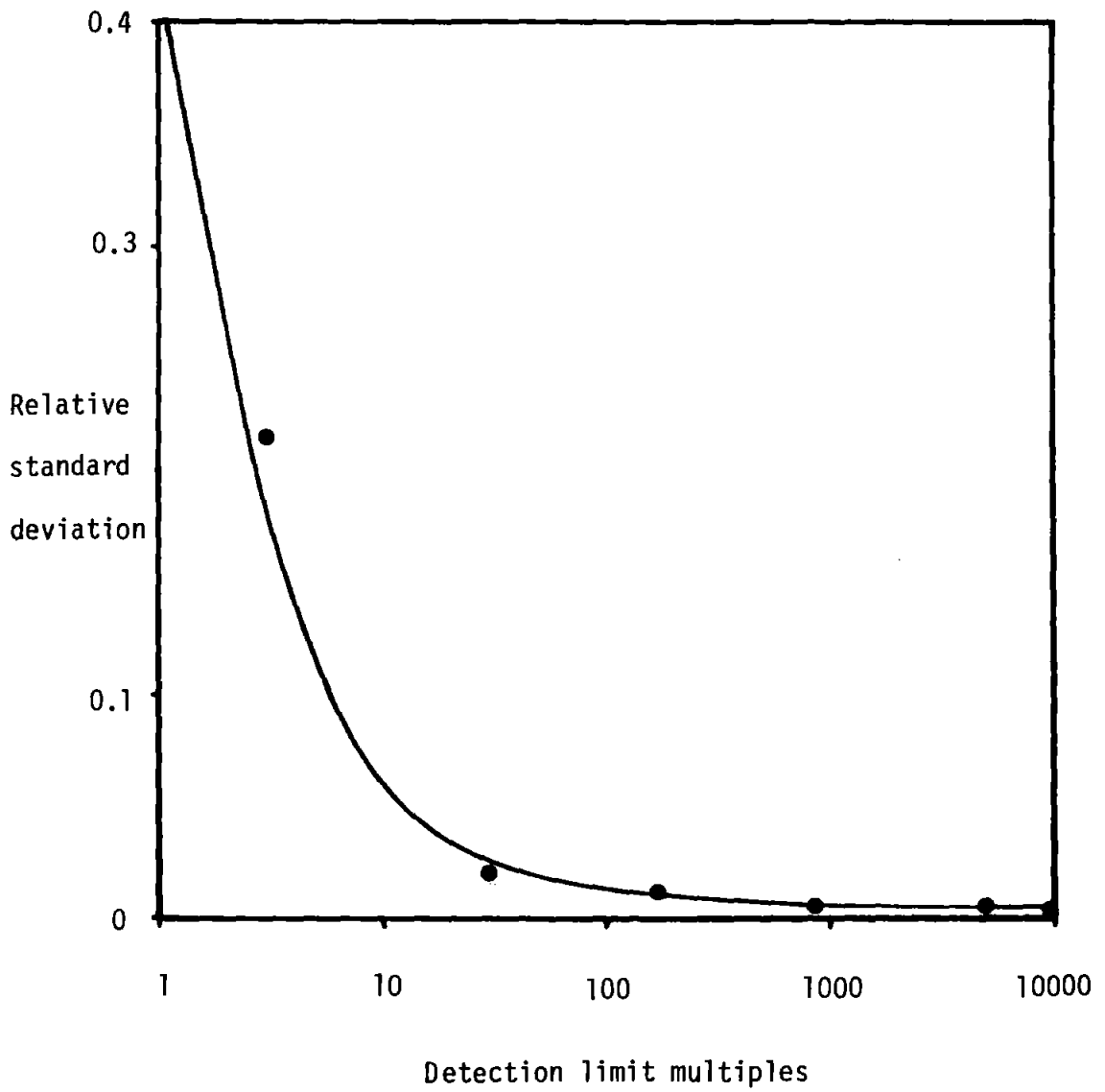

where, x_{LOD} is a measure of the LOD.

$\overline{x}_{BL}$ is a mean blank measure.

s_{BL} is an estimate of the standard deviation of the blank measure.

This definition of LOD is normally referred to as "3σ limits" in the literature but, in fact, "3s limits" would be more accurate.

Limits of detection are obviously not the only performance characteristics to consider when choosing or comparing plasma systems. However, for forensic science purposes, the knowledge of practical LOD's may be essential to decide whether analysis is feasible on a very small fragment of sample. Limits of detection were determined for the 16 polychromator elements available at the time of this investigation, this experiment was then repeated on the scanning monochromator using the same element lines. The data are shown in Table 2.4 together with published data for similar equipment.

It can be seen that the polychromator results generally compare favourably with the literature values. The performance of the monochromator was poor at wavelengths below $\sim$300 nm, this was considered to result from the low efficiency of the holographic grating in this region (the maximum efficiency is $\sim$ 50% at 500 nm)

Experiments were performed in an attempt to improve the low wavelength performance of the monochromator. Monitoring lines between 200 and 300 nm at the second order diffraction (i.e. 2 x wavelength) indicated a large increase in signal intensity. However, the large contribution from the first order plasma background (i.e. 400 - 600 nm) resulted in lower signal to background ratios (SBR's) for these lines.

A broadband UV filter (Oriel Scientific Ltd., Surrey, UK.) was used to block the first order plasma background but transmit the low

Table 2.4

Comparison of Limits of Detection[x] in $\mu g\ ml^{-1}$

Element	Wavelength (nm)	Monochromator	Polychromator	Reported Concentrations	
				Monochromator[+]	Polychromator[*]
Zn	213.8	0.03	0.007	0.0018	0.0075
Pb	220.3	1.10	0.07	0.042	0.033
Ni	231.6	0.40	0.025	0.015	0.011
Co	237.8	0.25	0.015	0.0097	-
Mn	257.6	0.009	0.0015	0.0014	0.0006
Fe	259.9	0.03	0.006	0.0062	0.0015
Cr	267.7	0.02	0.009	0.0071	0.003
Mg	285.2	0.004	0.002	0.0016	-
Sn	303.4	0.35	0.2	-	0.09
Cu	324.7	0.008	0.003	0.0097	-
Ti	334.9	0.002	0.002	0.0038	-
Zr	343.8	0.003	0.005	0.0071	-
Al	396.1	0.02	0.01	0.028	-
Sr	407.8	0.0001	0.0001	0.00042	0.00015
Ba	455.4	0.0002	0.0005	0.0013	0.00009
Li	670.8	0.03	0.03	-	-

x All calculated as 3s (3 standard deviations of the background variation).

\+ Ref. (119)

* Ref. (120)

wavelength lines. Thus, the low wavelength lines could be detected in second order free from the first order background. The results obtained for a selection of Zn and Sn lines are shown in Table 2.5.

Table 2.5

Comparison of Low Wavelength Limits of Detection on the M1000 Monochromator

Element	Wavelength nm	Detection Limit $\mu g\ ml^{-1}$			
		1st Order	2nd Order	2nd Order (Filtered)	Reported+
Zn	202.55	0.05	1.3	0.009	0.004
Zn	206.20	0.06	1.3	0.008	0.006
Zn	213.86	0.03	0.2	0.003	0.002
Sn	224.61	0.85	6.0	0.15	0.12
Sn	235.48	0.50	-	0.10	0.096
Sn	242.95	0.40	-	0.10	0.096

\+ Ref. (119)

These results indicated the considerable improvement in performance which could be obtained from monitoring low wavelength lines in second order with a broadband UV filter. This work considerably enhanced the usefulness of the monochromator as a large proportion of sensitive plasma lines are found in the 200 - 300 nm region because of the energetic nature of the excitation source.

2.4.4 Calibrations

Linear calibrations of intensity versus concentration over 4 orders of magnitude have been obtained from both spectrometers, thus confirming the optically thin nature of the ICP source.

The monochromator electronics would require signal autoranging to achieve this range automatically, at present the amplifier gain has to be manually changed. The polychromator electronics can cover this concentration range, higher concentrations requiring gain changes. Examples of calibration curves obtained with the polychromator are shown in Figure 2.10.

2.4.5 Interferences

An evaluation of any analytical technique is not complete unless possible interferences have been considered. Potential major interferences are shown in Table 2.6 together with their observed effects in ICP-OES.

In general, good analytical procedures can overcome the effects of most interferences. At this stage of the evaluation, the major interferences were briefly considered in order to estimate the magnitude of their effects.

The high temperature of the ICP source virtually eliminates the formation of refractory species such as $Ca_2P_2O_7$ (or $Ca_3(PO_4)_2$) or $Ca\ Al_2O_4$ which can cause considerable problems in flame emission spectrometry.

Transport interferences caused by the nebulisation process can be overcome by careful matching of the acid concentrations of sample and standard solutions. However, these interferences were considered sufficiently problematical to warrant further study and are considered in more detail later (see Chapter 4).

Overlap of spectral lines can be a major problem particularly if the emission spectrum of the matrix is complex. However, the use of M.I.T. wavelength tables (121) together with line coincidence tables (122) permit spectral interferences to be recognised and, in certain cases, the effects can be predicted.

Figure 2.10

Examples of Polychromator Calibration Curves

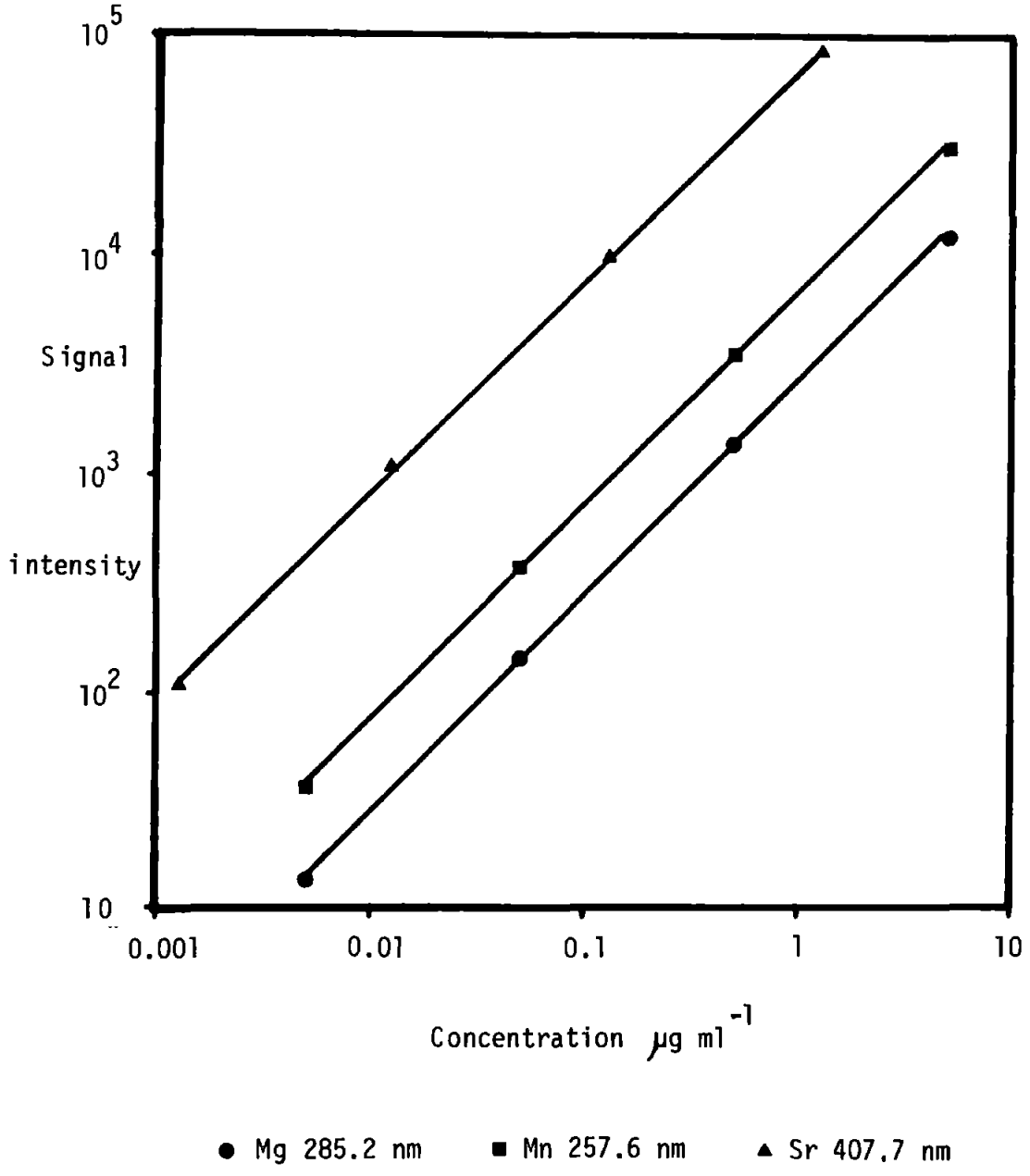

Table 2.6

Potential Major ICP-OES Interferences

Type	Cause	Effect
Chemical	Formation of refractory species in the source.	Negligible as a result of high source temperature.
Transport	Nebulisation affected by different physical properties of solutions e.g. acid content.	Emission intensities reduced with increasing acid concentration.
Spectral		
a. line overlap	Overlap of analyte emission line by interfering line.	Positive interferences.
b. line broadening	Broadened emission line profiles as a result of physical processes in the ICP..	Positive interference from the wings of an adjacent stray line.
c. recombination	Recombination of matrix ions and electrons causing continuum emission.	Positive interferences from background shift.
Stray Light	Light scattering inside polychromator when matrix containing intensely emitting species e.g. Ca, Mg.	Shifts in plasma background, generally positive interferences. Can be severe if analysis line close to matrix line.
Ionisation	Shift in atom-ion equilibrium due to presence of easily ionisable elements.	Variable effect, possibly significant when high concentrations of alkali metals present.

A wide variety of different materials can be encountered in forensic investigations and a polychromator with a fixed set of spectral lines will inevitably experience spectral overlap interferences. However, experience has shown that careful choice of the line set will permit the determination of most elements in most matrices. The analysis of steels has proved to be an exception as a result of the line rich iron spectrum. For this work, interference free element lines were selected and the analyses performed on the monochromator.

Line broadening and recombination emission (90) can cause enhancement of the plasma background. Dynamic background correction for polychromator analyses is probably the only effective means of overcoming these. These interferences did not present any major problems for the dilute solutions analysed in this work.

Stray or scattered light effects can arise from optical imperfections and poor design in spectrometers. The intense emission from Ca and Mg in the ICP source has highlighted this type of interference. Stray light effects can be severe in polychromators as a result of complex optical arrangements. High quality engineering, light traps and baffles, holographic gratings and dielectric filters have been shown to reduce scattered light significantly (120,123,124).

An experiment was performed by nebulising solutions of 100 $\mu g\ ml^{-1}$ Ca and Mg and determining apparent concentrations for the polychromator element set. The results are shown in Table 2.7. It can be seen that both positive and negative effects can be obtained and while generally these are small, significant positive interferences can be obtained at the Pb, Cr and Al wavelengths. The large interference at the Al 396.15 nm line results from the close proximity of the intense 393.37 nm and 396.85 nm Ca lines. This Al line has subsequently been changed to the less sensitive but interference free

Table 2.7

Concentration Equivalents from Scattered or Stray Light

Element	100 μg ml^{-1} Mg	100 μg ml^{-1} Ca
Zn	<0.007	0.04
Pb	0.1	0.22
Ni	0.04	0.05
Co	0.03	0.05
Mn	0.004	0.002
Fe	0.03	0.009
Cr	0.1	0.01
Mg	-	<0.002
Sn	<0.2	<0.2
Cu	<0.003	-0.005
Ti	-0.004	0.006
Zr	-0.009	-0.007
Al	-0.02	1.25
Sr	-0.0004	0.0004
Ba	-0.0009	0.0008
Li	0.06	0.07

308.215 nm line.

In an attempt to reduce the effects of scattered light, additional baffles were installed in the secondary optics and the exit slits were sealed to the slit plate. The interferences at the Pb and Cr wavelengths were then re-determined but little change was observed. Thus, these interferences probably result from reflections in the main body of the spectrometer and their elimination would require design modifications or the installation of interference filters at individual exit slits.

Interference from easily ionisable elements (EIE) have been recognised for some time and a wealth of research work has been published. However, the effects of these interferences have been described as "a study in confusion" (93) because of inconsistent data and a lack of appropriate fundamental studies. Results so far reported (93,125,126) indicate that studies of spatial effects probably offer the most appropriate means of understanding the factors affecting analyte emission in the ICP.

The evaluation and possible reduction of interference effects was considered too complex for a preliminary investigation, but is studied later in this work. At this stage of the investigation, the magnitudes of some interferences were determined by analysing test solutions prepared in nitric acid solution (5%, by volume) both with and without 1000 $\mu g\ ml^{-1}$ Na. The observed interference effects are shown in Table 2.8 and it can be seen that all are less than 10%. This was considered acceptable for the present studies. Interestingly all the interferences are negative which could result from nebuliser efficiency changes or the properties of the particular plasma region monitored for this experiment.

2.5 Preliminary Applications Studies

2.5.1 Certified Reference Materials

The analysis of certified reference materials is a valuable means of verifying analytical methods; a set of 6 reference samples were thus chosen for analysis on the polychromator. The set consisted of 4 metals (Bureau of Analysed Samples, Middlesborough, UK), a float glass

Table 2.8

Interference Effects of 1000 $\mu g\ ml^{-1}$ Sodium

Element	Conc $\mu g\ ml^{-1}$	Signal Change %
ZnI	0.2	-4.7
PbII	5.0	-1.5
MnII	0.1	-7.4
MgI	0.2	-6.7
AlI	3.0	-7.1
SrII	0.01	-9.1

(British Glass Industry Research Assoc., Sheffield, UK), and a sample of human liver tissue which had been previously ashed and analysed by spark source mass spectrometry (46) at the CRE.

Duplicate analytical solutions were prepared by dissolution of the reference materials in suitable mineral acids and subsequent dilution. The final liver ash solution contained 1000 $\mu g\ ml^{-1}$ and the glass and metal solutions contained 100 - 200 $\mu g\ ml^{-1}$ of analyte. These are greater dilutions than would normally be used for elemental analysis but they were chosen to represent typical solution concentrations which may be obtained from casework samples. Multielement standards were diluted from 1000 $\mu g\ ml^{-1}$ stock solutions (BDH Chemicals Ltd., Poole, UK) in acid concentrations to match the sample solutions.

The results of these determinations are shown in Table 2.9. Some spectral interferences and background changes were encountered and corrected for in the metals samples. The data show very good agreement with the reference values, confirming that quantitative results from trace elements to major constituents can be obtained from dilute solutions of a variety of materials.

Table 2.9

Analysis of Reference Materials

Element	Zn/Al Alloy BCS 300/1 %	Nimonic 901 BCS 387 %	Mild Steel BCS 453 %	High Tensile Brass BCS 179/2 %	Human Liver Tissue* ppm	Float Glass BGIRA EC1.1 %
Al	- -	0.26 (0.24)+	- -	2.28 (2.27)	- -	0.60 (0.57)
Cr	0.15 (0.13)	12.66 (12.46)	0.24 (0.24)	- -	- -	- -
Cu	1.33 (1.27)	0.032 (0.032)	0.14 (0.15)	58.3 (58.5)	4.9 (4.8)	- -
Fe	0.25 (0.24)	35.0 (36.0)	- -	0.99 (1.02)	246 (240)	0.074 (0.072)
Pb	- -	- -	- -	0.39 (0.35)	- -	- -
Mg	2.85 (2.74)	- -	- -	- -	- -	2.23 (2.28)
Mn	0.35 (0.33)	0.08 (0.08)	0.05 (0.04)	0.85 (0.86)	1.6 (1.4)	0.01 -
Ni	- -	42.1 (41.9)	0.10 (0.11)	0.59 (0.56)	- -	- -
Ti	0.095 (0.09)	3.00 (2.95)	- -	- -	- -	0.028 (0.024)
Zn	5.92 (5.87)	- -	- -	35.8 (35.8)	46 (45)	- -
Zr	0.19 (0.18)	- -	- -	- -	- -	- -

* Ref (46)

\+ "True values"

2.5.2 Human Tissues and Body Fluids

Inductively coupled plasma - optical emission spectrometry has been used for the determination of toxic metals in support of casework investigations. These analyses were performed on the monochromator and the samples prepared by a combined dry ash - nitric acid oxidation procedure (127).

A selection of these results is shown in Table 2.10 compared with values for normal tissue (128). Lead and Tl were determined as part of a toxic metal screen, the limits of detection were adequate as acute poisoning levels are known to be significantly higher than normal tissue concentrations. The Cd determinations were requested in a case of suspected industrial poisoning, and together with other evidence, the elevated liver and kidney concentrations were shown to be consistent with chronic cadmium poisoning. Blood and liver iron concentrations were obtained following a fatality, possibly from an overdose of capsules containing an iron salt. The data showed low Fe concentrations, more consistent with the anaemic condition of the deceased, thus eliminating suggestions of an overdose.

Water-borne aluminium has been recognised for some time as a contributory factor in the dialysis encephalopathy syndrome (129). Patients undergoing renal dialysis, in regions where tap-water concentrations of aluminium are high, are more likely to develop encephalopathy when dialysed with softened water than when deionised water is used to prepare the dialysate (130). The Al concentrations shown in Table 2.11 were obtained from tissue samples in a suspected dialysis dementia fatality. The Al levels are considerably higher than those for normal tissue, and the elevated brain, muscle and bone results are consistent with published data (131).

Table 2.10

Analysis of Human Viscera and Blood

Element Determined	Wavelength (nm)	Sample	Wet Tissue Concentrations ($\mu g\ g^{-1}$) This Work	Literature*
Pb	405.8	Liver	<2	2.3 ± 0.6
Tl	535.0	Liver	<1	~0.009
Cd	228.8	Liver	28.6	4.3 ± 1.0
Cd	228.8	Kidney	83.1	13.9 ± 0.7
Fe	259.9	Liver	101	176 ± 28.9
Fe	259.9	Blood	395	493 ± 3.9

* Ref (128)

Table 2.11

Aluminium Determinations in Dialysis Dementia Fatality

Sample	Wet Tissue Concentrations ($\mu g\ g^{-1}$) This Work	Literature*
Brain - cerebral lobe	3.8	0.5 ± 0.1 (whole brain)
Brain - stem	3.5	0.5 ± 0.1 (whole brain)
Muscle - thigh	9.7	0.5 ± 0.2
Liver	139	2.6 ± 1.3
Rib bone	75	32.4 ± 5.4

* Ref (128)

2.5.3 Metal Borides

Following the recovery of materials believed to have been stolen from a metallurgical company, the local operational laboratory was required to analyse them to provide proof of identity and origin. Inductively coupled plasma - optical emission spectrometry was the most suitable technique (in the HOFSS) for the quantitative determination of boron; low atomic number and insensitivity precluded XRF and AAS respectively.

Five samples of the Fe and Ni borides were submitted for analysis. A sodium carbonate - peroxide fusion, followed by dissolution of the melts in dilute hydrochloric acid, was used to prepare the solutions which were analysed on the monochromator using the 249.77 nm B line.

The results are shown in Table 2.12 together with data obtained by the metallurgical company using a neutron attenuation technique, and from a British Chemical Standard. These determinations confirm the accuracy and precision of ICP-OES and the capability for the analysis of refractory materials.

2.6 Conclusions and Recommendations

The instrumentation acquired during this investigation has been described and a preliminary evaluation of performance carried out. Inductively coupled plasma - optical emission spectrometry has been shown to be a stable and sensitive multielement technique which is relatively free from interferences. The following fundamental problems were identified and will be studied later:

1. multielement optimisation;

Table 2.12

The Determination of Boron in Metal Borides

Sample	%B ICP	%B Company Data
A	17.3	17.41
B	19.3	18.28
C	17.7	17.78
D	19.7	19.42
E	18.1	17.55
BCS 373 (Certified 15.1%B)	15.2	-

2. interferences from easily ionisable elements;
3. sample introduction and transport effects.

Analyses of standard reference materials have demonstrated that quantitative, multielement data from trace elements to major constituents can be obtained on small samples which may be recovered in forensic science casework. Other applications have indicated the versatility of ICP-OES for the quantitative determination of a range of elements in a variety of materials.

Inductively coupled plasma - optical emission spectrometry is, of course, a destructive analytical technique but its high sensitivity may allow small samples to be subdivided for analysis. The absolute data obtained could allow identification of manufacturing sources. In addition, the data should be useful to analysts whose techniques generate only qualitative or semi - quantitative data. Thus, a thorough investigation of ICP-OES for the analysis of evidential materials such as glass, metals, paint etc. was considered appropriate and detailed studies are presented later in this thesis.

3. SIMPLEX OPTIMISATION OF PLASMA PERFORMANCE

3.1 Introduction

Optimisation of an analytical procedure consists of the selection of operational parameters in order to obtain the most favourable response. The optimisation criterion should be a suitable objective function which has been selected to optimise the method. In analytical procedures, a maximum objective is normally sought; this may be a simple function e.g. signal to background ratio (SBR), or a composite function. Minimisation of interferences may also be important but a single criterion is normally selected and true multicriteria optimisations are rarely applied.

Forensic science analysis often requires the extraction of the maximum amount of information from the minimum quantity of sample; optimisation of analytical performance is thus a vital requirement. The performance of ICP-OES can be affected by a large number of parameters, including those associated with the plasma operation and spectrometer system. To achieve optimum plasma operating conditions and to allow meaningful comparisons of different plasmas it is necessary to choose a criterion of merit which is independant of the light detection and measuring systems.

Detection limits are normally quoted to indicate the performance of an analytical system. However, this criterion is not the most suitable if different plasmas need to be compared as it is dependant on the background noise and hence the magnitude of the background. The spectral background emitted by an argon plasma can be low and thus the measured spectrometer background may consist largely of photomultiplier dark current. It has been shown that the intrinsic

merit of different plasmas can be assessed on a given spectrometer by comparing their net SBR's (132). The plasma with the highest SBR will be the best plasma on any spectrometer but, depending on spectrometer gains, this plasma may or may not yield the best limits of detection (LOD's).

The operational parameters of plasmas (power, observation height and 3 gas flows) are interrelated and thus true optimisation is not readily achieved by iterative, univariate searches. However, an alternating variable search technique (133) has been reported for the optimisation of plasma performance. Matrix interference corrections for the determination of Ta in Au by ICP-OES have been determined by factorial analysis (134). This method is appropriate for statistical significance testing and is essential if a non-continuous variable is included in the optimisation e.g. selection of the best nebuliser. Simplex optimisation is conceptually simple and optimisation can readily be achieved when wide variations of a number of operational parameters are considered.

Application of the simplex optimisation technique for the optimisation of plasma performance is reported in this chapter. Single element optimisation has been investigated for the comparison of 2 sample introduction systems. An appropriate objective function for multielement optimisation has been evaluated and the technique extended to investigate suitable conditions for the reductions of easily ionisable element (EIE) interferences.

3.2 The Simplex Method

A simplex is a geometrical figure defined by a number of vertices (angular points) such that:

$$V = P + 1 = D + 1$$

where,

V = vertices of the simplex

P = parameters in the optimisation

and D = dimensions of the factor space

For example, in 2 and 3 dimensional factor spaces the simplex is a triangle and a tetrahedron respectively. In multi-dimensional factor space, the simplexes are less readily visualised but this is not a requirement for the successful operation of the method.

The movement of the simplex (for a 2 parameter optimisation) is governed by the following rules.

1. The new simplex is formed by rejecting the point with the worst result in the preceding simplex and replacing it with its reflection across a line defined by the remaining 2 points.
2. If the new point in a simplex has the worst response, do not apply rule 1 but reject the point with the second lowest response and obtain the new simplex from its reflection.
3. If a point is retained in 3 successive simplexes (i.e. n+1 parameters, where, in this case n=2) then redetermine the response at this point.
4. If a point falls outside one of the boundaries (e.g. parameter limit), assign an artificially low response to it and proceed with rules 1 - 3.

An example of a 2 parameter simplex optimisation is shown in Figure 3.1. The contours are lines of isoresponse and the movement of the simplex across the response surface is illustrated. This fixed step size simplex was first reported by Spendley et al.(135). This technique is very dependant on the choice of the initial step size;

Figure 3.1

The Fixed Step Size Simplex

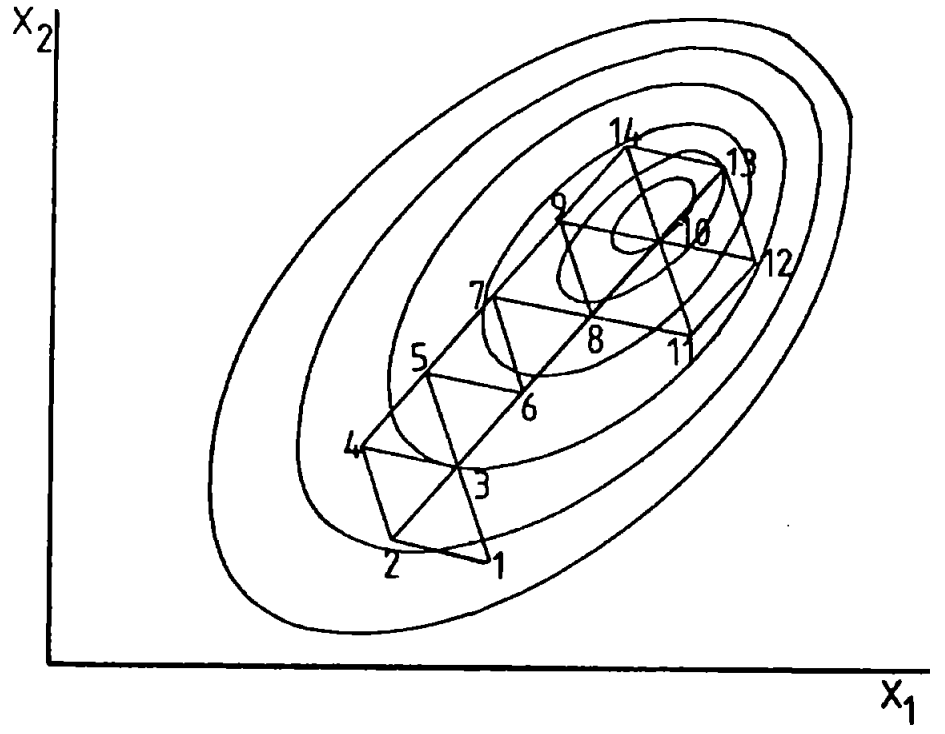

if too small compared to the factor space, the optimisation will be slow and if too large, the optimum will be imprecise. Long (136) proposed decreases in the final step sizes to achieve a more accurate determination of the optimum. However, Nelder and Mead (137) formulated a more elegant modification in which the step size is variable (within defined limits) throughout the optimisation. The typical movement of this simplex is shown in Figure 3.2 and the expansion and contraction capabilities are illustrated. This method was introduced and clearly explained by Morgan and Deming (138) and a later publication by these workers (139) illustrates a useful flow chart for experimental optimisation.

The movement of the variable step size simplex (for a 2 parameter optimisation) is governed by similar rules to the fixed step size simplex. The additional movements of the variable step size simplex are illustrated in Figure 3.3 where:

P = the centroid of the line joining B and A

W = the point with the worst response

R = the new simplex vertex

E = the expanded vertex

Cr = a contracted vertex

Cw = a contracted vertex

Rule 1 can thus be modified to allow for expansion and contraction.

1. The new simplex is formed by rejecting the point with the worst result in the preceding simplex (W) and replacing it with its reflection (R) across a line defined by the remaining 2 points (B and A). Using position vectors, this basic step can be defined as follows:

$$R = \bar{P} + (\bar{P} - W)$$

Figure 3.2

The Variable Step Size Simplex

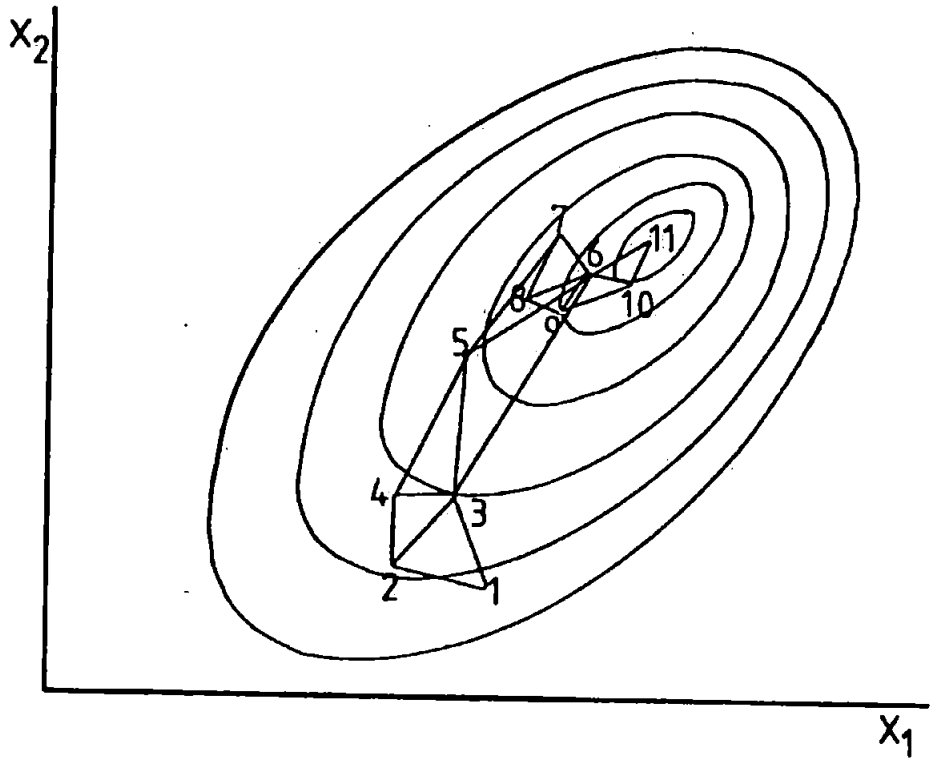

Figure 3.3

Variable Step Size Simplex Moves

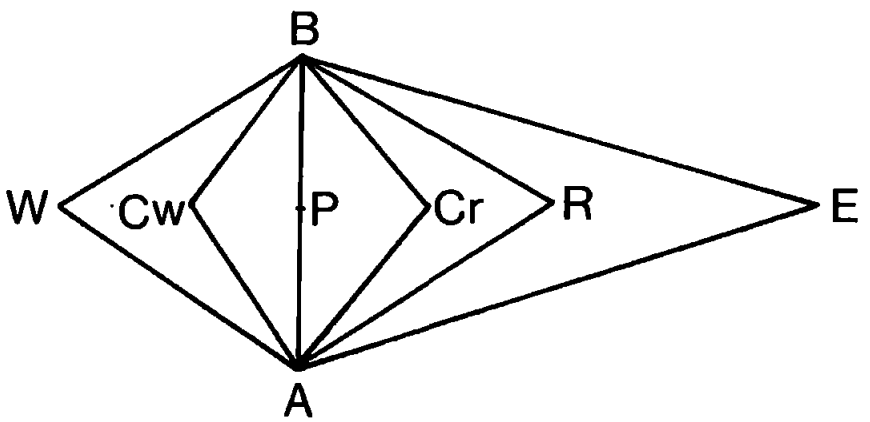

P = the centroid of the line joining B and A

W = the point with the worst response

R = the new simplex vertex

E = the expanded vertex

Cr = a contracted vertex

Cw = a contracted vertex

If R is better than the previous best then E can be defined by:

$$E = \bar{P} + e\ (\bar{P} - W)$$

where,

e = an expansion factor (usually 2)

The better response from these vertices defines the vertex in the new simplex. If the original response for R is poor then one of the following contractions may be defined according to the rules (139).

$$Cr = \bar{P} + c\ (\bar{P} - W)$$

$$Cw = \bar{P} - c\ (\bar{P} - W)$$

where,

c = a contraction factor (usually $\frac{1}{2}$)

The choice of the initial step size is a critical factor in the optimisation procedure. Yarbro and Deming (140) have demonstrated the desirability of starting with a large step size to ensure the majority of the factor space is explored before the simplex contracts to the optimum. The matrix and accompanying equations, described by these authors, were used to design the initial simplex. The three dimensional initial simplex was set up as shown in Figure 3.4. The value Sn is called the step size for the n th variable and is calculated by subtracting the lowest feasible value (Xn) from the highest feasible value. The lowest and highest values depend on the physical constraints of the instrument and whether or not a stable plasma can be formed. The values Pn and Qn can be calculated for each variable and by adding these values to the appropriate Xn value the initial simplex can be formed.

A number of simplex optimisation applications have been reported in connection with elemental analysis. Michel et al. (141) have optimised the preparation of electrodeless discharge tubes. Cave et al. (142) described the variable step size simplex for individual element optimisation and interference reduction and Ebdon et al. (143)

Figure 3.4

The Initial Simplex Matrix

Vertex	Dimensions 1	2	3	n-1	n
1	X_1	X_2	X_3	X_{n-1}	X_n
2	$P_1 + X_1$	$Q_2 + X_2$	$Q_3 + X_3$	$Q_{n-1} + X_{n-1}$	$Q_n + X_n$
3	$Q_1 + X_1$	$P_2 + X_2$	$Q_3 + X_3$	$Q_{n-1} + X_{n-1}$	$Q_n + X_n$
4	$Q_1 + X_1$	$Q_2 + X_2$	$P_3 + X_3$	$Q_{n-1} + X_{n-1}$	$Q_n + X_n$
n	$Q_1 + X_1$	$Q_2 + X_2$	$Q_3 + X_3$	$P_{n-1} + X_{n-1}$	$Q_n + X_n$
n+1	$Q_1 + X_1$	$Q_2 + X_2$	$Q_3 + X_3$	$Q_{n-1} + X_{n-1}$	$P_n + X_n$

where:-

$$Pn = \frac{Sn}{n\sqrt{2}} \left(\sqrt{n+1} + (n-1)\right)$$

$$Qn = \frac{Sn}{n\sqrt{2}} \left(\sqrt{n+1} - 1\right)$$

compared the performance of alternative plasmas. Terblanche et al. (144) optimised a high power plasma and Leary et al. (145) were the first to propose an objective function for multielement optimisation. Wade (146) proposed a modified simplex to optimise flow injection analysis and Harper et al. (147) optimised the ultrasonic extraction of atmospheric particulates. McCaffrey and Michel (148) used an 8 factor simplex to optimise the operation of a metastable nitrogen plasma with carbon furnace sample introduction. Moore et al. (149) evaluated a procedure for a sequential optimisation of maximum SBR then minimum interference. Montaser et al. (150) reported the simplex optimisation of a low gas flow ICP torch and Lukasiewicz and Dewalt (151) recently advocated the use of limit of detection instead of SBR as an objective function for optimisation.

The studies performed in this section of the thesis used the variable step size simplex and each of the factors was varied according to the rules of the algorithm (137). All computations have been performed with a hand held calculator although a Basic computer program was briefly investigated. Recent modifications to the simplex procedure such as the weighted centroid and super modified simplex have been reported (152, 153, 154) but were not considered appropriate for the manual calculations employed in this work.

3.3 Preliminary Experiments

All optimisations reported here have been performed on the polychromator; during the course of these experiments the instrument was uprated from 16 to 32 element channels.

Problems were initially experienced with optimisation using the criterion of maximum SBR. The simplex appeared to be moving to a

minimum plasma background to achieve a maximum SBR; small changes in plasma background thus caused large fluctuations in SBR's. An example of these results is shown in Table 3.1 and it can be seen that a high signal to plasma background ratio does not give the best detection limit performance.

The total signal observed during nebulisation of a blank includes the plasma background, photomultiplier dark current and electronic offset. The offsets were reduced to a minimum and the total blank signal used as background for all subsequent optimisations as improvements in the practical, analytical performance was the ultimate aim. It was considered that the smaller SBR's could make optimisation more difficult, but that the concept of the intrinsic merit of alternative plasmas on a given spectrometer would be unaffected.

Table 3.1

Preliminary Optimisation Results for Mn

Simplex Function	SB plasma R	SB total R	LOD $\mu g\ ml^{-1}$
Signal/plasma background	11.93	0.71	0.003
Signal/'total background'	2.78	1.81	0.0009

Initial optimisations were performed by varying the following 5 parameters: plasma gas, auxiliary gas, injector gas, generator power output and observation height above the load coil. Using manual calculation, an average of 3½-4 hours was required to complete each single element optimisation. In an attempt to achieve more rapid optimisation, the significance of each parameter was investigated. Increasing the auxiliary flow appeared to raise the plasma and visibly increase the argon flow in the injector channel. The plasma background

remained relatively constant but emission signals decreased, resulting in a decrease in SBR. Varying the auxiliary flow did not appear to offer any advantage and was therefore not considered to be a significant parameter. Increasing the plasma gas flow-rate produced a slimmer and more elongated plasma. SBR's were increased as a result of an increased pinch effect on the axial channel, this reached an optimum at 18-24 l min^{-1} for most elements. Therefore, for all further optimisations, the auxiliary flow was set at zero and the plasma gas at 18 l min^{-1}.

The corrosion resistant sample introduction system has been used for the majority of studies and, following preliminary experiments, the starting conditions shown in Table 3.2 were calculated as previously described and have been used for all optimisation experiments. It was found that a precision of 1%-1.5% on the SBR's from 4 vertices provided an acceptable stopping condition for the optimisations.

Table 3.2

Starting Conditions for Simplex Optimisation of the Corrosion Resistant System

Vertex	Injector Flow l min^{-1}	Power kW	Observation Height mm+
1	0.80	0.40	6
2	1.25	0.65	11
3	0.95	1.20	11
4	0.95	0.65	22

+ Above load coil.

The results obtained from a Mn optimisation are shown in Table 3.3; this optimisation performed with a solution concentration of 1 $\mu g\ ml^{-1}$ took 18 moves, and was completed in 2 hours. Univariate searches of these parameters are shown in Figures 3.5 to 3.7 and confirm the accuracy of the simplex predictions. In addition, searches were performed of the auxiliary and plasma gas flow rates. These are shown in Figures 3.8 and 3.9 respectively and support their omission from the optimisation.

The flow rate of solution supplied to the nebuliser was set at 1.6 ml min^{-1} following preliminary experiments. At the simplex conditions, Mn signal and background were monitored as the pump flow was changed. It was found that no advantage was obtained when the solution flow was increased to 2.75 ml min^{-1}, but the SBR decreased when the solution flow was reduced below 1.6 ml min^{-1}. Therefore, it was not considered necessary to change the solution flow from the original value.

Table 3.3

Final Vertices for Mn Optimisation

Injector Flow l min^{-1}	Power kW	Observation Height mm	SBR
0.99	0.60	11.0	10.48
0.99	0.60	11.5	10.29
1.02	0.65	11.5	10.36
0.97	0.60	10.5	10.24
Mean = 0.99	0.60	11.0	

Figure 3.5

Univariate Search of Injector Gas Flow at Mn Simplex Conditions

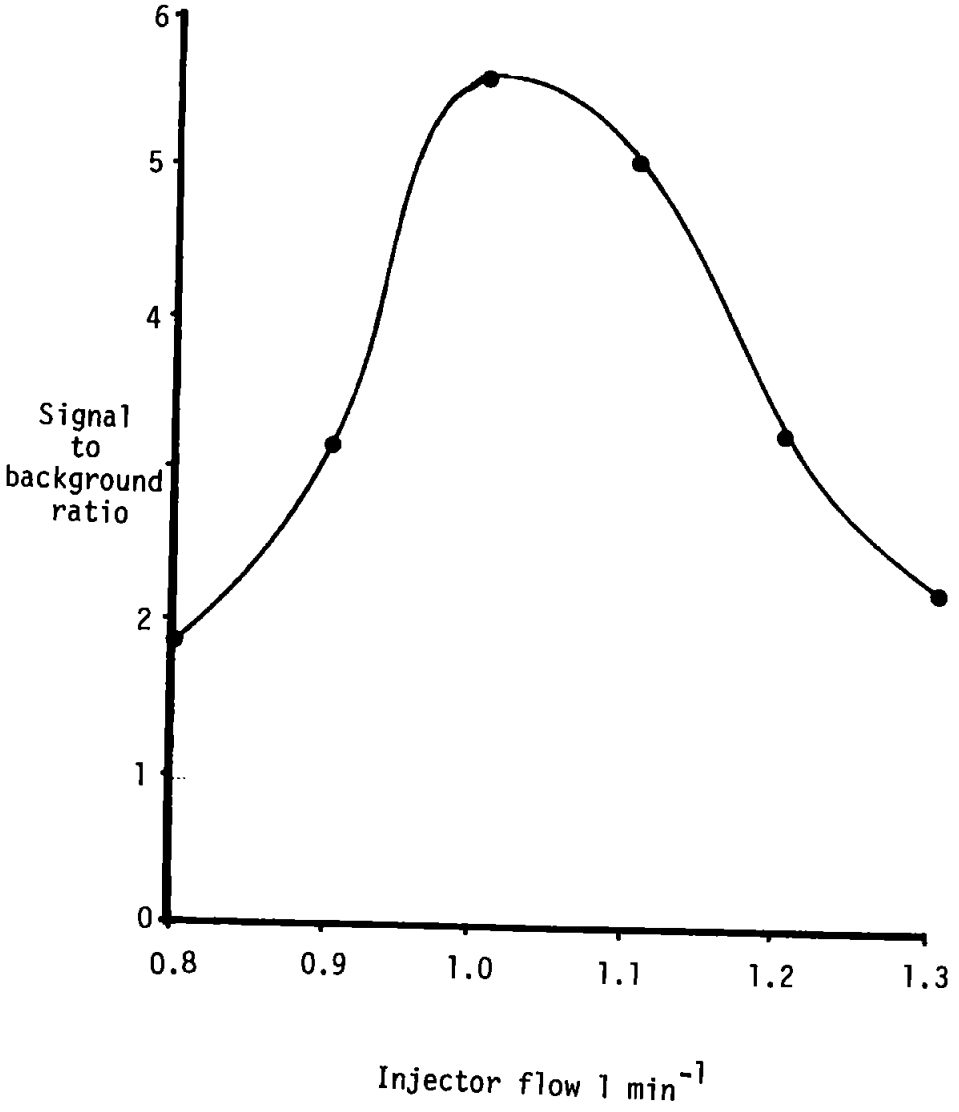

Figure 3.6

Univariate Search of Power at Mn Simplex Conditions

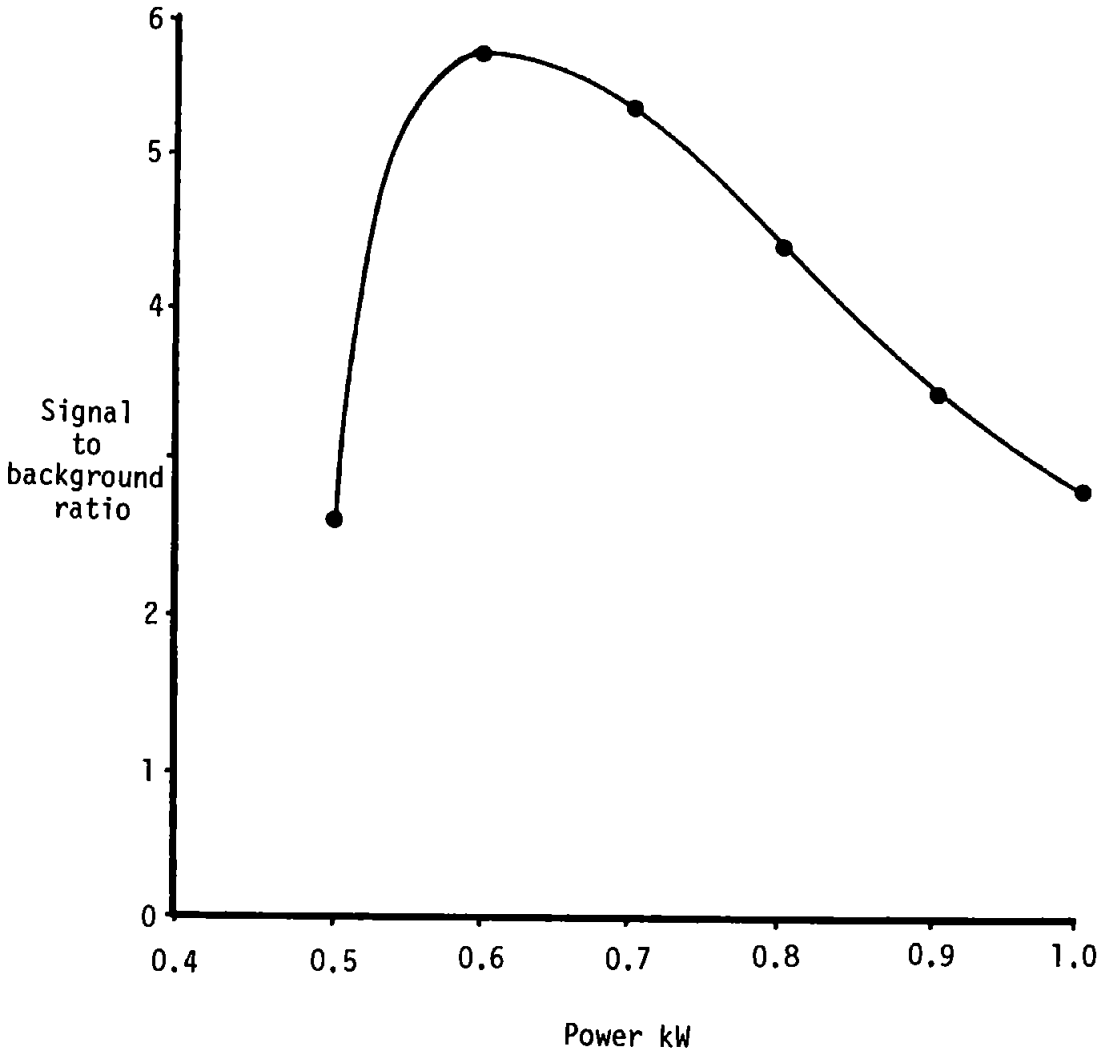

Figure 3.7

Univariate Search of Observation Height at Mn Simplex Conditions

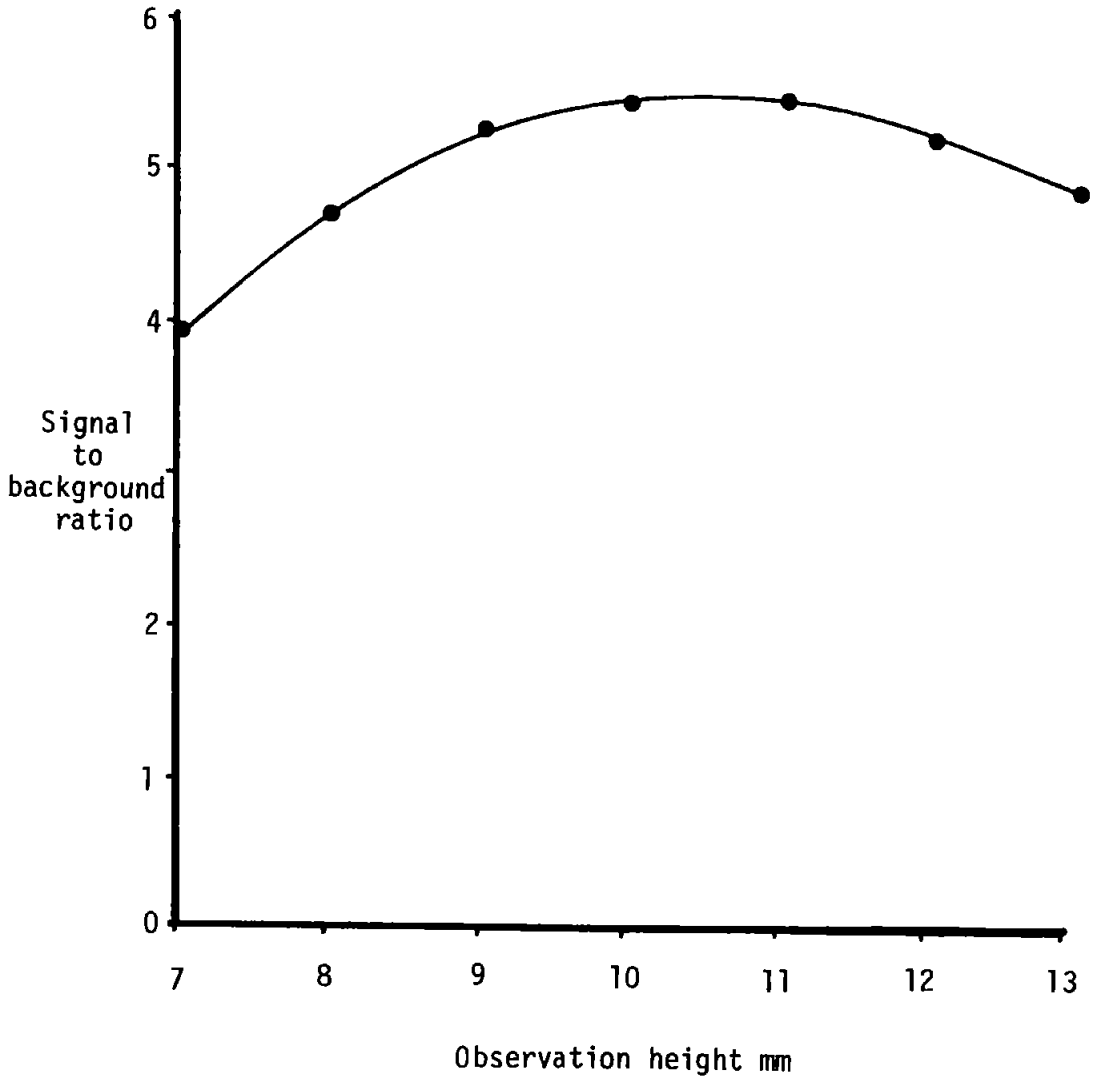

Figure 3.8

Univariate Search of Auxiliary Gas Flow at Mn Simplex Conditions

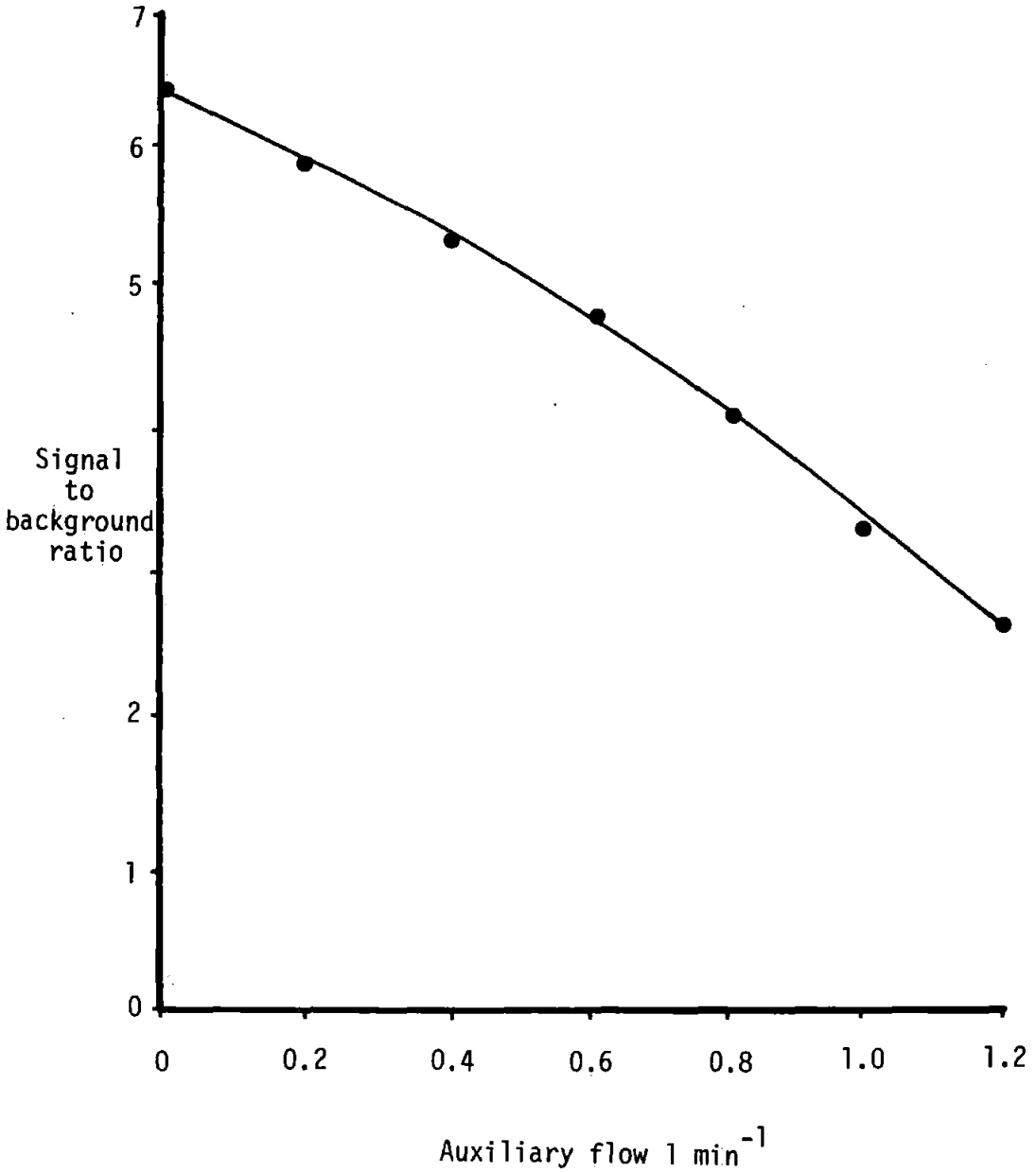

Figure 3.9

Univariate Search of Plasma Gas Flow at Mn Simplex Conditions

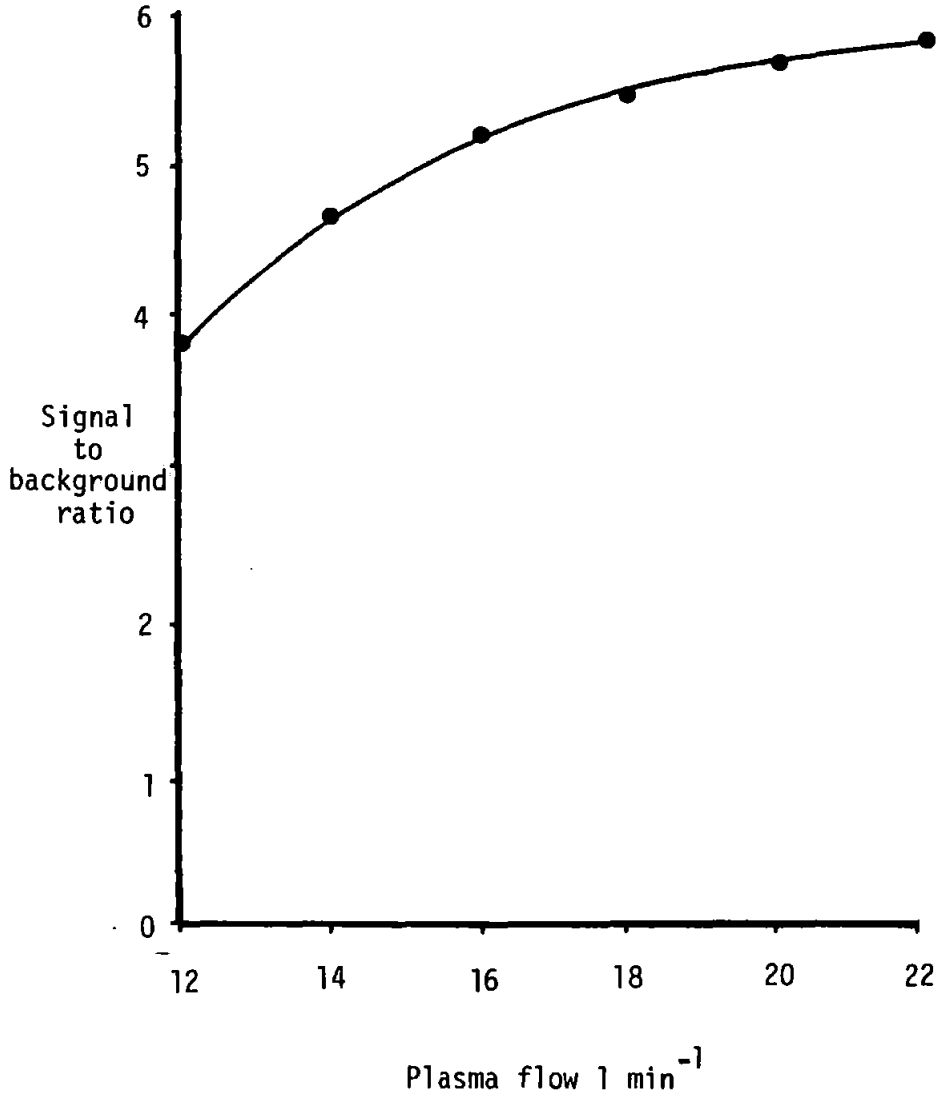

During the course of these experiments, a Basic computer program was obtained on loan for trial purposes. This program, OPT1 (155), was written for an Apple 11e micro-computer (Apple Computer Inc. Cupertino, California, USA.) and utilised the variable step size simplex. The results are shown in Table 3.4 and show excellent agreement with the manual simplex in Table 3.3.

Table 3.4

Final Vertices for Mn Optimisation (OPT1 program)

Injector Flow $l\ min^{-1}$	Power kW	Observation Height mm	SBR
1.02	0.60	11.20	10.36
1.02	0.57	10.98	10.36
0.98	0.60	10.59	10.29
0.98	0.65	11.12	10.35
Mean = 1.00	0.61	10.97	

This computer optimisation was quicker and easier to apply than the manual version and would obviously be more appropriate for a more complex, multielement optimisation. Unfortunately, the Apple machine was interfaced to another instrument and could not be spared for future simplex applications.

The optimum Mn conditions were found to provide acceptable performance for a variety of elements and were therefore used for most determinations. After a period of 6 weeks Mn was re-optimised and the results shown in Table 3.5. The parameters show good agreement with those obtained earlier although the SBR is somewhat reduced. This indicates, as expected, that long term stability of optimised conditions

can be achieved with a stable system.

Table 3.5

Final Vertices for Mn Optimisation
(Repeat after 6 weeks)

Injector Flow min^{-1}	Power kW	Observation Height mm	SBR
0.90	0.55	11,5	5.90
0.95	0.55	11.0	5.88
0.97	0.55	11.5	5.78
0.96	0.55	11.5	5.84
Mean = 0.95	0.55	11.5	

The accuracy with which the individual parameters could be set was dependant on their calibrations. For these experiments the calculated parameters were rounded up to the following practical increments: injector flow 0.02 l min^{-1}, power 0.05 kW and height 0.5 mm.

3.4 Comparison of Sample Introduction - Plasma Torch Configuration.

The ultimate aim of these studies was to achieve compromise operating conditions for simultaneous, multielement analysis by ICP-OES. It was considered appropriate to use simplex optimisation to compare the 2 available systems to determine the most suitable for compromise, multielement analyses.

Details of the elements used for these studies are shown in Table 3.6. The 2 system configurations have been described earlier (section 2.3.2).

Table 3.6

Element Details for Single Element Optimisation

Element	Wavelength nm	Difficulty of Excitation eV*
Mn II	257.61	12.2
Fe II	259.94	13.0
Mg I	285.21	4.3
Al I	308.22	4.0
Sr II	407.77	8.7
Ba II	455.40	7.9

* Excitation + ionisation potential where appropriate.

Six elements were optimised with the glass - silica system and the results are shown in Table 3.7. Three of these elements were re-optimised using the hydrofluoric acid resistant system, the results of these experiments are shown in Table 3.8.

Table 3.7

Simplex Optimised Plasma Parameters
(Glass - silica system)

Element	Injector Flow l min^{-1}	Power kW	Observation Height mm
Mn II	0.89	0.90	15.5
Fe II	0.90	1.10	16.0
Mg I	0.92	0.90	14.0
Al I	0.82	0.65	13.5
Sr II	0.96	0.90	22.5
Ba II	0.99	0.90	21.5

The effectiveness of the simplex procedure was confirmed with univariate searches.

Table 3.8

Simplex Optimised Plasma Parameters
(Hydrofluoric acid resistant system)

Element	Injector Flow $l\ min^{-1}$	Power kW	Observation Height mm
Mn II	0.99	0.60	11.0
Mg I	0.95	0.50	9.0
Sr II	0.99	0.50	12.5

Considerable variation of parameters exists between these systems, particularly for input power and observation height. It was considered that nebuliser or spray chamber alterations would be unlikely to cause these differences. The internal diameters of the silica and alumina injector tubes of the 2 torches were 1.5 mm and 2 mm respectively. Thus, for a given flow rate the injector gas velocity is lower using the alumina injector resulting in lower optimal observation heights. These height differences have previously been reported in connection with the position of the "sodium bullet" in the injector channel (156). The lower optimal power for the demountable torch results in a smaller, more compact plasma thus confirming the interrelation of plasma operating parameters.

The optimum observation zones for the demountable torch are very compact. Those for Mg I and Sr II, 'soft' and 'hard' lines respectively on the criteria proposed by Boumans (157), vary only from 9 mm to 12.5 mm. Whereas, using the smaller bore injector tube, the variation is from 14 mm to 22.5 mm. As previously reported (158),

optimal viewing heights for ion lines are higher than for atom lines.

The reduction in gas velocity for the larger bore injector suggests that atomisation of the sample aerosol is taking place closer to the load coil as a result of the longer residence time. A considerable potential advantage appears to exist for this system as its compact characteristics facilitate the choice of multielement compromise conditions. The univariate searches for observation height, power and injector gas flow rate generally illustrate the less critical dependence of SBR on these parameters for the larger diameter injector tube (Figures 3.10 to 3.12) than for the smaller diameter injector tube (Figures 3.13 to 3.15). Thus, the sacrifice in resetting to compromise conditions from single element optimal conditions is less for the torch containing the wider bore injector tube.

Detection limits were estimated for 3 elements with both systems using both preliminary and simplex optimised conditions. The results are shown in Table 3.9. The simplex predictions demonstrated improvements in detection limits for all elements with both sample introduction systems. These improvements were small but consistent. The average optimisation time of 1½ to 2 hours demonstrated that a number of elements could be readily re-optimised following changes to the sample introduction system.

The hydrofluoric acid resistant sample introduction system fitted with the larger bore torch injector tube gives rise to a smaller, more compact plasma with less variation of operational parameters between elements. This system was thus selected for further studies into multielement optimisation.

Figure 3.10

Univariate Searches of Observation Height with the

Wide Bore Injector Tube

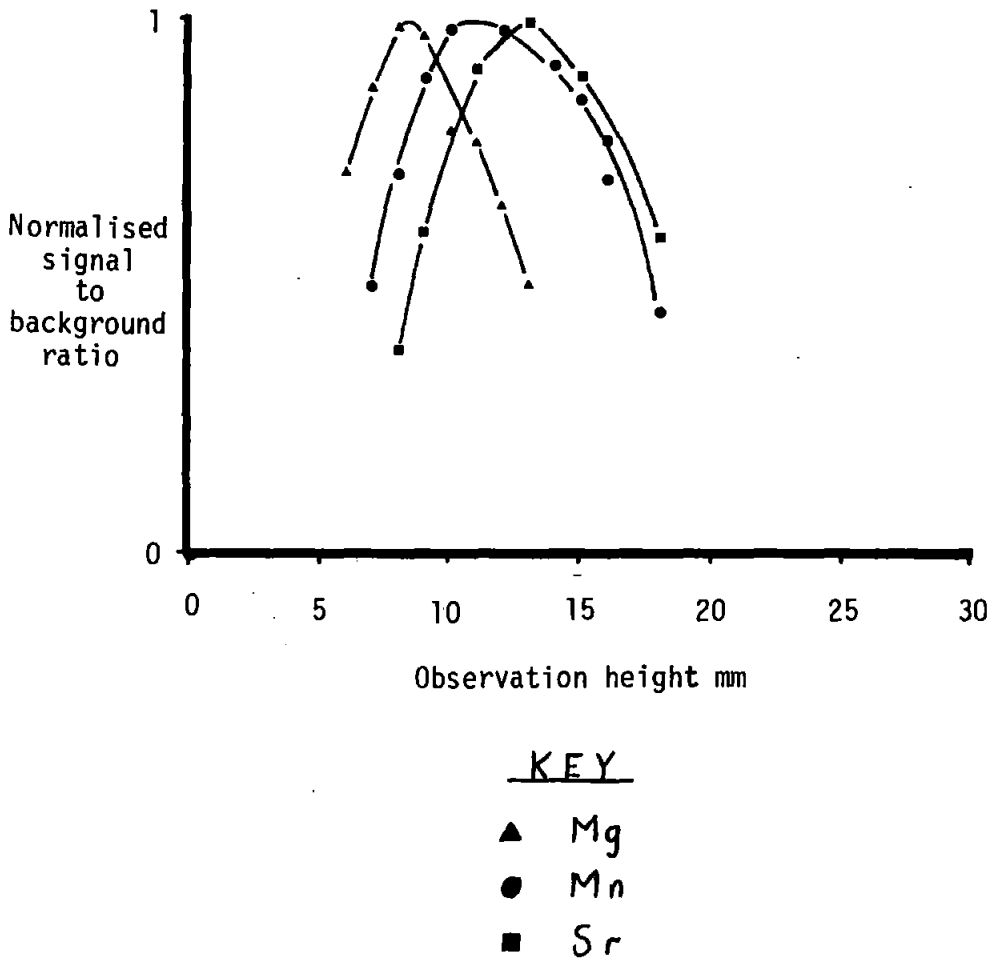

Figure 3.11

Univariate Searches of Power with the Wide Bore Injector Tube

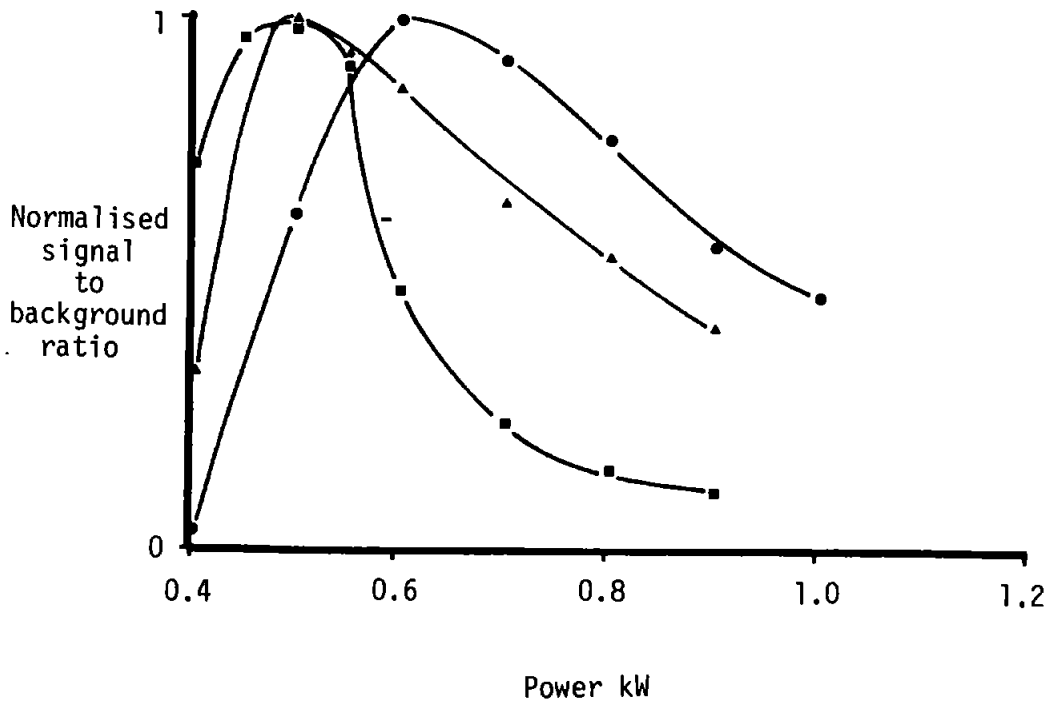

Figure 3.12

Univariate Searches of Injector Gas Flow with the Wide Bore Injector Tube

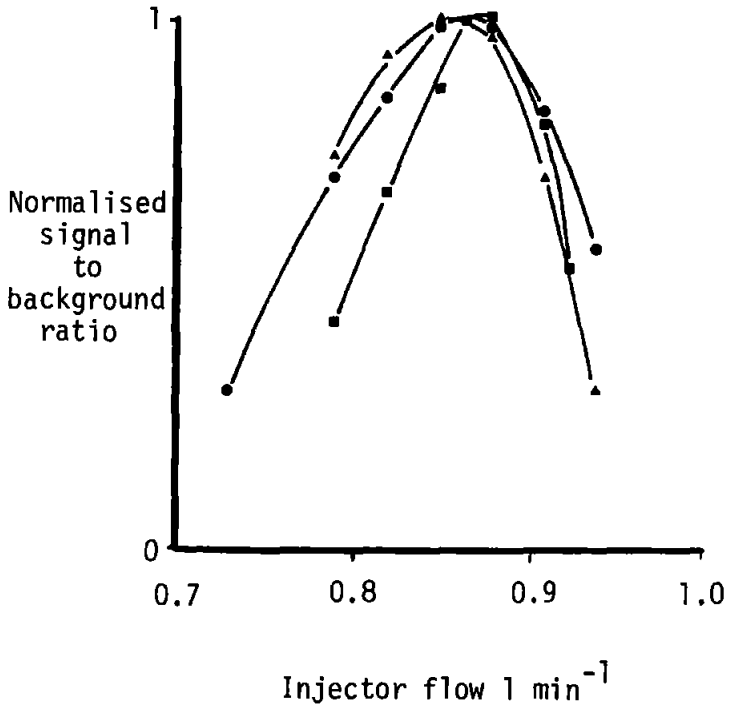

Figure 3.13

Univariate Searches of Observation Height with the Narrow Bore Injector Tube

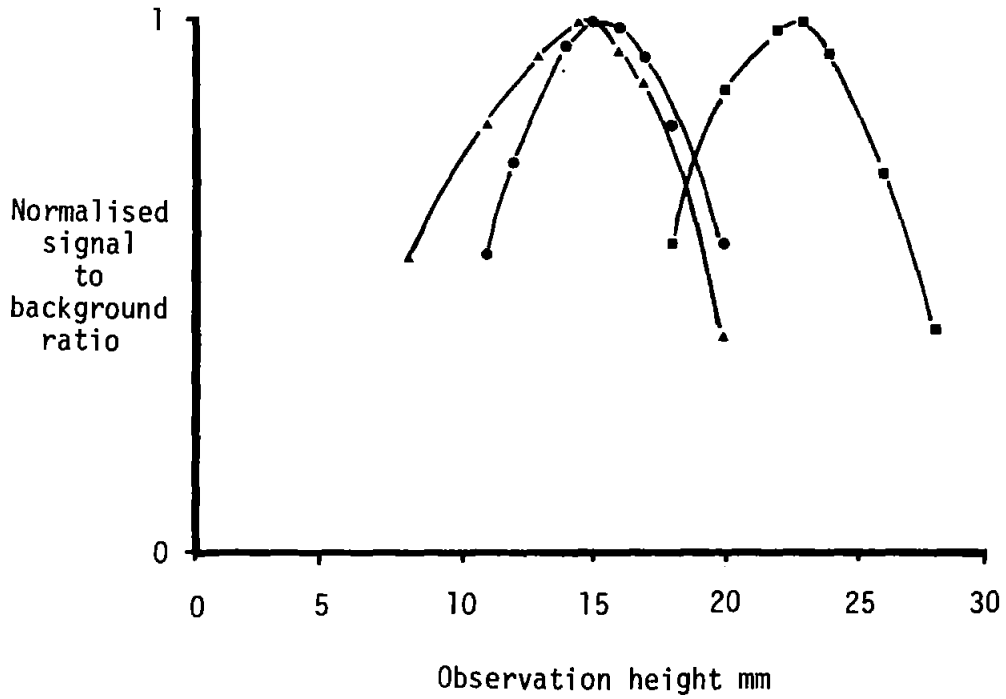

Figure 3.14

Univariate Searches of Power with the Narrow

Bore Injector Tube

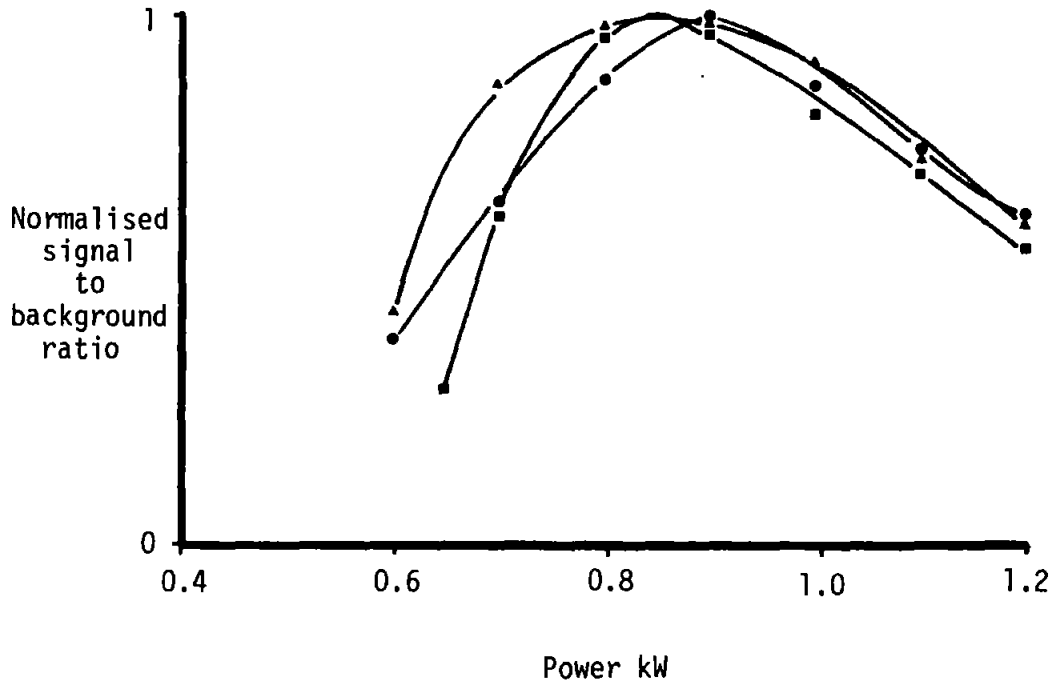

Figure 3.15

Univariate Searches of Injector Gas Flow with the Narrow Bore Injector Tube

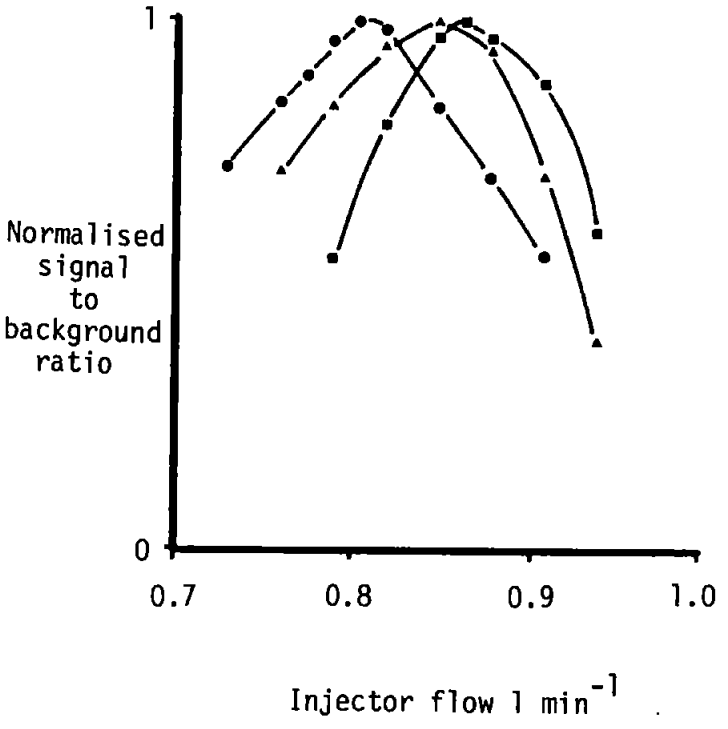

Table 3.9

Comparison of Limits of Detection ($\mu g\ ml^{-1}$)

Criterion	Mn	Mg	Sr
1. Compromise	0.0015	0.002	0.00015
Simplex	0.0008	0.001	0.00005
2. Compromise	0.0008	0.0015	0.0001
Simplex	0.0004	0.0009	0.00003

1. Glass-silica system. Compromise conditions: Injector flow 0.87 $l\,min^{-1}$, Power 1.0 kW, Observation height 18.0 mm.
2. Hydrofluoric acid resistant system. Compromise conditions: Injector flow 1.15 $l\ min^{-1}$, Power 1.0 kW, Observation height 18.0 mm.

3.5 Multielement Optimisation

3.5.1 Introduction

Inductively coupled plasma - optical emission spectrometry is a multielement analytical technique which is generally operated with a single set of analytical conditions. Spectroscopists rarely perform a true multielement optimisation and prefer to use compromise conditions obtained from the literature, manufacturers or as a result of single element studies. The versatility of the ICP source is such that good performance can generally be obtained. However, only a comprehensive multielement optimisation can ensure that the best performance is achieved for a particular application.

The establishment of compromise conditions for multielement optimisation has been reported by a number of workers. Boumans and De Boer (159) commented on the ideal nature of (argon) ICP-OES for simultaneous, multielement analysis and presented a set of compromise conditions. Greenfield and Thorburn Burns (133) compared the performance of argon cooled and nitrogen cooled torches under optimised conditions. Berman and McLaren (160) advocated the use of "ion line" conditions as a good compromise for optimum LOD's and interference reduction. These conclusions were also reported by Boumans and Lux-Steiner (157) and Bamiro et al. (161). Ebdon et al. (143,162) and Montaser (163) identified the argon plasma as more suitable for compromise analysis than the nitrogen cooled plasma.

Moore et al. (149) performed univariate searches on a nitrogen cooled argon plasma and identified optimum conditions for atomic and ionic lines and also compromise analysis. Leary et al. (145) reported the application of an objective function for multielement

simplex optimisation of an argon plasma. The forward power and observation height were optimised for a set of 5 elements and the simplex was terminated after 30 moves. This technique was employed by Montaser et al. (150) to optimise a low gas flow torch. Six parameters were optimised for a set of 20 elements and the performance of this torch shown to be comparable to a conventional ICP. Moore et al. (164) optimised a nitrogen cooled argon ICP with the same objective function but added a second stage for minimisation of ionisation interference effects. These workers achieved an analytically useful plasma combining good detection limits and minimum interference effects.

A multielement optimisation would obviously be appropriate to assist the acquisition of the maximum information from small samples encountered in forensic investigations. The evaluation of a 10 element, 3 parameter simplex optimisation was thus undertaken.

3.5.2 Preliminary Studies

Successful multielement optimisation requires the selection of a suitable objective function to represent the composite response from a group of elements of interest. The general weighted average incorporating SBR^{-1}, as reported by Leary et al. (145), appeared simple to apply and as elegant as the simplex optimisation itself. This calculation takes the following form:

$$F = n \Big/ \sum_{i=1}^{n} (SBR)_i^{-1}$$

where F = objective function

and n = the number of analyte elements

In addition, the following optimisation strategies were considered:

a. The element concentrations in the test solution should be similar to the particular samples requiring analysis.

b. The element concentrations in the test solution should be similar and related to particular sample types by the application of suitable weighting functions to individual elements.

c. For unknown materials the optimum conditions should be chosen to provide the minimum deviation from individual element optimum conditions.

To assist the simplicity of calculations in these studies, the first strategy was selected i.e. the test solution should match the sample type and the trace elements should be at the lowest expected levels.

This optimisation strategy is obviously weighted towards the lowest concentration trace elements, whereas the major element responses can change markedly without the overall performance being affected. Elements of intermediate concentrations should make some contribution to the objective function to avoid degradation of performance.

Assuming a typical background signal of $\sim$1000 (5 second integration) and an RSD of $\sim$ 0.35%, the complete analytical range of the polychromator is 0.01 SBR (i.e. 3s LOD) - 150 SBR or 1.5×10^4 concentration units. For optimisation purposes, an analytical range of 0.01 SBR - 5 SBR i.e. 5×10^2 concentration units was considered appropriate. The sensitivity of the objective function is determined by the SBR^{-1} function and Table 3.10 illustrates some alternatives together with their response ranges. It can be seen that a concentration range of 500 is represented by a corresponding range of 500 for SBR^{-1}, this implies a very high sensitivity for small response changes. The $SBR^{-0.7}$ function appears more appropriate as the range of the response function is a contraction of the concentration range.

Table 3.10

Alternative SBR Functions

	SBR	$SBR^{-0.5}$	$SBR^{-0.7}$	SBR^{-1}	$SBR^{-1.5}$
	0.01	10	25	100	1000
	0.1	3.2	5	10	32
	1	1	1	1	1
	5	0.45	0.32	0.2	0.09
Range =	500	22	77	500	11111

This proposal was tested by performing a 4 element, 3 parameter simplex optimisation using the following objective function:

$$F = n \Big/ \sum_{i=1}^{n} (SBR)_i^{-0.7}$$

The optimisation took 2¾ hours but was complicated by a malfunctioning nebuliser. However, the final SBR's for the elements were artificially varied to test the variation in the response of the objective function. Some of these calculations are summarised in Table 3.11. It can be seen that the SBR^{-1} function is most sensitive to a 10% change in trace element response (Mn) but totally insensitive to a 150% change in major element response (Ba). However, the $SBR^{-0.7}$ function is less sensitive to the trace element change but does respond to the major element change. Therefore, this $SBR^{-0.7}$ function was selected for the full optimisation as its performance appeared to be more appropriate for these studies.

Table 3.11

Variation in Response of Objective Function

	SBR				Objective Function	
	Zn (0.5)+	Mn (0.02)	Mg (0.05)	Ba (0.5)	$SBR^{-0.7}$ (% change)	SBR^{-1} (% change)
1.	0.69	0.05	0.09	2.91	0.261	0.122
2.	1.04	0.05	0.09	2.91	0.267 (+2.2)	0.123 (+0.8)
3.	0.69	0.055	0.09	2.91	0.271 (+3.8)	0.129 (+5.7)
4.	0.69	0.05	0.09	7.28	0.265 (+1.5)	0.122 (0)

+ Element concentration in $\mu g\ ml^{-1}$.

1. SBR's at end of simplex optimisation.

2. 50% increase in minor element concentration.

3. 10% increase in trace element concentration.

4. 150% increase in major element concentration.

Before the full multielement studies were performed, the polychromator element set was increased from 16 to 32 elements, a burnt out RF connector was replaced, the torch was completely rebuilt and the cross-flow nebuliser fitted with new gas and solution capillary tips. These major alterations were expected to change future optimum conditions from those previously obtained.

3.5.3 Multielement Simplex Optimisation

A set of 10 elements was selected to test the optimisation routine. These were not derived from a particular sample type but represent a compilation of elements encountered in forensic analyses.

The element set is shown in Table 3.12 together with concentrations and other fundamental data. It can be seen that these elements range from a difficulty of excitation of 4.0 eV for Al to 14.7 eV for Pb. In addition, 5 of these element lines could be classified as "soft" and 5 as "hard" according to the criteria of Boumans (157).

Table 3.12

Element Set for Multielement Simplex Optimisation

Element	Wavelength nm	Concentration $\mu g\ ml^{-1}$	LOD factor+	Difficulty of Excitation eV	Boumans' Classification*
Tl I	351.9	1	5	4.5	Soft
Zn I	213.8	1	500	5.8	Hard
Pb II	220.3	10	100	14.7	Hard
Mn II	257.6	0.005	5	12.2	Hard
Fe II	259.9	0.05	10	13.0	Hard
Mg I	285.2	0.5	500	4.3	Soft
Al I	308.2	5	100	4.0	Soft
Ti II	334.9	0.05	10	11.1	Hard
Sr II	407.8	0.05	100	8.7	Soft
Ba II	455.4	0.01	10	7.9	Soft

\+ LOD multiple, estimated from previous data.

* Ref. (157).

Three optimisation experiments were performed over a period of 3 weeks, an average time of 3 hours 30 minutes was required for an optimisation consisting of about 18 moves. The simplex conclusions are shown in Table 3.13 and demonstrate an acceptable precision.

Table 3.13

Multielement Simplex Optimisations (3 experiments)

	Injector Flow l min^{-1}	Power kW	Height mm
	0.89	0.55	11
	0.85	0.55	9.5
	0.85	0.5	9.5
Mean =	0.87	0.55	10

In order to test the performance of the simplex optimisation, the LOD's were determined on 3 separate days using both the mean simplex conditions and the previous compromise conditions. The mean results are shown in Table 3.14. The multielement simplex conditions demonstrate an overall improvement in LOD's. However, only minimal improvements were obtained for Mn and Tl which were the trace elements in this study and expected to show the greatest improvements. In all probability the data obtained for these elements, with both sets of conditions, are approaching the optimum obtainable for this particular sample introduction - torch - spectrometer configuration.

At the simplex conditions the LOD's of the "soft" lines improved by an average of 26% and the "hard" lines improved by 14%. This could be a characteristic of the low observation region in this plasma but the overall improvement confirms the earlier observations (section 3.4) that this compact argon plasma is very appropriate for compromise multielement analysis.

Table 3.14

Comparison of Limits of Detection[+] ($\mu g\ ml^{-1}$)

Element	Multielement Simplex	Previous Compromise
Tl	0.18	0.19
Zn	0.0015	0.002
Pb	0.045	0.055
Mn	0.0008	0.001
Fe	0.004	0.005
Mg	0.0015	0.002
Al	0.035	0.05
Ti	0.001	0.001
Sr	0.00009	0.0001
Ba	0.0004	0.001

+ Mean of 3 determinations.

An alternative to the multielement simplex could be the optimisation of the trace elements in a test solution and the subsequent use of these conditions for the full multielement analysis. Both Tl and Mn (the elements with the lowest LOD factor in Table 3.12) were individually simplex optimised and their predicted optima together with LOD's are shown in Table 3.15. These results are similar to those previously obtained with the multielement simplex and thus confirm its successful operation. The LOD's obtained for the individual optimisations suggest that this approach could be a viable alternative

to a full multielement optimisation. However, the time required for 2 individual optimisations (~3 hours) is only slightly shorter than the full 10 element optimisation which is inherently superior for multielement analysis.

Table 3.15

Individual Simplex Optimisations

Element	Injector Flow l min^{-1}	Power kW	Height mm	LOD $\mu g\ ml^{-1}$
Mn	0.86	0.65	11.5	0.0008
Tl	0.89	0.55	11.0	0.15

The results obtained from the individual simplex optimisations are very interesting as a result of the similarity in optimum conditions for a "soft" line with a difficulty of excitation of 4.5 eV (Tl I) and a "hard" line with a difficulty of excitation of 12.2 eV (Mn II). The maximum intensities of "hard" lines have been reported at higher positions in plasmas than "soft" lines (157,161). Spectral studies performed by Kawaguchi et al. (165) and Blades and Horlick (158) indicated the presence of 2 regions in the aerosol channel of an argon plasma. A lower, thermal region was identified where "soft" line behaviour was observed and a higher, non-thermal region where "hard" line behaviour was observed.

The results of all studies reported in this thesis have been based on the SBR which is of greater analytical value than maximum intensity. The relationship between maximum signal and maximum SBR is dependant on the plasma background and thus similar optimum regions may not be obtained. However, the argon plasma used in these studies is

unlikely to differ from the previously reported systems except in its more compact analytical region as a result of the larger bore injector tube.

Occasional difficulties were experienced in terminating the simplex optimisation experiments performed in these studies. These appeared to result from the gently sloping response surfaces which enabled similar performance to be obtained at different analytical conditions. These problems were investigated further by examining the response surfaces of a number of elements. The injector flow rate ($0.87\ l\ min^{-1}$) obtained for the multielement optimisation was used; the observation height was varied between 8 and 12 mm and the power varied between 0.4 and 0.9 kW. The response surfaces (using SBR) obtained for Mn and Tl are shown in Figure 3.16. These (and other) element maps confirmed the presence of gently sloping response surfaces, except below 0.5 kW where the response decreased quite rapidly. Ridges and plateaus could be identified which explained the similar performance obtainable at differing analytical conditions. Multiple optima were not detected during these experiments which agrees with the findings of numerous simplex optimisation experiments with this plasma system. Response surface mapping is not a viable alternative to simplex optimisation because of the number of parameters involved. However, the technique can be used to visualise a section of the response surface to assist the interpretation of results.

Figure 3.16

Response Surfaces (SBR) for Mn and Tl

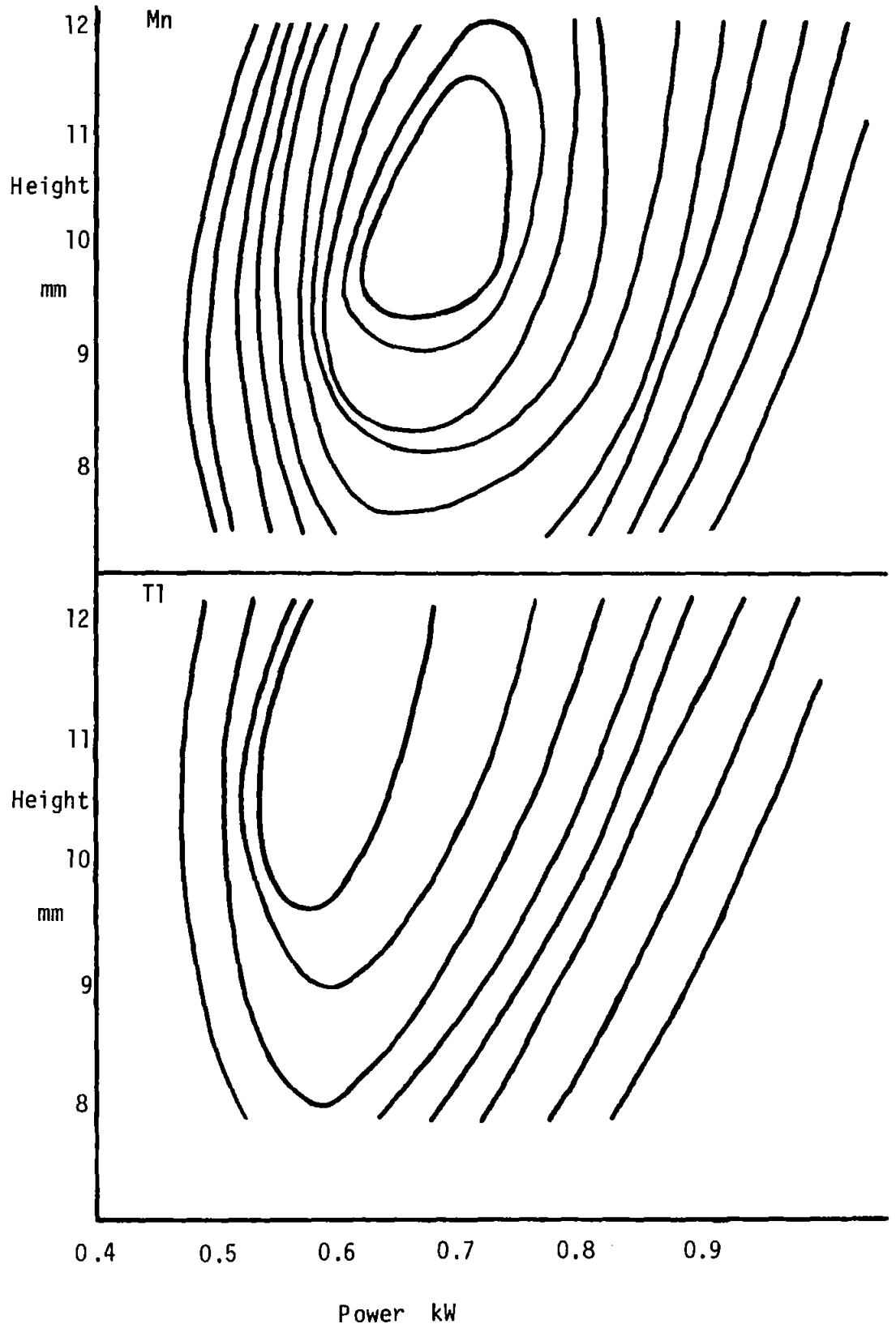

3.6 Simplex Optimisation for Interference Reduction

3.6.1 Introduction

Excluding spectral interferences, the effects of easily ionisable elements (EIE) on analyte emission are the major source of interferences in ICP-OES. A vast quantity of studies have been reported on the characterisation of this type of interference as a result of the ubiquitous nature of EIE's, especially Na and K, Blades and Horlick (93) described a literature survey of the effects of an excess of EIE's as "a study in confusion". This confusion has arisen because of apparent inconsistencies in reported data and the lack of understanding of the mechanisms of these interferences.

Fundamental characterisation of the ICP is inhibited by the spatial complexity of the plasma. The initial confusion of conflicting reports has been clarified to a great extent by spatial studies of analyte emission profiles (158,166) together with the effects of EIE's (93,167,126,168). Mass spectrometric studies (91) and spatial distributions of electron number densities (169,170,171,172) are providing further information on the high ion-atom emission intensity ratios (suprathermal ionisation)in argon ICP's. An eventual understanding of the fundamental ICP mechanisms will probably arise from a combination of these studies and the mathematical modelling of Boulos and Barnes (173) and Mills and Hieftje (174).

A number of different approaches have been reported for interference minimisation during multielement analysis. The use of ion or "hard" line conditions has been advocated for compromise analysis (161,160,157). The use of higher power has been reported for interference reduction (149,150,175) but observation heights and

injector flows were also changed from the optimum LOD conditions. Ebdon (162) has illustrated the critical dependance of EIE interference on observation height and to a lesser extent on injector flow.

The studies reported in this section are concerned with the application of a simplex optimisation technique to the minimisation of EIE interferences in an argon ICP.

3.6.2 Preliminary Studies

Initially, the interference effect of 0,5% Na was studied for a selection of elements using both the multielement simplex (LOD) conditions and the previous compromise conditions. To estimate the reproducibility of the interference effects, these determinations were performed on 5 separate days. The results are shown in Table 3,16.

The mean results obtained from these experiments appear acceptable as the worst interferences are of the order of 10% (in each case a depression). However, considerable variations exist from day to day which makes the prediction of interference effects quite difficult. The reproducibility of interference effects is significantly better for the compromise conditions than the LOD simplex conditions; only the Mg and Sr variations are not significantly different at the 5% confidence level. The reproducibility of the LOD simplex conditions may be poorer because of the lower observation height in a more turbulent region of the plasma.

Table 3.16

Interference Effects of 0.5% Na Over a 5 Day Period

Analytical Conditions	% Interference							
	Tl I	Zn I	Pb II	Mn II	Mg I	Al I	Ti II	Sr II
LOD Simplex	-4.2	-2.8	-2.5	-9.8	-8.5	-8.3	-4.1	-11.2
	-0.8	+1.9	+1.9	-5.6	-2.3	-3.7	-2.5	-6.0
	-11.6	-7.6	-9.0	-15.9	-15.8	-13.5	-13.5	-18.6
	-4.3	-3.6	-4.5	-11.1	-10.6	-8.7	-6.9	-12.5
	-6.7	-5.4	-6.5	-12.1	-10.2	-10.0	-8.3	-14.0
$\bar{x}$	-5.5	-3.5	-4.1	-10.9	-9.5	-8.8	-7.1	-12.5
RSD	0.727	1.011	1.009	0.343	0.511	0.400	0.600	0.365
Compromise	-3.1	-4.3	-1.8	-8.7	-7.4	-8.3	-5.7	-7.9
	-2.9	-4.3	-1.9	-7.5	-6.4	-8.2	-6.0	-7.3
	-4.4	-4.2	-1.9	-9.7	-12.1	-8.2	-7.4	-12.2
	-4.5	-5.2	-2.5	-7.5	-9.7	-7.4	-6.4	-10.5
	-4.2	-4.7	-1.5	-7.4	-6.7	-7.1	-5.2	-9.1
$\bar{x}$	-3.8	-4.5	-1.9	-8.2	-8.5	-7.8	-6.1	-9.4
RSD	0.200	0.092	0.191	0.124	0.285	0.071	0.136	0.211

Using the LOD simplex conditions, univariate searches of power, observation height and injector flow were performed to determine the variation in interferences for 0.5% Na. Figures 3.17 to 3.19 illustrate the results obtained for some elements using 10 second integrations. Increasing the power from 0.5 kW to 1.0 kW appears to decrease the interference effect and also reduce the variation between elements. An increase in observation height from 8 mm to 13 mm causes an increase in the interference effect from a mean of -2% to a mean of -19%. The variation between elements is reduced as the height of

Figure 3.17

Variation of Interference Effect (0.5% Na)

with Applied Power

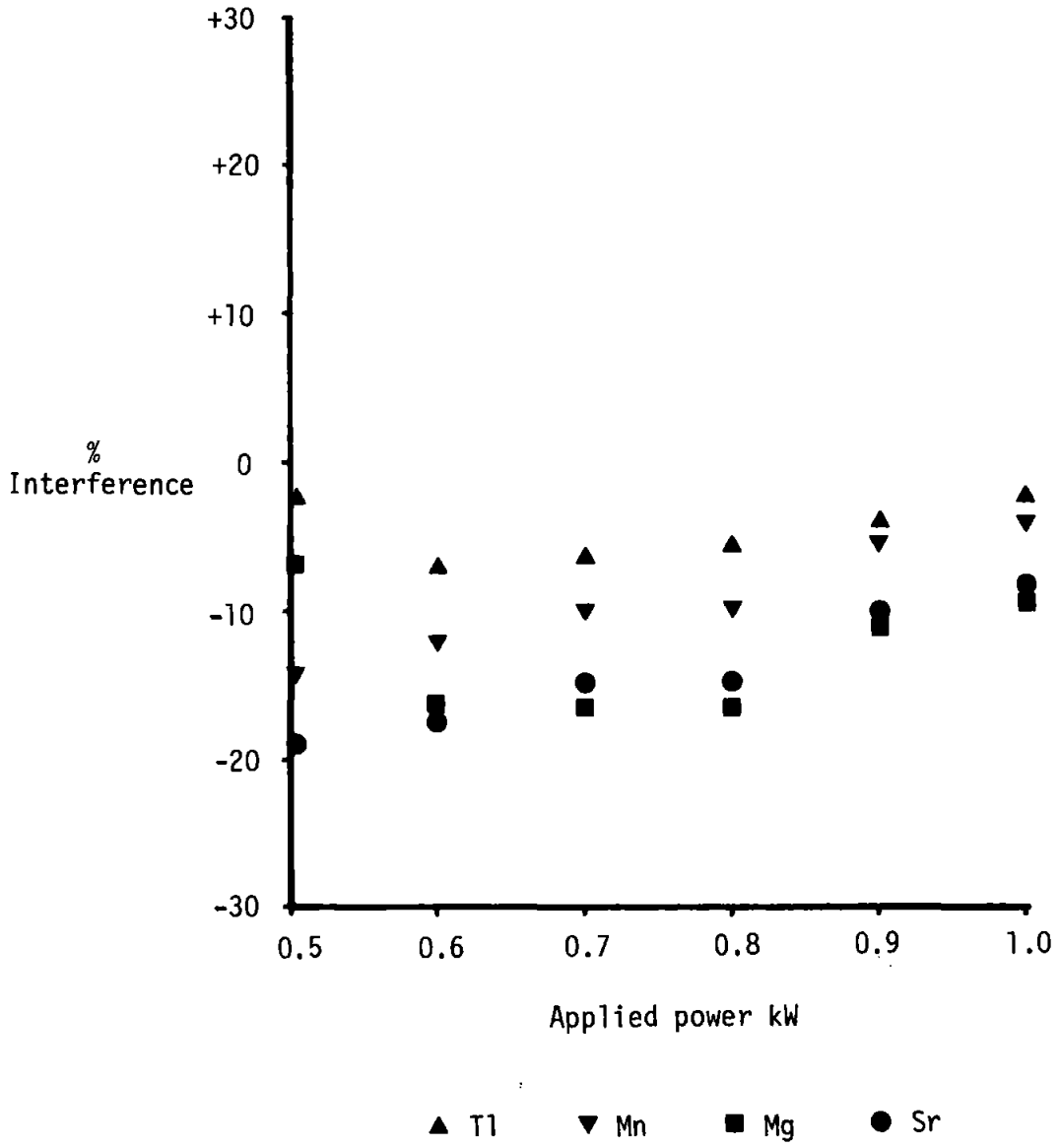

Figure 3.18

Variation of Interference Effect (0.5% Na) with Observation Height

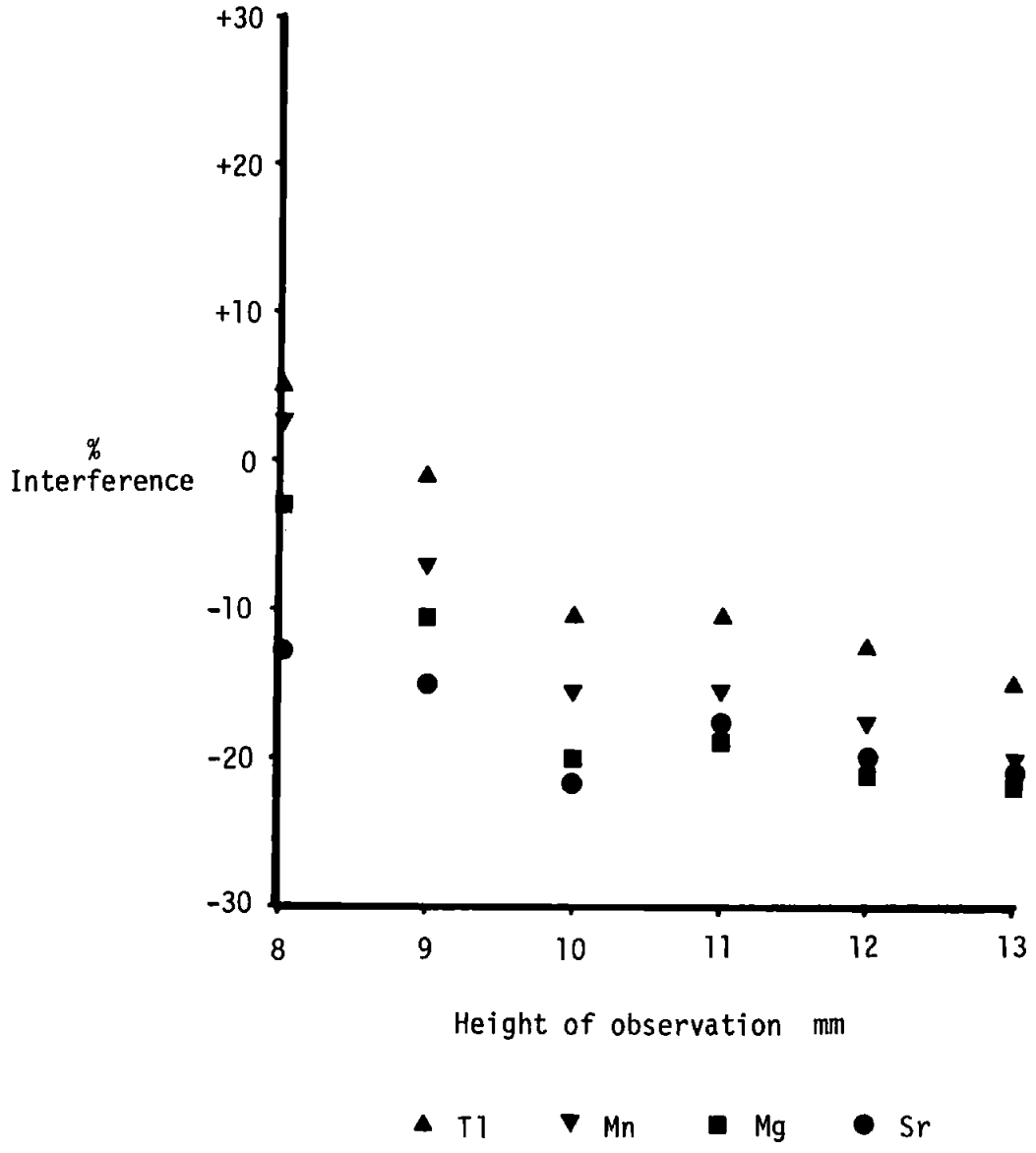

Figure 3.19

Variation of Interference Effect (0.5% Na) with Injector Gas Flow

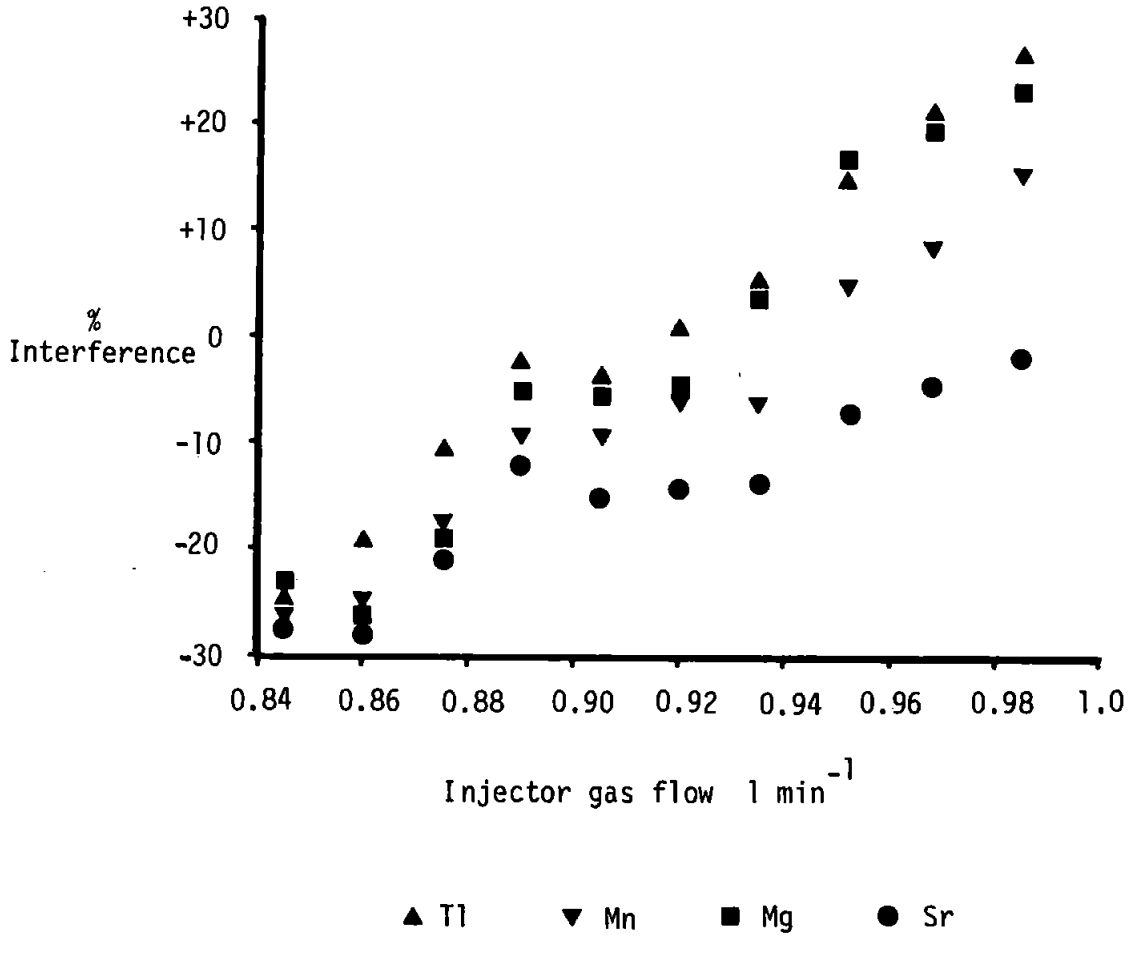

observation is increased. As previously mentioned, this may indicate a less turbulent region higher in the plasma. The variation in injector flow from 0.85 l min^{-1} to 0.99 l min^{-1} changes the mean interference effect from -25% to +16%, although with considerable variation for individual elements. The determination of these interference effects demonstrated considerably greater fluctuations than previously determined analytical signals, thus the data shown in Figures 3.17 to 3.19 should be interpreted as general trends.

The following general observations can be made from these experiments.

a. The interferences of EIE's are affected markedly by variation of injector flow and to a lesser extent by variation of observation height. These observations are in agreement with those of Ebdon (162). Using the nomenclature system proposed by Koirtyohann et al. (176), enhancement occurs in the lower region of the normal analytical zone (NAZ) and extends down into the initial radiation zone (IRZ). Suppression occurs in the NAZ and increases with an increase in height of observation. An interference free zone appears to exist between these 2 distinct regions. These observations have been reported by other workers (165,167,168,158, 177) and Blades and Horlick (93), in particular, have demonstrated the shift in this spatial crossover point as parameters are changed.

b. An increase in power reduces the observed suppressions. The IRZ moves lower as more energy is available to heat the incoming gas and as previously reported (156) this can be offset by a corresponding increase in injector flow. This provides additional confirmation of the interrelationship of parameters in the argon plasma and thus the importance of the simplex optimisation technique.

As demonstrated for the LOD optimisation, the choice of a suitable response function for interference minimisation is an important consideration. Because of the gently curving response surfaces illustrated earlier, it seemed appropriate to perform a complete optimisation based on the minimisation of the % interference of 0.5% Na. The individual element performances could then be compared with the data obtained from the LOD simplex optimisation.

3.6.3 Multielement Simplex Optimisation for Interference Minimisation

The response function used for this optimisation was as follows:

$$R = n \Big/ \sum_{i=1}^{n} (I)_i^2$$

where I is the % interference resulting from the presence of 0.5% Na in the test solution. The squared function was found to increase the sensitivity and selectivity of R. All solutions contained 5% nitric acid (by volume) and 10 second integrations were used. The optimisation for 4 elements required 2½ hours and Figure 3.20 illustrates the movement of the simplex. Log R has been plotted for the convenience of illustration, Table 3.17 shows the results obtained for the worst vertex - 2, and the best vertex - 18.

This Table illustrates the massive interferences which could be obtained during improper operation, and also illustrates the sensitivity of the response function. The simplex moved rapidly to a region of minimum interference but termination of the optimisation was difficult because of variations in the interference effects.

Figure 3.20

Variation of the Response Function for Interference Minimisation During the Simplex Optimisation

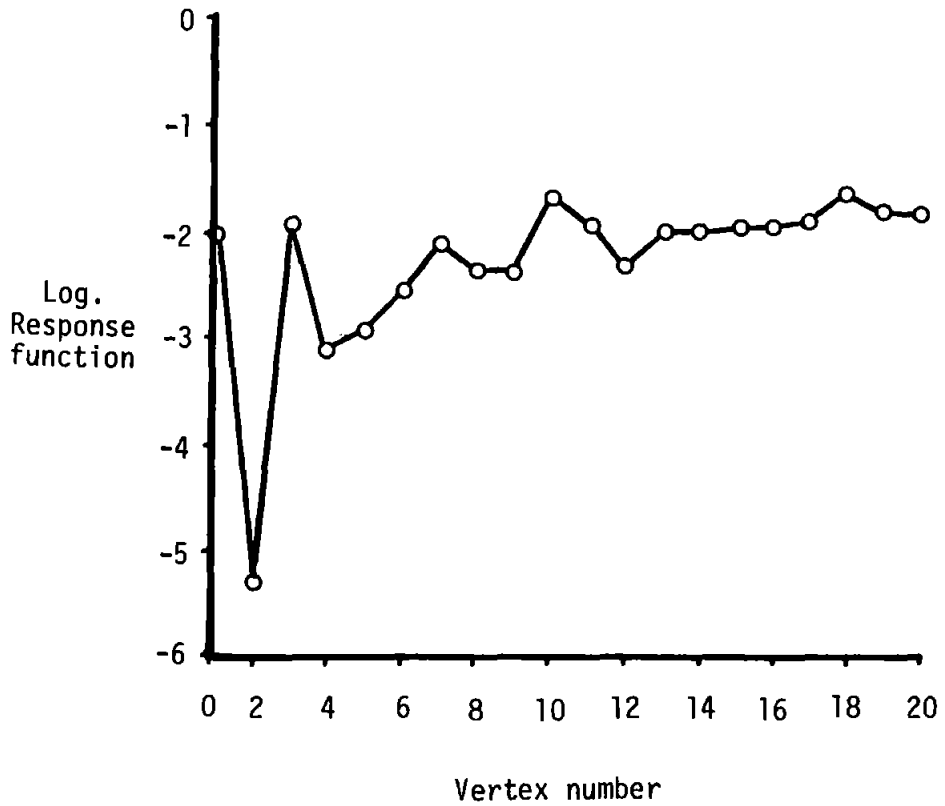

Table 3.17

Results Obtained for the Worst and Best Vertices

During the Interference Minimisation Simplex Optimisation

Vertex	Injector Flow $l\ min^{-1}$	Power kW	Height mm	% Interference Tl	Mn	Mg	Sr	R
Worst	1.27	0.6	12.0	+701	+272	+295	+482	0.000005
Best	0.88	0.75	8.0	+5.3	+5.1	-3.1	-6.7	0.037

The parameters used to obtain the optimum interference minimisation were as follows:

Injector flow 0.88 $l\ min^{-1}$, Power 0.75 kW and Observation height 8.0 mm. Compared to the LOD simplex conditions, the power had increased by 0.2 kW and the observation height decreased by 2 mm. Table 3.18 shows a comparison of the LOD's for both optimisations.

Table 3.18

Limits of Detection Obtained for Optimisations

Element	Optimum LOD $\mu g\ ml^{-1}$	Minimum Interference $\mu g\ ml^{-1}$
Tl	0.18	0.70
Zn	0.0015	0.003
Pb	0.045	0.08
Mn	0.0008	0.0015
Fe	0.004	0.007
Mg	0.0015	0.006
Al	0.035	0.10
Ti	0.001	0.003
Sr	0.00009	0.0003

As previously reported (93), an increase in power decreases the magnitude of the matrix effects. The lower observation region for the interference minimisation (IM) region obviously coincides with a spatial crossover point between enhancements and depressions. This null interference region has been reported by other workers (168,176, 177) and confirms the reality of interference free analysis with an argon ICP. However, the selection of analytical parameters is critical and without access to suitable instrumentation for spatial studies, simplex optimisation can rapidly and efficiently locate the interference free zone.

The LOD's obtained from the IM conditions are up to a factor of 4 worse than the optimised LOD conditions. The "soft" lines show a greater decrease than the "hard" lines which perhaps indicates the greater sensitivity of the "soft" lines to power and height changes. The poorer performance at the IM conditions would not be expected to cause problems during analysis for the majority of elements. Increased confidence in the accuracy of results would outweigh some loss of LOD performance.

Two major problems were encountered during these interference minimisation studies; a drift in injector gas flow-rate and, as previously mentioned, short term fluctuations. The injector gas flow changes could be recognised by the interferences becoming increasingly positive or negative during stability studies. Figure 3.19 indicates the importance of accurate flow control and together with subsequent experiments it was established that the injector flow stability should be $\pm$ 0.0025 l min^{-1} to ensure minimum drift. The Plasma Therm gas control system is totally inadequate for this accuracy and precision of flow control and it is probable that a mass flow controller would be required.

The short term fluctuations appeared to be associated with the observed "bounce" at the tip of the "sodium bullet". The range of this "bounce" was ~ 1.5 mm and illustrates the difficulty of location of the interference free zone. The results shown in Table 3.19 represent a series of determinations made at 10 minute intervals and indicate the magnitude of these variations. In addition, this experiment achieved the most accurate location of the interference free zone and indicated the performance which could routinely be obtained with accurate and precise flow control.

Table 3.19

Signal Fluctuations at the Interference Free Zone[+]

	% Interference[x]				R
	Tl	Mn	Mg	Sr	
	+2.7	+3.7	+3.0	+4.1	0,085
	+2.4	+4.9	+1.3	+0,1	0.127
	-0.3	+1.8	+1.1	0.0	0.881
	+3.1	-0.9	+0.2	+4.5	0,130
	-0.6	+4.5	+1.0	-1.4	0.170
	+1.9	+2.9	+2.0	+3.9	0,128
	-2.8	-3.6	-4.8	-3.3	0.073
$\bar{x}$	0.91	1.90	0.54	1.13	0.228
s	2.19	3.11	2.51	3.06	0.290
RSD	2.41	1.64	4.65	2.71	1.272
Range	-2.8 to +3.1	-3.6 to +4.9	-4.8 to +3.0	-3.3 to +4.5	0.073 to 0.881

+ Determinations at 10 minute intervals.

x 0.5% Na

Examination of the data from the test solutions confirmed the greatest signal instability was obtained from the solutions containing the EIE. It was considered that these fluctuations could arise from the spray chamber drain, peristaltic pump pulsations or pressure pulses from the nebuliser.

A new glass wool plug was fitted in the spray chamber outlet but this did not increase the signal stability, neither did the incorporation of a wetting agent into the solutions. The frequency of droplets draining into the waste tube was $\sim 30\ min^{-1}$ and was obviously not the cause of the high frequency pulsations visible at the tip of the "sodium bullet".

The Perkin Elmer nebuliser would not operate satisfactorily without a pumped solution supply, therefore it seemed appropriate to use an alternative nebuliser which could be operated in either a pumped or free running mode. The previously used Meinhard nebuliser was fitted to the Perkin Elmer spray chamber and simplex optimised for the best Mn LOD. The optimised conditions are shown in Table 3.20 and compared with the data obtained for the Perkin Elmer crossflow nebuliser.

Table 3.20

Simplex Optimisations for Mn with Alternative Nebulisers

Nebuliser	Injector Flow $l\ min^{-1}$	Power kW	Observation Height mm
Meinhard	0.85	0.60	11.0
Perkin Elmer	0.86	0.65	11.5

The similarity of these optimum conditions suggests that a nebuliser change does not affect the overall optimisation. The injector flow is

obviously a critical factor as the Meinhard and Perkin Elmer nebulisers were operated at 27 psi and 16 psi respectively.

The Meinhard nebuliser was operated at the IM conditions determined for the Perkin Elmer nebuliser and the stabilities for pumped and free uptakes determined. The mean results are shown in Table 3.21.

Table 3.21

Variations in Interference Signals[+] for the Meinhard Nebuliser with both Free and Pumped Solution Uptake

Operation	% Interference Tl	Mn	Mg	Sr	R
Free uptake[x]					
$\bar{x}$	5.24	8.76	1.70	0.16	0,051
s	3.27	5.20	2,53	2.46	0,036
RSD	0.62	0.59	1.49	15.38	0,708
Pumped uptake[x]					
$\bar{x}$	8.73	10.49	4.43	1.56	0,021
s	3.33	1.27	1.44	2.49	0.009
RSD	0.38	0.12	0.33	0.63	0.428

+ Mean of 7 determinations at 10 minute intervals.

x Solution uptake 1.5 ml min^{-1}, 0.5% Na.

The free uptake results for the Meinhard nebuliser are very similar to typical results obtained with the Perkin Elmer nebuliser. However, the pumped uptake results for the Meinhard nebuliser show significantly less variation. These results indicate the fluctuations

in interference signals to be derived from the nebuliser and not the pump.

Myers and Tracy (178) used varying lengths of plastic tubing to filter the aerosol between the spray chamber and the ICP torch. They reported a reduction in emission noise because of a reduction in larger droplets entering the plasma and improved aerosol mixing, they also suggested a reduction in pressure fluctuations. Rybarczyk et al. (126) used a similar system but did not determine whether the stability improvement resulted from large droplet removal or less turbulent gas delivery to the plasma. However, they did report their plasma to have no visible flicker in the IRZ region. Belchamber and Horlick (179,180) related fluctuations in the analyte emission signal to pressure fluctuations in the nebuliser. They designed a sand-trap soak-away drainage system to improve analytical precision.

It seems reasonable to infer from these studies, that nebuliser derived pressure fluctuations are the major cause of the "bounce" observed at the tip of the "sodium bullet" and hence the instability of EIE interferences. Location and stability of the interference free zone are obviously critical, and a nebuliser which performs well for aqueous analysis may not be appropriate for stable, interference free determinations.

3.7 Conclusions

An ICP torch fitted with a wide bore injector tube has been shown to be most appropriate for multielement analysis because of the compact NAZ. Using a suitable objective function, a 10 element 3 parameter multielement optimisation was performed with this system. The multielement conditions were reproducible and demonstrated small but

consistent improvements in LOD's compared to previous data.

The effects of EIE interferences were investigated and the injector flow shown to be the critical parameter for the location of an interference free zone. However, the power and observation height are also relevant parameters for interference minimisation as a result of the spatial complexity of the ICP. A response function based on % interference was used to simplex optimise 4 elements for the minimisation of interference effects from 0.5% Na. An interference free zone was rapidly located which exhibited only a small degradation in the LOD performance when compared to the optimum values. Thus, the argon plasma used in these studies was shown to be ideal for multielement analysis because of its good LOD performance when operated using interference minimisation conditions.

Two problems were identified during the interference minimisation studies. Drifting of the interference free zone was shown to result from inadequate control of the injector gas flow. High frequency fluctuations of the interference free zone appeared to arise from pressure fluctuations in the nebulisation process. The choice of suitable nebuliser and gas flow control is thus more critical for stable minimisation of interferences than for optimum LOD performance.

4 FORENSIC SAMPLE INTRODUCTION STUDIES

4.1 Introduction

Sample introduction is generally recognised as the "weak link" in ICP-OES. While it can be argued that there has been a shortage of fundamental studies, a wide variety of practical techniques have been reported for sample introduction and significant advances have been made. The major sample introduction techniques are illustrated in Figure 4.1, both well established and experimental techniques are included.

Pneumatic nebulisation is the commonest technique and used for most samples because it offers stability, simplicity and cheapness. In addition, the sample presented for analysis is in the form of a homogeneous solution. However, the poor efficiency of these nebulisers (typically 1-2%[181]) can be a major disadvantage if the analysis of very small samples is contemplated. Results reported later (Chapter 5) demonstrate the capability of this technique for quantitative, multielement analyses of ~100µg samples dissolved in 1 ml of solution. The aim of this section was to investigate the introduction of small samples. This has been achieved by discrete nebulisation for the simultaneous, multielement analysis (via the polychromator) of samples weighing less than 100µg. In addition, a recirculating nebuliser has been evaluated for the sequential, multielement analysis (via the monochromator) of 1 ml solution samples.

Figure 4.1

Sample Introduction Techniques for ICP-OES

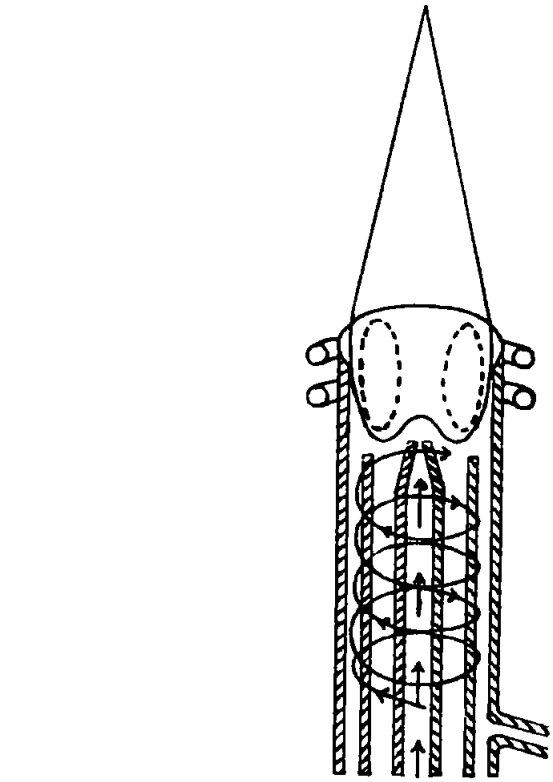

Solid	Liquid	Gaseous
Slurries	Pneumatic nebulisation	Hydrides
Laser ablation	Ultrasonic nebulisation	Volatile chelates
Arc/spark	Electrothermal vapourisation	Mercury vapour
	Graphite probe	

4.2 Discrete Nebulisation

4.2.1 Introduction

The nebulisation of small solution droplets (termed 'discrete nebulisation') has been utilised very successfully with atomic absorption spectrometry (AAS). This method has normally been used either to avoid nebuliser/burner clogging when analysing solutions containing a high concentration of dissolved solids or for multielement analyses on small solution volumes. Reported applications have included the analysis of biological materials (182), plant tissue digests (183), sediments (184), waters (185), steels (186) and glass fragments for forensic science purposes (187).

The feasibility of the direct analysis of solution microsamples using a high power ICP was demonstrated in 1972 for oil, organic compounds and blood (188). This technique was extended to the determination of trace elements in whole blood and serum (189). Little work has been reported with low power ICP's because of the problems of air entrainment between samples causing plasma instability. Broekaert and Leis (190) overcame this by using argon flushed microsampling cups for the analysis of waste water microsamples and subsequently for the analysis of biological solutions (191). More recently, a simpler system has been reported using teflon (PTFE) sampling cups and rapid manual transfer of the nebuliser tube between sample droplets and wash solutions (192).

In this section a discrete nebulisation technique has been studied for the analysis of alloy fragments, weighing <100 ug, which may be encountered in casework.

4.2.2 Experimental

4.2.2.1 Instrumentation and Operating Conditions

The polychromator was used for all analyses. The corrosion resistant sample introduction system was installed and operational parameters were as follows: power 1 kW, height 18.0 mm, injector argon flow 1.1 l min^{-1}, plasma argon flow 18.0 l min^{-1} and nil auxiliary argon flow. A peristaltic pump (Buchler Instruments, NJ, U.S.A.) supplied solution to the nebuliser at a rate of 1.2 ml min^{-1}.

Air entrainment was found to extinguish the plasma when the lower power, simplex optimised conditions were employed. Thus, for this work, the higher power was essential and a slight sacrifice in performance was acceptable (see Chapter 3).

4.2.2.2 Discrete Nebulisation

The only modification made to the system used for continuous introduction of solution was the fitting of a narrow bore platinum - iridium tube in the end of the nebuliser tube. This facilitated its accurate positioning in the solution droplets.

Solution droplets (100 μl) were aspirated from thin PTFE tape stretched over a perspex block (Figure 4.2). The smooth PTFE surface ensured minimum contact of the solution droplets and allowed complete aspiration to be readily observed. Pre-integration and integration times (10s and 5s, respectively) were selected to give the best signal to background ratio and were used for all analyses.

Figure 4.2

The Discrete Nebulisation Technique

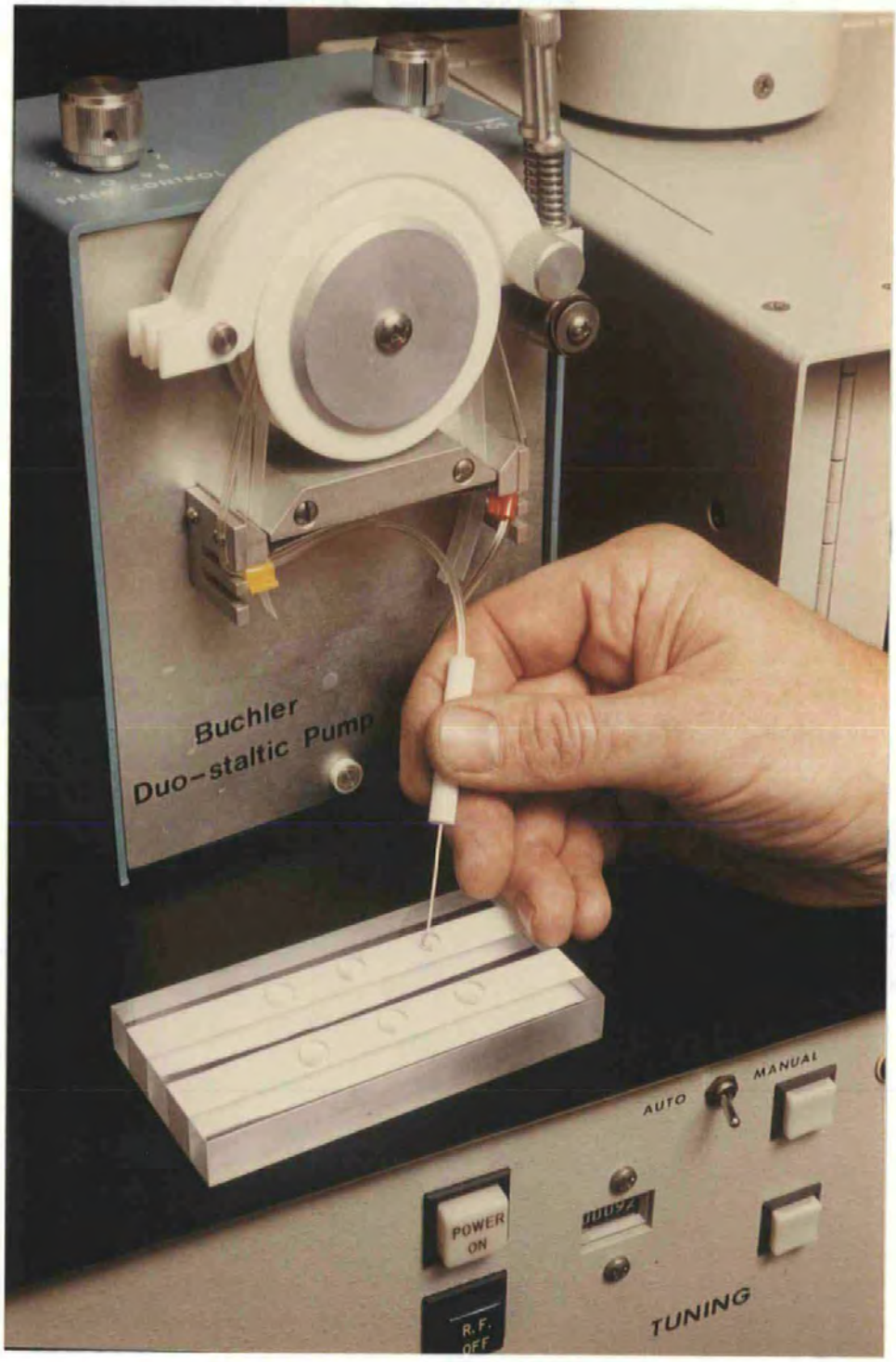

4.2.2.3 Sample and Standards Preparation

Time consuming weighing of samples was minimised and weighing errors associated with small samples were eliminated by the use of a concentration ratio technique that required the acquisition of only relative not absolute solution concentrations (193). Concentration ratios of all elements to the major constituent were determined from intensity ratios. The concentration of the major constituent could then be determined and hence the individual element concentrations. For this calculation to be valid it is necessary to measure the concentration of all major and minor elements present and to ensure that all determinations are carried out within the linear calibration range of the instrument. Provided sufficient element coverage is available from the detection system then prior knowledge of the sample type or elemental composition is not required.

Metal particles were degreased with 1,1,2-trichloro-1,2,2-trifluoroethane and were placed in pre-cleaned 1.5 ml polypropylene centrifuge tubes (Hughes and Hughes Ltd, Romford, Essex). Acid cleaning was inappropriate because of the danger of selective dissolution of the major constituents. Nitric acid (120 μl,25% by volume) was added to each tube and the samples allowed to stand until dissolution was complete.

Multielement standards were prepared from 1000 $\mu g\ ml^{-1}$ stock solutions (BDH Chemicals Ltd., Poole, Dorset) in the same acid concentration as the samples.

4.2.2.4 Cutting Experiments

A small hacksaw (Eclipse Junior, 6 inch blade, 32 teeth per inch) was used for cutting experiments on a previously analysed brass rod (0.25 inch diameter, 60/40 brass). Four new, cleaned blades were used to cut through the rod and the fragments generated in each case were retained. Particles adhering to 3 of the blades were removed with a stainless steel needle. Before the remaining blade was examined for brass particles it was used to cut through a mild steel rod (0.25 inch diameter).

In a second experiment, turnings from a standard brass (BCS 385; Bureau of Analysed Samples Ltd, Middlesborough, UK) were divided with a clean scalpel blade to provide a range of fragment sizes for analysis.

In a third experiment to simulate a possible casework situation, a clean, fine needle file was used to score the surface of a standard copper-nickel alloy (BCS 180/2). The file was examined under a low power binocular microscope and a collection of small alloy fragments removed for analysis.

4.2.3 Results and Discussion

4.2.3.1 Discrete Nebulisation

Detection limits obtained for the discrete nebulisation technique were up to a factor of 3 poorer than those previously obtained for continuous solution introduction. Data obtained for the 6 elements used in this study are shown in Table 4.1. The poorer performance resulted from a combination of a slightly higher and

noisier plasma background and a reduction in signal intensity. However, the discrete nebulisation technique gave better detection limits ($\mu g\ g^{-1}$) from small solid samples because of reduced dilution effects. In addition, sample throughput was quicker as a result of the reduction in wash time between samples.

Table 4.1

Analytical Wavelengths and Detection Limits for Discrete Nebulisation

Element	Wavelength nm	Detection Limit $\mu g\ ml^{-1}$
Zn	213.8	0.006
Pb	220.3	0.080
Ni	231.6	0.017
Mn	257.6	0.001
Fe	259.9	0.011
Cu	324.7	0.003

4.2.3.2 Fragment Generation and Analysis

The average total weight of brass fragments removed from each of the 3 hacksaw blades used to cut the brass rod was found to be 3 mg. Some of these were quite firmly fixed between the teeth of the blades because of the ductility of the brass. The fragment weights varied from 0.2 μg to 200 μg with most between 5 μg and 50 μg. The remaining blade, which had subsequently cut a mild steel rod, was found to be free of brass fragments: presumably it had been effectively scoured by cutting the harder metal.

Brass fragments of varying weights, obtained from these experiments, were analysed by discrete nebulisation and the results are shown in Table 4.2 together with that obtained for the 105 μg fragment analysed by continuous solution introduction. It can be seen that the copper and zinc results are consistent for fragments weighing from 8.5 μg to 105 μg suggesting that no problems arise from inhomogeneity of the alloy. However, the result obtained for the 0.5 μg fragment is significantly different and indicates that samples of this size are not representative of the bulk material.

Table 4.2

Analysis of Fragments from 60/40 Brass

Fragment Weight μg	Element % Cu	Zn
0.5	54.5	45.5
8.5	60.9	39.1
14.5	60.6	39.4
31.0	60.6	39.4
105*	60.9	39.1

* Analysed by continuous introduction

Analyses were carried out on a range of fragments taken from the standard brass (BCS 385). This material was chosen as representative of a leaded duplex brass; lead is added to improve the machining properties and is present as isolated globules in the alloy. The results of these determinations are shown in Table 4.3. Although the data for the major constituents are, as before, consistent down to the smaller fragments, the lead values generally increase as fragment size

decreases. Lead acts as a solid lubricant in these alloys and spreads over the surface during machining. The increasing lead value is believed to result from the relative increase in surface area of fragments as their volume decreases. This reaffirms the need for careful interpretation of analytical data from small fragments of a non-homogeneous alloy.

Table 4.3

Analysis of Brass Standard (BCS 385)

Fragment Weight µg	Element % Cu	Zn	Pb
10	55.7	41.0	2.85
15	58.5	38.3	2.70
20	58.9	38.6	2.40
50	58.3	38.6	2.63
70	58.6	38.5	2.43
Certified Values	58.7	38.5	2.24

Analytical data from 8 fragments of the standard copper - nickel alloy (BCS 180/2) are shown in Table 4.4 together with the certified values. This material is a coinage alloy of known fine grain structure. The data for the major constituents are good, a mean sample weight of 2.7 µg was used and a range of 0.6 - 7.2 µg. The high Fe value probably arises from contamination by the file; 15 ng of Fe on the mean fragment weight would be sufficient to cause this elevated result.

Table 4.4

Analysis of Copper - Nickel Standard (BCS 180/2)*

Element	Wavelength nm	Certified %	ICP %	Standard Deviation	Relative Standard Deviation %
Cu	324.7	68.12	68.7	1.99	2.9
Ni	231.6	30.35	29.1	1.57	5.4
Fe	259.9	0.68	1.26	0.35	27.8
Mn	257.6	0.75	0.94	0.19	20.2

* n = 8, mean sample weight 2.7 μg, range 0.6 - 7.2 μg.

4.2.4 Conclusions

A discrete nebulisation technique has been developed for the multielement analysis of 100 μl solution droplets by ICP-OES. The performance of the technique is only slightly degraded when compared to continuous solution introduction. The advantages of this technique are the increased speed of analysis, the ability to analyse small solution volumes and, hence, the reduction of dilution factors when analysis is required on small solid samples. A logical extension to this work would be the incorporation of flow injection analysis (FIA) (194) as reported for ICP-OES by Greenfield (195). This would allow the rapid, automated analysis of small sample volumes with the added advantages of automatic dilution and calibration.

In a simulated case involving cutting a brass rod with a hacksaw, a relatively large number of fragments were found to be adhering to new, fine cut blades. Some of these would be expected to have long persistence times because of the firmness of their attachment. However, when one of these subsequently cut a mild steel rod, all

evidence of the previous brass cuts was removed.

The results obtained from the materials examined here indicate the caution required in the interpretation of analytical data from small alloy fragments. It is unlikely that the analysis of fragments of non-homogeneous alloys weighing less than 100 μg will provide relevant comparative data for forensic scientists. Analytical data from fragments of homogeneous alloys weighing less than 10 μg require careful interpretation as a result of the effects of sample contamination.

4.3 Recirculating Nebuliser

4.3.1 Introduction

The poor efficiency of pneumatic nebulisation has previously been considered. This can present an acute problem if a sequential, multielement analysis is required and only a minimum volume of sample solution is available. This situation commonly occurs with forensic samples and the ability to renebulise solution which would normally drain to waste would be a considerable advantage.

Recirculating nebulisers are uncommon in the ICP-OES literature. Novak et al.(196) described the construction and characteristics of a glass cross-flow recirculating nebuliser. Hulmston (197) reported a recirculating nebuliser system which utilised a Meinhard concentric nebuliser (J.E. Meinhard Associates Inc., Santa Ana, California, USA) and allowed stable aerosol production for at least 10 minutes from 1 ml of solution. He and Barnes (198) reported a modified version of this nebuliser which is now commercially available (J.E. Meinhard Associates Inc.). Hulmston (199) has

subsequently reported a microprocessor controlled system for his nebuliser which offers the opportunity for automatic sample analysis. A modified GMK nebuliser (200) has been applied to studies of solvent evaporation and aerosol ionic redistribution during the evaluation of this nebuliser.

Compressed air nebulisers have been used for many years for inhalation toxicological studies where recirculating systems generate monodisperse aerosols for long periods of time. A variety of nebulisers have been developed and these have been reviewed (201) together with other techniques for aerosol generation and characterisation. A system originally developed by Laskin has been reported (202), this is basically a cross-flow nebuliser operating inside its own spray chamber. This nebuliser was operated at between 6 l min^{-1} and 23 l min^{-1} of air and generated aerosols with a volume mean diameter (VMD) of 1.5 μm - 8.5 μm depending on conditions. A more compact version of this nebuliser was later reported (203) for the generation of aerosols from 20 ml volumes of radioactively tagged, polystyrene suspensions.

The objective of this work was to construct a smaller version of this nebuliser to analyse solution volumes of 1 ml. Further requirements were that the construction should be simple and resistant to hydrofluoric acid.

4.3.2 Experiments with the Initial Modified Laskin Nebuliser

4.3.2.1 Nebuliser Construction and Preliminary Experiments

The operating principle of this nebuliser is shown in Figure 4.3. Solution is drawn up through the capillary tube and a fine spray produced by the jet of gas at right angles to the tube tip.

Figure 4.3

Operating Principle of the Laskin Nebuliser

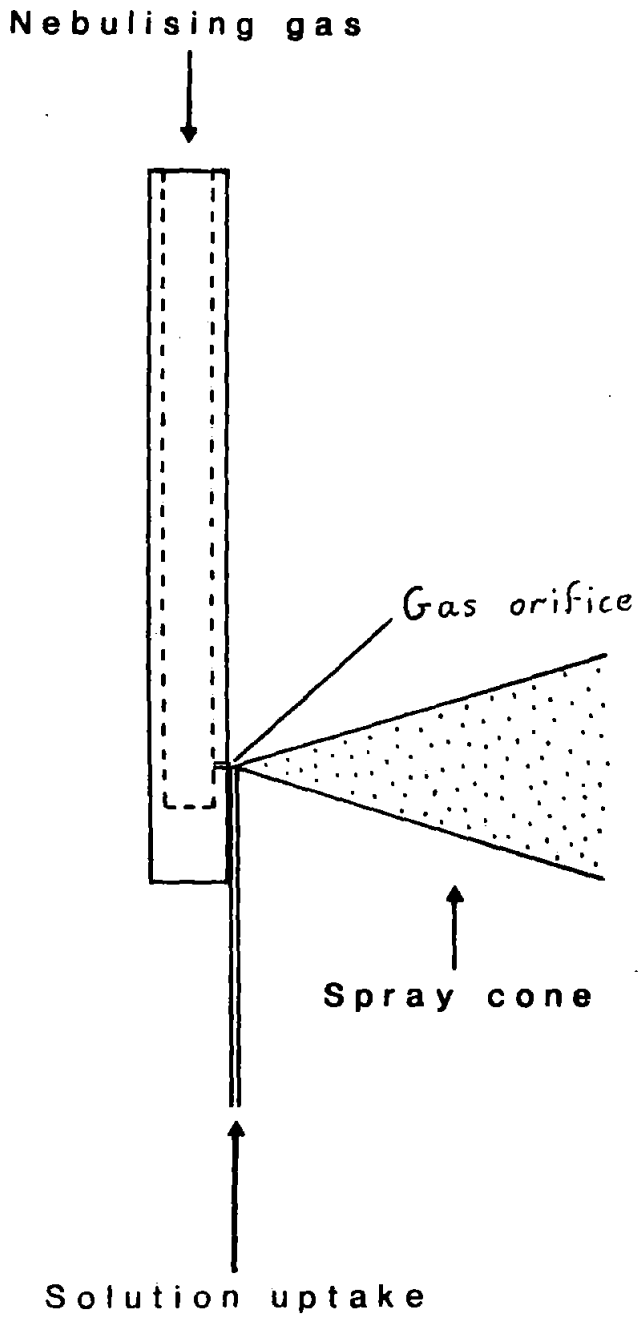

The spray cone strikes the wall of the nebuliser and the larger solution droplets coalesce and run down to the solution reservoir. Fine aerosol droplets are deflected from the wall and are carried out of the nebuliser in the gas stream.

A prototype nebuliser was constructed from a 50 ml polythene bottle with a nebuliser tube (for gas introduction) of perspex. Sample solutions (1 ml) were presented to the nebuliser in 1.5 ml polypropylene centrifuge tubes (Hughes and Hughes Ltd, Romford, UK). This prototype was used to investigate the feasibility of nebulising small solution volumes with this system.

Following preliminary experiments, a PTFE nebuliser - spray chamber was designed which used a Pt - Ir tube for solution uptake. A number of different configurations of nebuliser tube were investigated and the final version is shown in Figure 4.4. The spray chamber and nebuliser tube were produced in a PTFE workshop, the gas orifice and solution uptake tube were drilled and fitted at the CRE.

4.3.3 Results and Discussion

The prototype nebuliser was not particularly robust or stable but was shown to be successful as a recirculating system for 1 ml solution volumes. This was considered reasonable for a prototype and justified further work with the PTFE version.

Aerosol production and transfer, nebulisation time and signal stability for 1 ml of solution, and detection limits were the major factors considered during the evaluation of the PTFE system. The initial PTFE nebuliser was produced with a 0.35 mm diameter gas orifice and alignment of the solution uptake tube was found to be critical for aerosol production. Optimum aerosol production (by visual inspection)

Figure 4.4

The PTFE Laskin Nebuliser

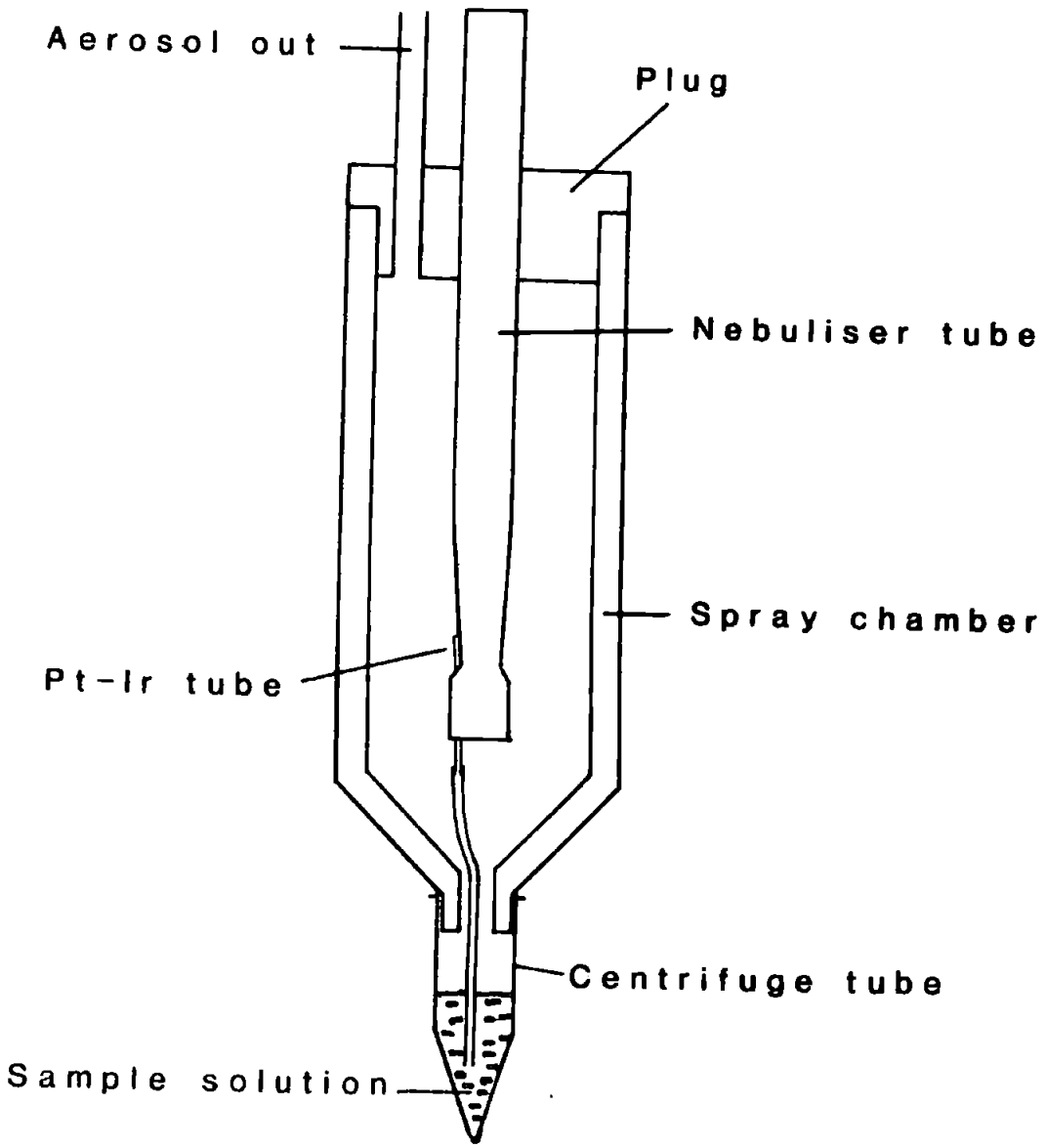

was obtained when the tip of the solution uptake tube half covered the gas orifice. However, small positional changes made large differences to the operating pressure and solution uptake.

Maximum sensitivity, i.e. solute transfer, was obtained when the spray cone struck the chamber wall directly below the aerosol outlet. Rotation of the nebuliser tube through 90^{o} and 135^{o} reduced the signal to 70% and 55% respectively. Sample aerosol was carried to the plasma via a 0.75 m long, 4 mm ID PTFE transfer tube.

Analytical studies were performed with a power of 1 kW and an observation height of 18 mm, the injector flow was optimised for Mn signal to background ratio. Using these conditions the solution uptake of the nebuliser was 2.5 ml min^{-1}. The entrainment of small amounts of air during sample tube changes precluded the use of the lower power, simplex optimised conditions (Chapter 3) as the plasma could easily be extinguished. Limits of detection were determined for a number of elements and were, on average, a factor of 5 poorer than those obtained for the simplex optimised conventional sample introduction system (Section 3.5.3).

During the course of these experiments it was observed that the analytical signals increased with increasing nebulisation time. Typical increases for 3 elements are shown in Figure 4.5. After 16 minutes nebulisation the mean signal increase for 6 elements was 38.5%, the relative standard deviation of this figure was 0.038. This agreed well with the actual concentration increase of the elements in the residual solution, determined as 37.5% by conventional analysis. This work indicated that solvent evaporation was a major factor in restricting the use of the nebuliser for routine analysis.

Experiments were performed using humidified argon as the nebuliser gas in an attempt to reduce or eliminate the evaporation

Figure 4.5

Intensity Variations with Time for the Initial Modified Laskin Nebuliser

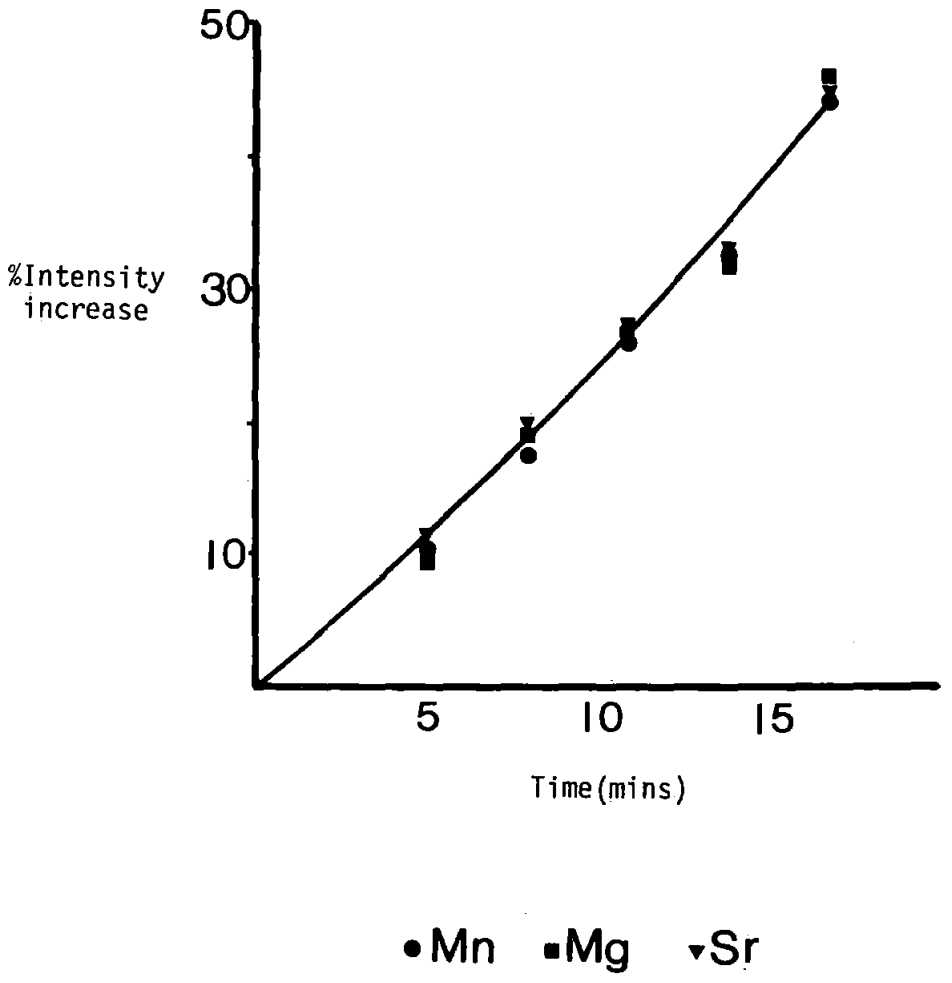

effects. Preliminary experiments with a commercial humidifier demonstrated a large dilution of the sample solution as a result of carry-over of water droplets in the gas stream. A humidifier was constructed in the laboratory and 2 stage filtration was incorporated to remove water droplets >1 μm in diameter. Intensity data obtained for 3 elements during an analytical run with humidified argon are shown in Table 4.5. These appear excellent for the 17 minutes nebulisation but when the actual element concentrations were determined in the residual solution they were found to be elevated by ~15%. The results obtained in Table 4.5 are therefore probably slightly fortuitous as a result of a small change in nebuliser characteristics. However, this work has indicated that humidified argon can lead to a large reduction in the solvent evaporation during the operation of this recirculating nebuliser.

Table 4.5

Signal Stability with Humidified Argon

Time (mins)		Intensities Sr	Mn	Mg
2		10542	10749	4282
5		10453	10692	4311
8		10418	10666	4323
11		10656	10889	4442
14		10608	10868	4439
17		10347	10727	4388
	$\bar{x}$	10504	10765	4364
	S	118.33	92.54	68.55
	RSD	1.12%	0.86%	1.57%

A modified Laskin nebuliser has thus been shown to be suitable for use as a recirculating nebuliser for ICP-OES. Solvent evaporation appears to be a major problem with this system, this has not been reported by other users of recirculating nebulisers (199,200). As evaporation of solvent will occur from the aerosol droplets being transported to the plasma, even at saturation humidity (204), the major cause of this problem could thus be from water evaporation from the liquid film on the spray chamber surface (205). Inspection of the spray chamber and transfer tube following 15 minutes operation revealed a large quantity of droplets adhering to the walls, thus providing additional evidence for the suggested origin of solvent evaporation.

An improved version of this nebuliser was thus constructed with particular attention paid to the reduction of solution uptake and the production of a finer aerosol.

4.3.4 Experiments with the Improved Modified Laskin Nebuliser

4.3.4.1 The Operational Nebuliser

An identical spray chamber-nebuliser tube configuration was employed but a 0.28 mm diameter gas orifice was drilled in the nebuliser tube. This nebuliser was operated at 70 psi (1.1 l min^{-1}) and the solution uptake tubing was selected to allow an uptake of 1.5 ml min^{-1}. In addition, a Y tube was fitted to the spray chamber outlet, one arm of which was fitted with a PTFE plug and the other arm connected to the aerosol transfer tube. A photograph of this nebuliser is shown in Figure 4.6.

Figure 4.6

The Improved Modified Laskin Recirculating Nebuliser

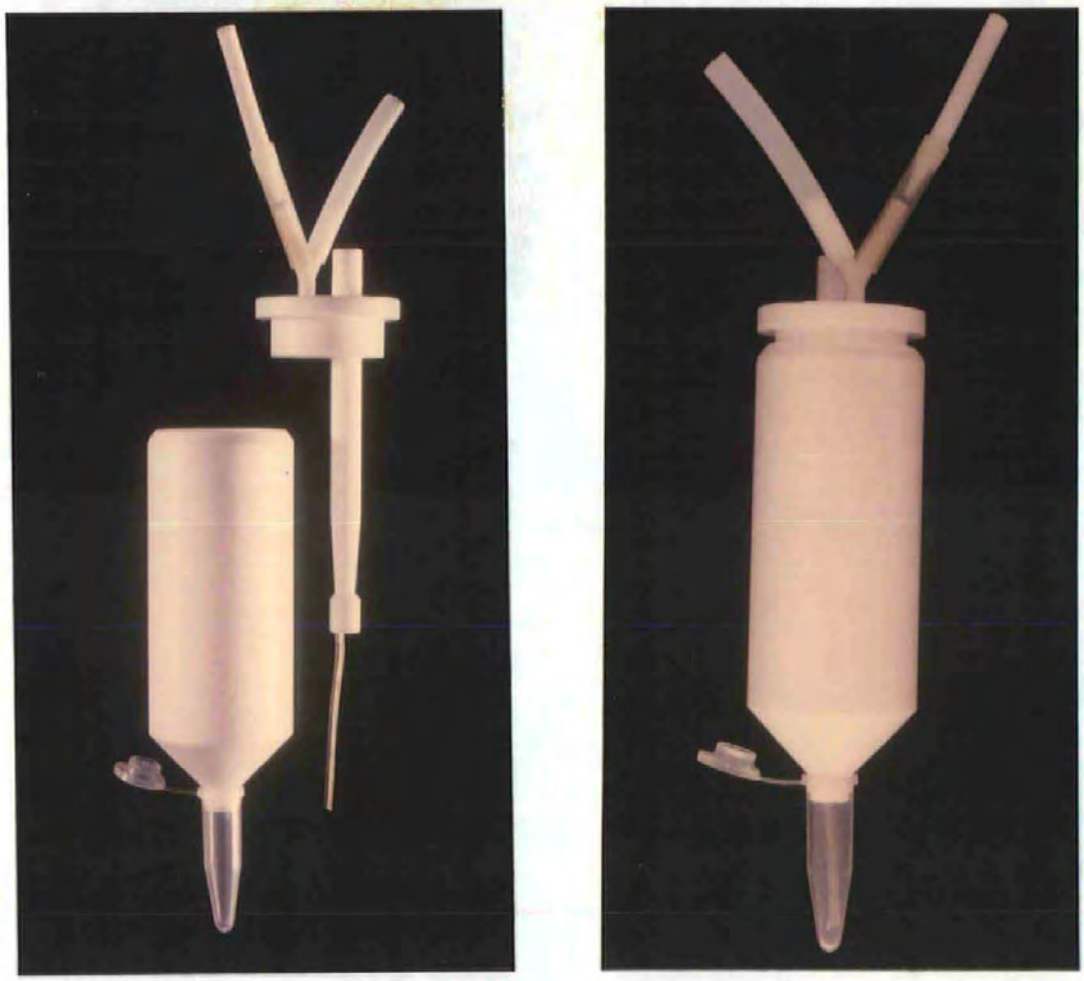

4.3.5 Results and Discussion

Signal stability and the time of useful nebulisation was initially investigated with a test solution containing 3 elements. The results from 3 separate experiments are shown in Figure 4.7, for illustration purposes the initial element intensities have been set at unity and subsequent results related to this. These experiments were started after a 1 minute stabilisation time and the background subtracted signals show an initial decrease, a stabilisation at 10 minutes followed by increasing signals for some elements after 15 minutes. After 20 minutes nebulisation, analysis of the remaining solution gave a mean relative intensity of 1.03 ± 0.05 (1s) for the 3 elements.

The solvent evaporation problem appears to have been overcome and stable nebulisation of 1 ml of solution can be obtained for at least 15 minutes. Examination of the inside of the spray chamber after 20 minutes nebulisation revealed only a small quantity of spray droplets. Thus, the reduced solution uptake and finer aerosol leads to less coarse droplet deposition inside the spray chamber, and, as a result of this the evaporation of solvent is much reduced.

Limits of detection were estimated for 10 elements and were, on average, a factor of 6 poorer than those obtained with the simplex optimised, corrosion resistant sample introduction system (Chapter 3). This data is shown in Table 4.8.

The precision of background measurements was better for the Laskin nebuliser than the Perkin Elmer system but the signal to background ratios were, on average, poorer by a factor of 9. This indicates a finer droplet size aerosol and reduced solute transfer to the ICP when the Laskin nebuliser is in use.

Figure 4.7

Stability of Element Signals with Increasing Nebulisation Time

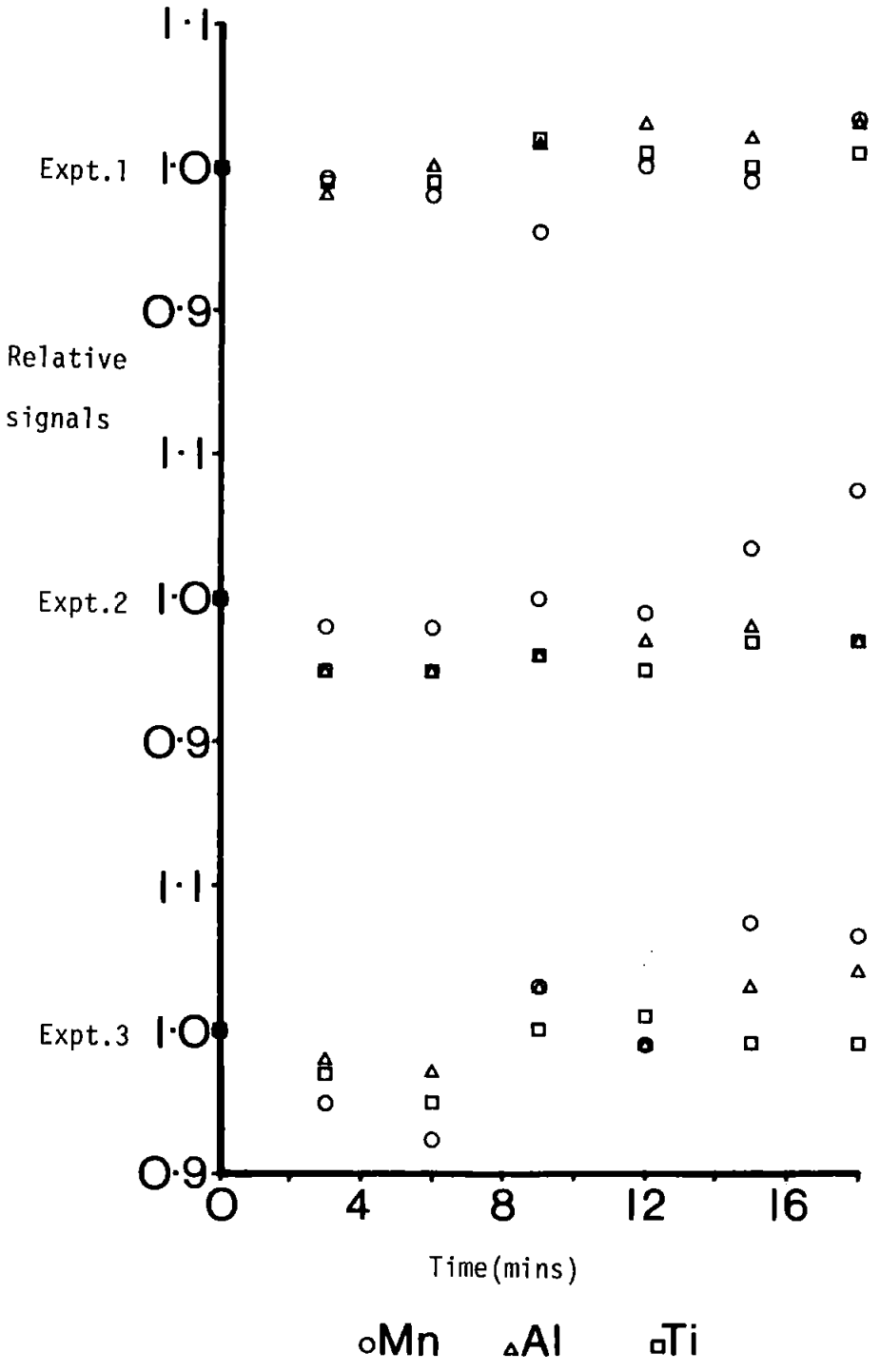

Table 4,8

Detection Limits Obtained with the Improved Laskin Nebuliser

Element	Detection Limits $\mu g\ ml^{-1}$ (3s) Laskin Nebuliser	Simplex Optimised Nebuliser+
Tl	0.90	0.18
Zn	0.015	0.0015
Pb	0,45	0.045
Mn	0.004	0.0008
Fe	0.02	0.005
Mg	0.008	0.0017
Al	0.25	0.034
Ti	0.007	0.001
Sr	0.0006	0.00009
Ba	0.0007	0.0004

+ Corrosion resistant, Perkin Elmer system

4.3.6 Mode of Operation of the Laskin Nebuliser

This nebuliser was found to be relatively simple to operate and permit rapid sample changes with negligible contamination or dilution of successive samples. This was achieved by changing the spray chamber with each sample, the sequence of operation for changing a sample is shown in Table 4.9.

Table 4.9

Procedure for Sample Changing with the Laskin Nebuliser

1. Increase auxiliary flow to 1.5 l min^{-1} (to raise plasma).
2. Remove plug from Y tube in outlet.
3. Remove spray chamber and sample tube.
4. Rinse and blow dry nebuliser tube.
5. Fit clean spray chamber plus sample tube.
6. After a 30 second argon flush of the spray chamber, replace the plug in the Y tube.
7. Reduce auxiliary flow to zero.
8. Commence analysis.
9. Rinse and dry spray chamber for next sample.

4.3.7 Nebulisation Effects with Acid Solutions

The necessity of matching the acid concentrations of sample and standard solutions is recognised by ICP spectroscopists. The change in signal intensity with acid concentration has been investigated by Greenfield et al. (206) using a high power plasma. The signal reductions were explained by viscosity changes for acid solutions of different concentrations.

It seemed appropriate to evaluate the effects of acid solutions with the Laskin nebuliser and to compare the results with other conventional nebulisers. A range of solutions of varying nitric acid concentrations were prepared, each containing 5 μg ml^{-1} Mn (acid blanks were also prepared). Details are shown in Table 4.10.

Figure 4.8 shows the results obtained for the Laskin nebuliser together with a Meinhard concentric nebuliser (J.E. Meinhard

Figure 4.8

Signal Variations with Varying Acid

Concentrations (free uptake nebulisers)

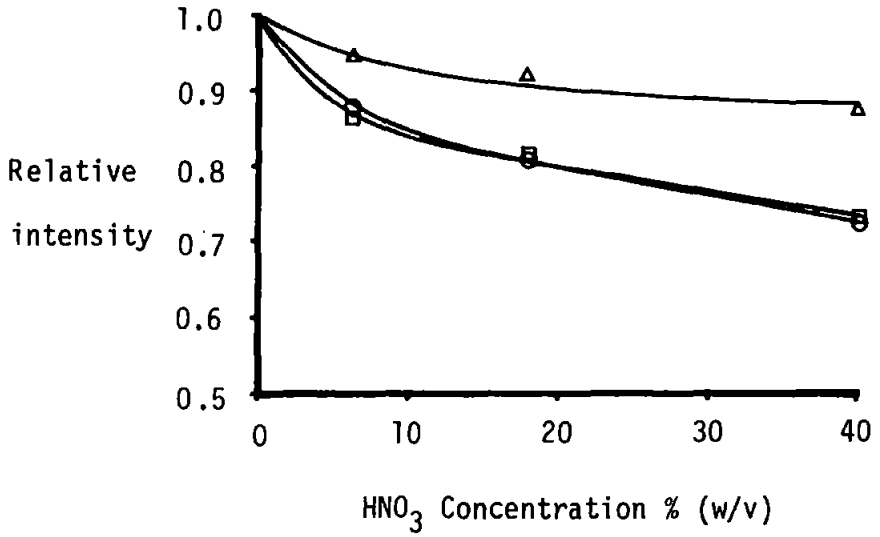

△ Jarrell Ash Crossflow

○ Meinhard Concentric

□ Laskin Recirculating

Associates Inc., Santa Ana, CA, USA) and a Jarrell Ash crossflow nebuliser (Jarrell Ash Division, Fisher Scientific Co, Waltham, MA, USA). These nebulisers were operated with free solution uptake.

Table 4.10

Test Solutions with Varying Nitric Acid Concentrations

Solution	Mn concentration $\mu g\ ml^{-1}$	Nitric Acid Concentrations $^{v}/_{v}$	$^{w}/_{v}$
1	5	1	1.4
2	5	4	5.6
3	5	12	16.8
4	5	30	42

Figure 4.9 shows the results of similar experiments using nebulisers with pumped solution supply. The Meinhard nebuliser was the same as before and was used with a Babington type nebuliser (207) and the Perkin Elmer crossflow nebuliser which has been used for most studies and applications in this thesis.

The results for both the free uptake and pumped nebulisers show the same trends of decreasing signal with increasing acid concentration. The Jarrell Ash crossflow nebuliser was the least affected by varying acid concentrations but the results obtained for the Laskin nebuliser were similar to those obtained with the other nebulisers.

The empirical relationship derived by Nukiyama and Tanasawa (208) successfully predicts the characteristics of experimentally produced primary aerosols. This equation takes the following form:

Figure 4.9

Signal Variations with Varying Acid Concentrations (pumped uptake nebulisers)

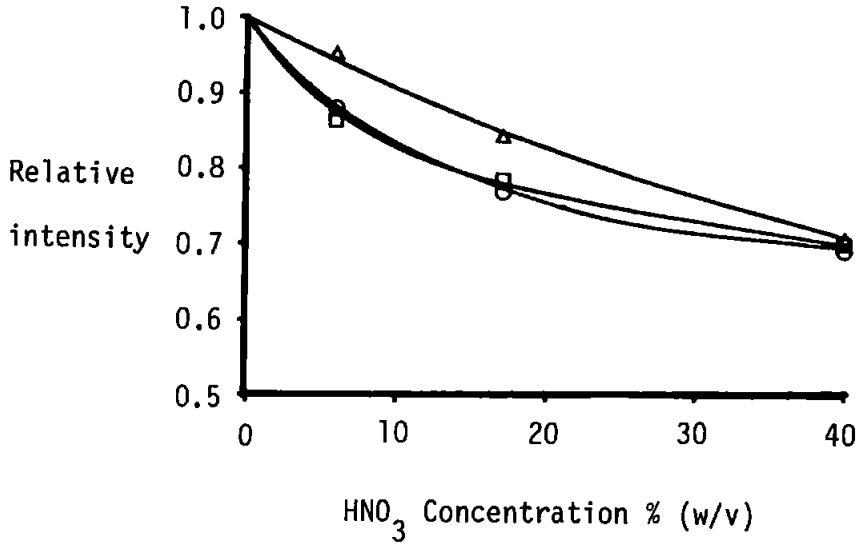

○ Meinhard Concentric

□ Perkin Elmer Crossflow

△ Babington

$$d_0 = \frac{585}{v}\left(\frac{\sigma}{\rho}\right)^{0.5} + 597\left(\frac{\eta}{(\sigma\rho)^{0.5}}\right)^{0.45} \cdot 1000\left(\frac{Q\ liq}{Q\ gas}\right)^{1.5}$$

where,

d_0 = mean droplet diameter (μm)

v = velocity difference between gas and liquid flows (ms^{-1})

σ = surface tension of the liquid (dyne cm^{-2})

ρ = density of the liquid (g cm^{-3})

η = liquid viscosity (Poise)

Q liq, Q gas = volume flow rates of liquid and gas respectively (cm^3s^{-1})

Changes in solution viscosity were earlier suggested as the major cause of signal reductions (206) as a result of reduced solution uptake. This is, perhaps, a little simplistic when the results in Figures 4.8 and 4.9 are compared, particularly for the Meinhard nebuliser. It seems more likely that the changing solution properties are affecting the primary droplet size distributions. That is, more coarse droplets are produced when solutions contain higher acid concentrations i.e. higher viscosities. These additional coarse droplets would be filtered out by the spray chamber and hence the secondary aerosol would contain significantly less solute and give rise to reduced signals.

Closely matched acid concentrations for samples and standards is as important for the Laskin nebuliser as it is for other nebuliser types, whether free running or pumped. Reference to Figures 4.8 and 4.9 indicates that less variation is experienced at higher acid concentrations. Matching is thus less critical but the analytical signals are significantly reduced, emphasising the folly of comparing acid digests with simple aqueous standards. The use of an internal standard would obviously be an alternative approach.

4.3.8 Analysis of Shotgun Steels

4.3.8.1 Introduction

Firearm usage in robberies is increasing and the sawn off shotgun is particularly attractive because of the ease of concealment of this short range weapon. The analysis of steels e.g. shotgun barrels for classification and discrimination purposes is complicated because of the line rich Fe spectrum. The present polychromator line set could not be used for steels analysis because of these spectral line interferences. For forensic purposes it may be necessary to analyse a small steel fragment recovered from a hacksaw and attempt to determine whether it matches the composition of a sawn off shotgun discarded at a robbery. It seemed appropriate, therefore, to evaluate the Laskin nebuliser for the analysis of small fragments of shotgun steels using the scanning monochromator for multielement detection.

4.3.8.2 Sample and Standards Preparation

Three samples of 12 gauge shotgun barrels were obtained and fragment samples were generated by cutting these with a hacksaw. A certified reference material was used for standardisation (ES 186-1, Bureau of Analysed Samples, Middlesbrough, UK) and an alternative material was used as a control sample to test the accuracy of the method (BCS 453).

The steel samples (100-300 μg) were weighed into clean, polypropylene centrifuge tubes, distilled water (10 μl) followed by concentrated nitric acid (25 μl) were then added. When the reaction had subsided, concentrated hydrofluoric acid was added (25 μl) and the

tubes placed in an ultrasonic bath, maintained at 70°C, for 30 minutes. After cooling, distilled water (940 µl) was added and the tubes shaken. All samples were prepared in duplicate.

The reference material was prepared in a similar fashion but a larger volume of a more concentrated solution obtained (0.05g sample in 50 ml).

4.3.8.3 Analytical Procedure

Inductively coupled plasma and nebuliser operating conditions were as previously stated in this chapter. The scanning monochromator details are as shown in Appendix B with 50 wavelength steps of 0.004 nm being used to scan each peak with a 0.5 second integration time per step. The Basic computer program was used for this analysis and, with storage of the raw data on disc, each sample required an analysis time of ~12 minutes for the determination of 5 elements.

The analytical lines selected for these steels analyses are shown in Table 4.11, these were chosen to be free from Fe interferences.

Table 4.11

Analytical Lines for Steels Analysis

Element	Wavelength nm
Si	288.16
Mn	293.31
Cu	324.75
Ni	351.51
Cr	425.44

4.3.8.4 Results and Discussion

The results obtained for the analyses of steel fragments are shown in Table 4.12.

Table 4.12

Results[+] for the Analysis of Shotgun Steels with the Laskin Recirculating Nebuliser

Sample	Si %	Mn %	Cu %	Ni %	Cr %
BCS 453	0.41 (0.36)*	<0.05 (0.04)*	0.20 (0.15)*	0.15 (0.114)*	0.21 (0.24)*
Greener G.P. (English)	1.75	0.47	0.23	0.23	<0.1
Modern Italian Weapon	1.00	1.11	0.17	0.10	<0.1
Boehler Blitz (Italian)	2.07	0.48	0.35	<0.05	<0.1

+ All results are the means of duplicate determinations.

* Certified values.

The acceptable accuracy obtained from the samples in this short feasibility study confirmed the suitability of the Laskin nebuliser for this type of analysis. Silicon was successfully determined as the PTFE construction of the nebuliser permitted the use of hydrofluoric acid dissolution.

All 3 shotgun steels could be readily discriminated on the basis of 4 elements, Cr could not be determined at the levels found in these steels. Because of the ubiquitous nature of low alloy steels, a large survey of shotgun steels would be necessary in order to assess

the usefulness of this application for forensic purposes.

4.3.9 Conclusions

A compact, corrosion resistant recirculating nebuliser has been constructed and shown to be capable of stable aerosol production from 1 ml of sample solution for up to 15 minutes. The nebuliser is simple to use and permits rapid sample changes with negligible contamination and dilution effects.

Limits of detection obtained with this system are poorer than those obtained by conventional nebulisation, although the difference is less important because of reduced dilution factors. The performance may be improved, however, by a more rigorous optimisation and improved design and construction of the nebuliser tube.

The Laskin nebuliser has been applied to the analysis of shotgun steels and shown to be appropriate for small fragment analysis using a scanning monochromator. The PTFE construction permits the determination of Si following hydrofluoric acid digestion, glasses and other refractory materials could also be readily analysed.

5 APPLICATIONS STUDIES WITH INDUCTIVELY COUPLED PLASMA - OPTICAL EMISSION SPECTROMETRY IN FORENSIC SCIENCE

5.1 Introduction

These studies were undertaken to evaluate the potential of ICP-OES for the analysis of forensic samples. Small fragments of glass and brass have been investigated in detail and methods proposed for the analysis of white household glass paints and the determination of metals on hands.

As a result of the time scale of these projects, different analytical conditions have been employed. The corrosion resistant sample introduction system was used for all analyses, the brass and paint determinations were performed using pre-simplex compromise conditions (Table 3.9) and the glasses and handswabs analysed with simplex optimised conditions (Table 3.13). The polychromator was used for all analyses and unless stated the element wavelengths were as shown in Chapter 2.

5.2 The Analysis of Small Samples of Brasses and their Classification by Two Pattern Recognition Techniques

5.2.1 Introduction

The techniques normally employed for alloy analysis in the Forensic Science Service are x-ray fluorescence (XRF), scanning electron microscopy with energy dispersive x-ray analysis (SEM-EDXA) and x-ray diffraction (XRD). XRF would not normally be used for quantitative analyses of the sample sizes considered in this work.

XRD is a valuable technique but its usefulness is limited to the identification of phases and the estimation of copper/zinc ratios in certain brasses (209). The most popular technique is SEM-EDXA for small samples, but to obtain quantitative data, closely matched standards are required. Problems can also be encountered from surface smearing of the lead in leaded brasses.

This section describes a detailed study of the quantitative analysis and classification of 37 brass items obtained from everyday objects and those from a metals supplier.

5.2.2 Composition of Brasses

Copper base alloys in which zinc is the major alloying element are termed brasses. The commercially useful alloys have zinc contents ranging from 5-42% with small additions of other elements (<5%) to modify the properties for certain applications.

The brasses can be broadly divided into 2 distinct groups, the alloys in each group having different properties. The first group comprises the alpha or cold working brasses which contain a maximum of 37% zinc and are characterised by their ductility at room temperature. The commonest member of this group is cartridge brass which contains 70% copper and 30% zinc. The second group comprises the alpha-beta, duplex or hot working brasses which contain between 38% and 42% zinc. Unlike the alloys of the first group their deformation at room temperature is very limited. They are, however, more plastic at elevated temperatures and can be extruded into bars or tubes or hot stamped into complex shapes.

Of the alloying additives designed to improve machinability, strength or corrosion resistance, lead is the most important. It is

insoluble in brass and acts as a solid lubricant to improve machining. Lead contents generally range from 1% to 4.5% depending on alloy and application. Tin, aluminium, iron and manganese can be added at low percentage levels to improve strength; these alloys are called high tensile brasses. Tin, aluminium and arsenic additions improve the corrosion resistance of the alloys. Tin (1%) or arsenic (0.02-0.04%) inhibit de-zincification in Naval and Admiralty brasses, and aluminium (2%) reduces surface erosion by modifying the nature of the surface protective film. Nickel is added to the Nickel (or German) Silvers to decolourise the brass, allowing it to take a high polish and imparting good corrosion resistance; contrary to their name, these alloys contain no silver.

5.2.3 Experimental

5.2.3.1 Sample Preparation

The surface of each brass item was degreased with 1,1,2 - trichloro - 1,2,2 - trifluoroethane, the sampling area cleaned with fine silicon carbide paper (600 grit) then rinsed with distilled water and dried. Analytical samples were taken by drilling with a cleaned No. 50 drill (1.8 mm), the drillings were then placed in a cleaned polythene container.

Nominal 100 μg samples (approximately 80 μg-120 μg) were taken from the drillings of each item and placed in acid-cleaned polythene snap-top containers (1.5 ml). Duplicate samples were taken from all items. Nitric acid (50%, 0.5 ml) was pipetted onto each sample, 30 minutes was allowed for dissolution, then distilled water added

(0.5 ml) and the containers capped and shaken.

To assess the accuracy and precision of the analyses, duplicate samples of a standard brass (British Chemical Standard 179/2, high-tensile brass) were prepared in a similar fashion. In addition, a bulk solution of this standard was prepared at a concentration of 100 $\mu g\ ml^{-1}$.

5.2.3.2 Choice of Elements and Standard Preparation

The element set was chosen by considering the major elements, alloying additions, and other minor constituents. Following preliminary experiments the set was reduced to 8 elements, the only alloying elements not determined being arsenic (generally 0.05%) and silicon (1% in silicon brasses). The elements and their analytical wavelengths are shown in Table 5.1 together with practical determination limits in the solid samples; based on 100 μg of sample in 1 ml.

Multielement standards were prepared from 1000 $\mu g\ ml^{-1}$ stock solutions (BDH Chemicals Limited, Poole) in nitric acid (25%, by volume). Linear calibrations over 3-4 orders of magnitude were obtained for all elements.

5.2.3.3 Interferences

Zinc and lead were shown to be subject to spectral interferences from the major constituents. The zinc wavelength was interfered with to a small extent by the copper 213.6 nm line, lead interference was caused by both copper and zinc and appeared to result from a change in the spectral background. Both effects were readily corrected for: the lead correction was the more significant,

particularly at low lead concentrations.

5.2.3.4 Calculation of Results

Time consuming weighing of samples was minimised and weighing errors associated with small samples were eliminated by use of a concentration ratio technique (193). For the computation to be valid it is necessary to measure the concentration of all elements present in significant quantities and to ensure that all determinations are carried out within the linear calibration range of the instrument.

5.2.4 Results and Discussion

5.2.4.1 Accuracy and Precision of Analysis

Standards were included with each batch of samples in the form of aliquots of a bulk solution, prepared from the brass standard BCS 197/2, and those prepared on each occasion from the solid standard. The sample analyses were carried out over five weeks during which seven duplicate results were obtained for the standard. The results, shown in Table 5.2, are considered to be a realistic estimate of the long term precision and accuracy of the method.

The overall accuracy of the determinations is excellent, while the degradation in precision from solution to solid samples reflects the problems of manipulating and preparing very small samples. However, except for lead, the precision is more than adequate for classification. The variation in the lead results arises from the poor detection limit for this element. However, the lead content of this standard is artificially low for a leaded brass and more precise

results can be expected from samples likely to be encountered in casework.

Table 5.1

Elemental Data

Element	Wavelength nm	Limit of Determination* %
Zn	213.8	Major Constituent
Pb	220.3	0.15
Ni	231.6	0.05
Mn	257.6	0.003
Fe	259.9	0.012
Sn	284.0	0.15
Cu	324.7	Major Constituent
Al	396.1	0.02

* Calculated as 6σ (6 standard deviations of the background variation) applied to the solid sample; 100 μg in 1 ml.

5.2.4.2 Analysis and Classification of Sample Set

Quantitative results for up to 8 elements were obtained from duplicate samples of the set of 37 brasses. Because brasses cover a wide range of copper and zinc containing alloys it was decided to attempt a simple classification to aid the presentation and interpretation of the data. Figure 5.1 shows a three dimensional plot of the data using Zn, Cu and Pb contents for the axes. A few samples

Figure 5.1

3-Dimensional Plot of Brass Samples

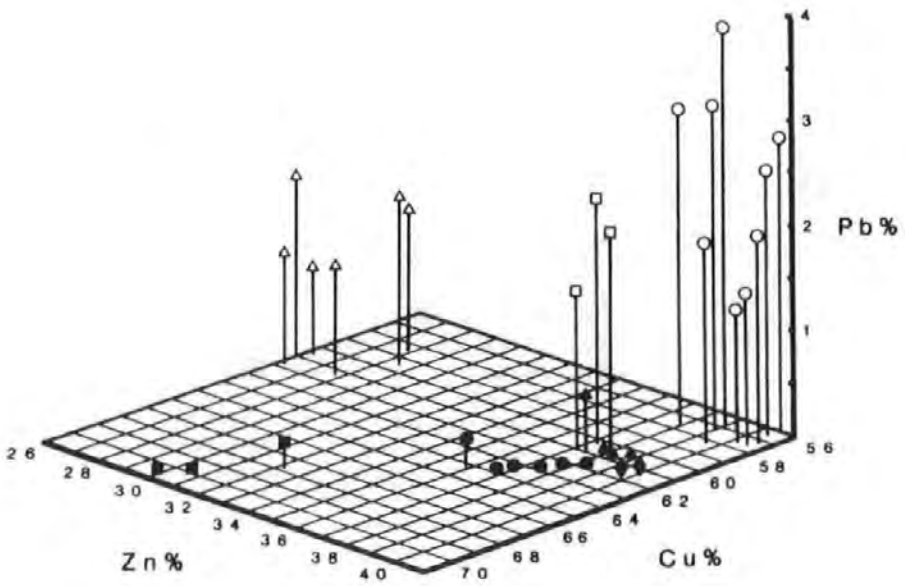

KEY

Group Identification

- ■ 2 Cartridge brass
- △ 3 Nickel silver
- ● 4 Common brass
- □ 5 Leaded alpha brass
- ▲ 6 Naval brass
- ◆ 7 Lead free duplex brass
- ○ 8 Leaded duplex brass

have been omitted from this plot either because of their similarity to others or, for one sample, a considerably different composition. The major alloy types are distinguished by the key.

Table 5.2

Accuracy and Precision of Brass Analysis

	Element % (w/w)							
	Zn	Pb	Ni	Mn	Fe	Sn	Cu	Al
BCS 179/2 Certified Data %	35.8	0.35	0.56	0.86	1.02	0.70	58.5	2.22
Solution Samples								
Elements %+	35.9	0.36	0.59	0.86	1.01	0.72	58.3	2.22
SD* (n=7)	0.40	0.08	0.02	0.01	0.03	0.03	0.29	0.05
RSDx	0.011	0.214	0.027	0.013	0.026	0.039	0.005	0.024
Solid Samples								
Elements %+	36.3	0.41	0.61	0.85	1.04	0.67	57.9	2.17
SD* (n=7)	0.59	0.12	0.04	0.04	0.06	0.05	0.39	0.11
RSDx	0.016	0.227	0.070	0.044	0.062	0.078	0.007	0.052

\+ Mean of duplicate determinations.

* Standard deviation.

x Relative standard deviation.

The samples of Nickel (or German) Silver are characterised by their approximately 10% Ni content and the Naval brasses by their tin content (~1%). The leaded alpha brasses form a compact group as do the leaded duplex brasses. The lead free brasses cover a wide concentration range and can be split into at least two sub groups. Table 5.3 shows a group classification based on the determination of the major and alloying constituents, and the complete analytical data for

these groups are shown in Table 5.4. Although the sample numbers in some of the groups are obviously limited, the sample of nickel brass in group 1 is clearly distinguished as are the three samples of cartridge and leaded alpha brass. The samples which are most difficult to separate are the common alpha and lead free duplex brasses in groups 4 and 7. The only feature which distinguishes between these is the threshold concentration of 38% Zn for duplex brass.

Table 5.3

Group Classification of Brasses

Group	Identification	Number of Samples
1	Nickel brass	1*
2	Cartridge brass	3
3	Nickel silver	6
4	Common brass	6
5	Leaded alpha brass	3
6	Naval brass	4
7	Lead free duplex brass	2
8	Leaded duplex brass	12

* Not shown in Figure 5.1

5.2.4.3 Pattern-Recognition

Two clustering techniques available on the laboratory Prime computer were applied to data on the brasses in an attempt to achieve a more objective means of classification.

The hierarchic clustering program AGCLUS (210) was used to

Table 5.4

Analytical Data for Grouped Brasses

	Element %+								Sample Number
	Zn	Pb	Ni	Mn	Fe	Sn	Cu	Al	
Group 1 - Alpha Brass									
Nickel brass blank Royal Mint	19.9	-*	1.07	-	0.07	-	78.8	-	4
Group 2 - Alpha Brass (Cartridge)									
Cartridge case, 0.22	29.6	-	-	-	0.03	-	70.3	-	13
Tube ¼", BS2871	30.1	-	-	-	-	-	69.9	-	30
Continental mains plug	32.0	0.21	-	-	-	-	67.7	-	3
Group 3 - Nickel Silver									
Dominion key	25.9	1.67	11.0	0.23	0.06	-	61.1	-	12
Betakey	27.7	1.02	9.8	0.11	0.14	-	61.2	-	19
Union padlock key	26.2	0.98	11.1	0.05	0.14	-	61.6	-	33
Union key	26.4	1.35	11.0	0.18	-	-	60.9	-	35
Union key	28.6	1.46	10.3	0.23	0.15	-	59.3	-	36
Yale key	27.8	1.34	11.3	0.34	0.20	-	58.3	0.03	37
Group 4 - Alpha Brass (Common)									
Gauze, 1 mm mesh	35.8	0.16	-	-	-	-	64.1	-	20
Washer, ⅜"	36.1	-	-	-	0.02	-	63.9	-	21
Car thermostat	36.5	-	-	-	-	-	63.5	-	24
Identity disc	36.9	-	-	-	0.02	-	63.1	-	14
Cup hook	37.3	-	-	-	0.03	-	62.7	-	18
Wood screw	37.9	-	0.04	-	0.02	-	62.0	-	17
Group 5 - Leaded Alpha Brass									
13 amp mains plug	37.1	2.34	-	-	0.05	-	60.5	-	2
35 mm pipe olive	37.4	1.47	-	-	-	-	61.1	-	8
Yale key	37.8	1.95	-	-	0.03	-	60.2	-	11
Group 6 - Naval Brass									
Vacuum coupling	37.4	0.47	-	-	0.24	1.32	60.6	-	23
Rod 1" BS2874	38.7	-	-	-	0.06	1.01	60.2	-	29
Rod ½" BS2874	37.6	-	-	-	0.05	1.37	61.0	-	31
Rod ¼" BS2874	37.9	-	-	-	0.09	1.37	60.7	-	32
Group 7 - Lead-Free Duplex Brass									
Screw, 0 BA	38.8	-	-	-	0.02	-	61.1	-	16
Flat bar, BS1949	39.2	-	-	-	-	-	60.7	-	27
Group 8 - Leaded Duplex Brass									
15 mm pipe fitting	40.7	1.98	0.10	-	0.10	-	57.2	-	5
6 mm pipe fitting	39.5	2.63	0.13	-	0.10	-	57.6	-	6
6 mm pipe fitting	39.0	2.98	0.14	0.007	0.19	-	57.7	-	7
6 mm pipe fitting	39.2	3.77	-	0.01	0.12	-	57.0	-	9
6 mm pipe fitting	39.5	2.61	0.11	0.004	0.15	-	57.6	-	10
5 amp mains plug	39.1	3.14	0.09	0.02	0.33	-	57.4	-	1
Hinge 1"	40.4	2.51	0.08	0.01	0.17	-	56.5	0.35	15
Wing nut	40.7	1.36	0.03	-	0.11	-	57.8	-	22
Angle ½"	40.7	2.79	-	-	0.19	-	56.0	0.26	28
Pipe clamp	39.6	1.94	0.12	0.005	0.16	-	58.2	-	25
Door chain block	40.5	1.33	-	0.02	0.11	-	57.8	0.18	26
Union padlock	39.3	3.01	-	-	0.19	-	57.5	-	34

\+ Means of duplicate determinations.

* Limits of determination as shown in Table 5.1

identify homogeneous groups or clusters in the data set using the farthest neighbour criterion applied to normalised data. Cluster analysis is conventionally displayed in the form of a dendrogram in which the individual samples and clusters are joined at nodes. Figure 5.2 shows part of the dendrogram obtained from these samples. The main features of cluster size, sample number and group identity can be clearly seen. The group assignment was based on the classification in Table 5.3. By consulting the dendrogram a subjective choice now has to be made on the number of groups into which the sample set can be split. As the set is relatively small, cluster sizes of three and four were chosen to split the samples. The cluster size of four gave six groups, (similar to the earlier assignment except that groups 5, 6 and 7 were combined into one). Division at a cluster size of three gave nine groups, where groups 6 and 7 were combined and 2 and 3 (not shown in Figure 5.2) were split. This clustering technique clearly needs a larger data base for groupings to be assigned with greater confidence.

A nonlinear mapping technique (211) was then applied to the samples in an attempt to identify their inter-relationships. Figure 5.3 shows a scattergram produced by the program from normalised data. The original groups can clearly be identified and except for groups 4 and 7 (as previously discussed) they are well separated. A second print-out from this program identifies the individual samples.

5.2.5 Conclusions

The determination of up to 8 elements in 100 μg samples of 37 brass samples has been reported. The analyses carried out by ICP-OES included elements from trace to major constituents. The accuracy and

Figure 5.2

Dendrogram of Some Brass Samples

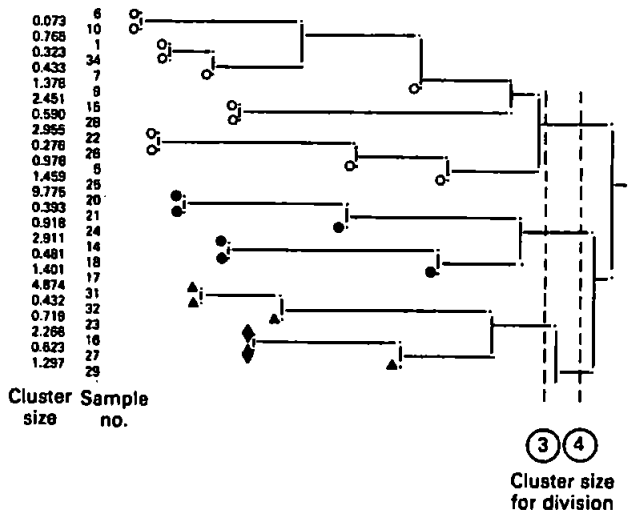

KEY

- ● Common brass (Group 4)
- ▲ Naval brass (Group 6)
- ♦ Lead free duplex brass (Group 7)
- o Leaded duplex brass (Group 8)

Figure 5.3

Scattergram of Brass Samples

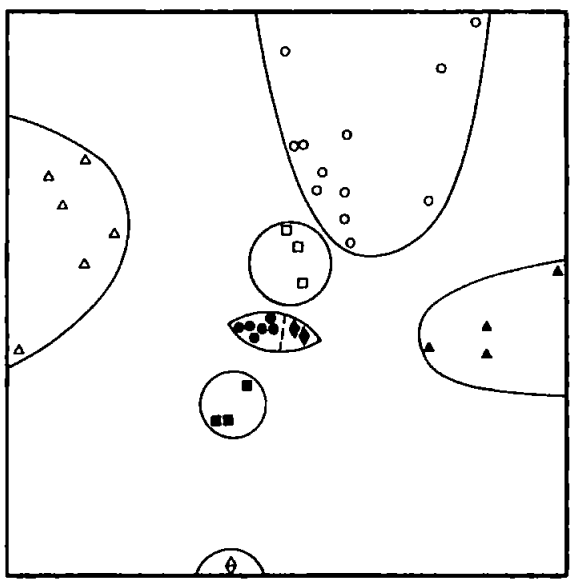

KEY

- ◊ Nickel brass
- ■ Cartridge brass
- △ Nickel silver
- ● Common brass
- □ Leaded alpha brass
- ▲ Naval brass
- ♦ Lead free duplex brass
- ○ Leaded duplex brass

precision of the method have been shown to be good from repeat analyses of a brass standard. The quantitative data are of potential use to forensic scientists as a reference collection and to assist the interpretation of alloy analyses.

Although the samples could be easily split into at least seven groups by considering their alloying constituents, a more objective classification was achieved by pattern recognition techniques. Nonlinear mapping was shown to be the most suitable method as the scattergram can be easily evaluated and the algorithm preserves the structural relationship between samples. The hierarchic clustering technique appears to be more useful for larger data sets where bigger clusters could perhaps be divided with greater confidence.

5.3 The Analysis of Small Fragments of Sheet Glasses

5.3.1 Introduction

Glass is one of the commonest types of material encountered by forensic scientists. Broken glass can arise in cases of murder, assault, criminal damage, road traffic accidents and burglaries. The commonest cases involving broken glass are burglaries, where glass fragments recovered from a suspect's hair, clothes or shoes are compared with a sample of control glass taken, for example, from a broken window at a crime scene.

When a window is forcibly broken by striking with a hard object, a cloud of glass fragments flies backwards from all parts of the window where cracks appear. This "backward fragmentation" showers the breaker of a window with a multitude of glass fragments of varying sizes. This was illustrated by Nelson and Revel (212) who published

photographs of a window being broken with a hammer blow. Pounds and Smalldon (213) later published data on the size and spatial distributions of glass fragments produced as a result of "backward fragmentation".

The forensic scientist will attempt to determine whether or not suspect fragments match the control glass (discrimination). He may also attempt to identify the type of glass from which the suspect fragments originated (classification).

The determination of refractive index (RI) is a fundamental technique for the discrimination of glass fragments. In the Home Office Forensic Science Laboratories the Becke line principle is employed (214) together with phase contrast microscopy and a silicone oil immersion medium. This technique can routinely determine refractive indices on glass particles as small as a few μg with typical standard deviations of 0.00005 for a mean sheet glass RI of 1.516 (231). Annealing techniques have recently been employed to identify toughened windscreen glass particles (215) and elimination of residual stresses in window glasses has been shown to enhance discrimination (216).

The measurement of refractive index alone is of limited use for classification purposes because of the overlap of refractive index distributions for sheet and container glasses (Figure 5.4) (232). Interference microscopy can be employed to identify original flat surfaces on small fragments of sheet glasses (217) and thus assist with their classification. In addition, the fluorescence from the tin rich surface of float glass can be used to distinguish this from non-float window glass (218).

Multielement analysis can provide significant additional information for the successful classification and discrimination of glass fragments. In the Forensic Science Service, scanning electron microscopy with energy dispersive x-ray analysis (SEM-EDXA) is the major

Figure 5.4

Refractive Index Distributions of Sheet and

Container Glasses

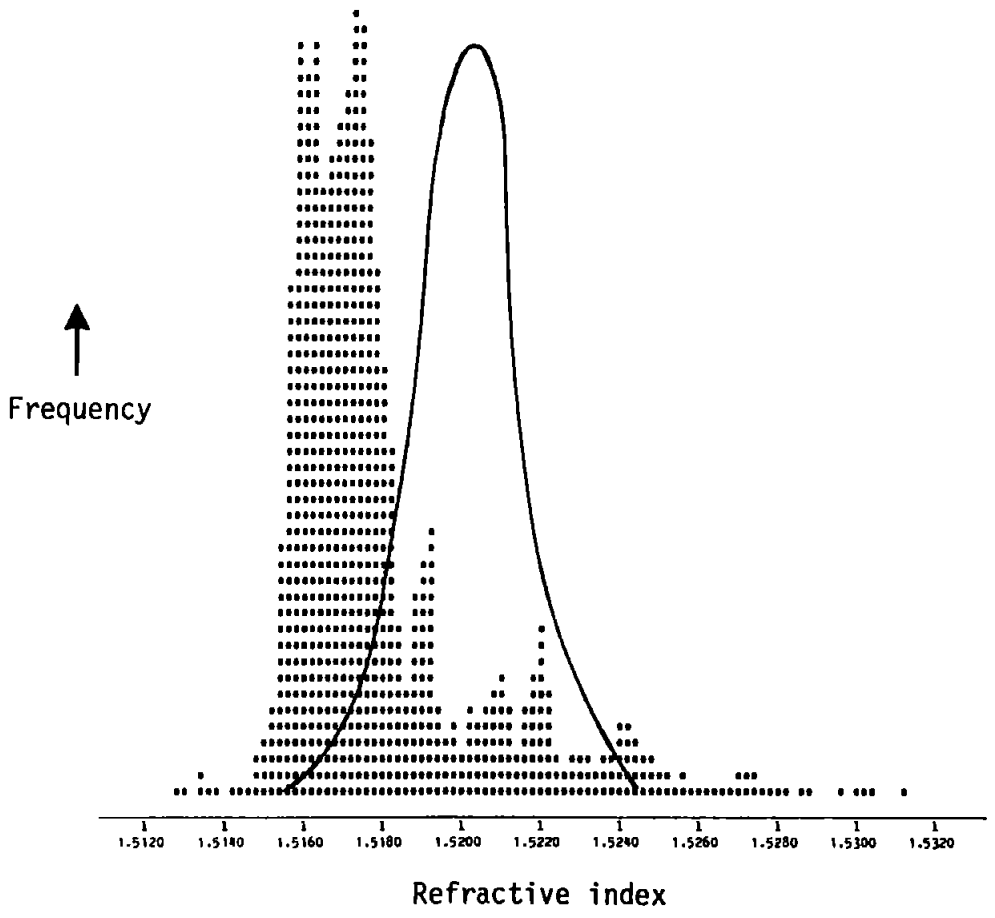

analytical technique used for the routine analysis of casework glass fragments, while x-ray fluorescence (XRF) may be used to provide additional trace element data for larger samples. SEM-EDXA is used primarily for classification of glass types and for comparative purposes where relative data may be sufficient. However, the benefits of quantitative results have been recognised and analysts are progressing towards the acquisition of absolute quantitative data for Si, Na, K, Mg, Al and Ca in casework glass fragments.

At the Metropolitan Police Forensic Science Laboratory ICP-OES has been used for the determination of 5 elements in small glass fragments (98). Data reported for 350 glass samples (99) has been used to formulate a glass classification scheme (100). A later study (219) identified Mg, Li, Co, Sr, Fe and As as good classifying elements and similar work (220) identified Ba, Rb, Sr, Fe, K, Mn and Li as good discriminating elements.

The major objective of the work reported here was to develop an ICP-OES technique for the simultaneous, quantitative analysis of up to 10 elements in casework size glass fragments with particular reference to the discrimination of sheet glasses of similar refractive index.

5.3.2 Composition of Glass

Glass can be regarded as a supercooled liquid and thus possesses the random structural nature of a liquid. The common glasses consist of a mixture of the oxides of Si, Na, Ca, Al and Mg with small amounts of K and Fe. These constituents can be classified according to the functions they perform during manufacture or in the glass.

Fused silica (SiO_2) is the major network former, i.e.

it can form a glass on its own. Sand is the commonest source of silica and its impurity content must be carefully controlled for the manufacture of colourless glasses. Alumina (Al_2O_3) is the most important intermediate glass former as it can form a glass in combination with another oxide. This compound imparts better chemical durability to silicate glasses and reduces the tendency to devitrification (crystallisation).

The next important group of oxides consists of fluxes or network modifiers which combine with the primary glass former to produce low melting point, low viscosity liquids. Soda (Na_2O) is the principal flux (added as Na_2CO_3) and K_2O regularly occurs as a result of raw material compositions. A deliberate addition of K_2O may be made to increase the brilliance of lead crystal glasses.

Divalent ion oxides stabilise the glass structure against chemical attack, they also reduce devitrification and increase electrical resistance by restricting the movement of monovalent ions. Lime (CaO) is the third largest component in most glasses, limestone is the principal raw material. Magnesium oxide acts similarly to CaO but is mainly added to lower the liquidus temperature and produce a slower setting glass.

Colourants and decolourants are used to control the appearance and redox state of the glass. Iron is the most troublesome impurity in colourless glasses, quality control of the raw materials is the most appropriate means of control. However, other colouring ions can be added during manufacture to provide complementary absorptions, or the Fe^{2+} Fe^{3+} equilibrium can be influenced by the addition of oxidising or reducing agents. Coloured glass can be produced by adding controlled quantities of Fe or Fe + Cr (green), Fe + S (amber), Se (yellow), Se + S + Cd (red), Co (blue), Mn (purple) and Ni (grey-brown).

Flat glass is encountered most frequently by forensic scientists. Until the late 1950's sheet glasses were produced by rolling or drawing but following the introduction of the float glass process (Pilkington Flat Glass Ltd, St. Helens, UK) the manufacture of sheet glass has been virtually eliminated. Other glass types which may be encountered are container, tableware and headlamp glasses. These major glass types can be classified using a combination of R.I. and major and minor element compositions. Typical compositions are shown in Table 5.5. The determination of R.I. alone may be sufficient to discriminate between a group of sheet or float glasses. However, if the R.I.'s are not significantly different then the determination of trace element concentrations may assist the discrimination.

Table 5.5

Typical Glass Compositions % (w/w)

Components	Float (%)	Bottle (%)	Drinking Glass (%)
SiO_2	72.0	72.7	72.3
Na_2O	13.4	15.7	13.7
CaO	8.6	6.6	6.7
MgO	3.8	2.8	3.4
Al_2O_3	1.1	1.1	1.9
K_2O	0.60	0.40	1.1
Fe_2O_3	0.10	0.04	0.03

5.3.3 Experimental

5.3.3.1 Preparation of Standards and Preliminary Samples

All glasses were initially crushed in a pestle and mortar under acetone to avoid loss of fragments. The glasses were cleaned with concentrated nitric acid, rinsed with distilled water then ethanol and dried. Glass samples (7-8 mg) were accurately weighed then placed in pre-cleaned and weighed polypropylene flasks (50 ml). Concentrated hydrochloric acid (1 ml) and concentrated hydrofluoric acid (0.5 ml) were then pipetted onto the samples. The flasks were then stoppered and placed in an ultrasonic bath at $60^{o}C$ for 1 hour to effect dissolution. After this period 5% boric acid solution (5 ml) was added and the flasks returned to the ultrasonic bath for 30 minutes. The concentration of glass in the final solution was $\sim 150\ \mu g\ ml^{-1}$, each sample was prepared in duplicate.

Multielement standards were prepared in a similar fashion from a certified standard float glass (ECl.1, British Glass Industry Research Association, Sheffield, UK). The concentration of glass in these solutions was 250, 500 and 750 $\mu g\ ml^{-1}$.

This preparation is a modification of that reported by Uchida et al. (221) for the analysis of silicates.

5.3.3.2 Analysis and Computation

Samples, standards and reagent blanks were analysed for Na, Ca, Mg, Al, Fe, Mn, Ti, Sr and Ba on the polychromator using simplex optimised conditions (Chapter 3). Integration times of 5 seconds were employed and background subtracted intensities recorded. Sample

concentrations were calculated from first or second order polynomial fits of the intensities of standards.

5.3.3.3 Preparation of Casework Size Glass Fragments

This preparation is basically a scaled down version of the method reported in Section 5.3.3.1.

Glass fragments (50-400 μg) were weighed into cleaned, polypropylene, snap top tubes (1.5 ml). Concentrated nitric acid (0.5 ml) was pipetted into each tube and the capped tubes were placed in an ultrasonic bath for 30 minutes. The nitric acid was then removed by suction, the fragments rinsed with distilled water then acetone and dried under vacuum. Concentrated hydrochloric acid (20 μl) and concentrated hydrofluoric acid (10 μl) were pipetted into each tube, the tubes capped then placed in an ultrasonic bath at 60°C for 1 hour to effect dissolution. After this period, boric acid solution (100 μl of 5%) was added to each tube, the tubes shaken then returned to the ultrasonic bath for a further 15 minutes. The tubes were allowed to stand for 45 minutes then distilled water (870 μl) added to give a total volume of 1 ml.

Glass samples were normally prepared in duplicate together with controls and reagent blanks.

5.3.4 Results and Discussion

5.3.4.1 Method Performance

Standard sheet glasses (7-8 mg samples) were analysed initially to assess the performance of the ICP method. Data for these glasses are shown in Table 5.6 and confirm the excellent accuracy of the technique. In addition to the elements reported, K, Zr and Si were monitored to determine their suitability for analysis. At the sample concentrations examined here K could not be detected with sufficient sensitivity; Zr concentrations appeared to be ~100 ppm in these glasses but the results were very erratic presumably because of the refractory nature of this constituent; and the wash out time of the sample introduction system was unacceptably long for Si determinations.

To assess the scaled down preparation for casework size fragments, duplicate samples of 3 glasses were prepared by both techniques and the analytical results are shown in Table 5.7. These results generally agree well for the 7 mg and 250 μg sample sizes. To test further the performance of this casework sample preparation technique, a set of 6 standard glasses were selected to cover a range of glass types, and sample weights of 80 μg to 300 μg taken for analysis. These results are shown in Table 5.8 and show excellent agreement with the reported data (where available) thus confirming the suitability of this technique for the quantitative, multielement analysis of a variety of glass types.

During the course of these and subsequent analyses, duplicate samples of the standard glass EC1.1 were analysed to assess the long term performance of the method. Over a 6 month period 9 results were obtained for sample sizes of 115 μg to 325 μg, these

Table 5.6

Analysis of Standard Glasses

		CL 16G[x]	CL 17G[x]	EC1.2[+]
Na%	ICP	9.67	9.64	10,80
	CERT.	9.64	9.62	10.55
Ca%	ICP	6.44	5.53	5.47
	CERT.	6.38	5.65	5.50
Mg%	ICP	1.90	2.32	2.43
	CERT.	1.95	2.40	2.42
Al%	ICP	0.55	0.68	0.64
	CERT.	0.51	0.65	0.64
Fe μgg^{-1}	ICP	680	1049	537
	CERT.	671	980	540
Ti μgg^{-1}	ICP	235	246	164
	CERT.	240	240	174
Mn μgg^{-1}	ICP	98	112	78
	MPL*	92	108	-
Sr μgg^{-1}	ICP	43	41	167
	MPL*	39	37	-
Ba μgg^{-1}	ICP	106	128	154
	MPL*	98	118	-

x Pilkington Flat Glass Ltd., St Helens, UK.

\+ British Glass Industry Research Assoc., Sheffield, UK

* Data Supplied by Dr. D. Hickman, Metropolitan Police Forensic Science Laboratory, London, UK.

results are shown in Table 5.9.

These results generally demonstrate very good accuracy and precision, the results for Ti are the poorest, and, as adequate sensitivity is available, this suggests the dissolution technique is not entirely satisfactory for this element. However, the majority of elements have relative standard deviations of 5% or lower which compares very favourably with the data reported by Catterick (101) who used a second monochromator to monitor an internal standard line for the analysis of similar sized glass fragments.

Table 5.7

Comparison of Large and Small Sample Preparation Techniques for Three Glasses

	Glass A+		Glass B+		Glass C+	
	7mg	250µg	7mg	250µg	7mg	250µg
Na %	10.29	10.93	9.27	9.51	9.54	9.87
Ca %	4.86	5.21	5.29	5.58	5.63	5.92
Mg %	2.19	2.29	2.32	2.36	2.31	2.37
Al %	0.78	0.80	0.64	0.64	0.66	0.69
Fe $\mu g g^{-1}$	1408	1367	1209	1274	602	756
Ti $\mu g g^{-1}$	347	258	253	215	96	112
Mn $\mu g g^{-1}$	50	49	108	114	114	115
Sr $\mu g g^{-1}$	112	117	102	104	182	185
Ba $\mu g g^{-1}$	90	86	4330	4553	138	154

+ All results are the means of duplicate determinations.

Table 5.8

Analysis of Small Samples of Standard Glasses

		Na %	Ca %	Mg %	Al %	Fe μgg^{-1}	Ti μgg^{-1}	Mn μgg^{-1}	Sr μgg^{-1}	Ba μgg^{-1}
+ SGT 5	CERT.*	11.61	4.68	1.66	0.59	304	-	-	-	-
	ICP	11.88	4.58	1.69	0.56	308	157	21	37	417
+ SGT 6	CERT.	10.87	7.13	0.06	0.89	240	-	-	-	-
	ICP	10.94	7.29	0.01	0.89	245	87	30	36	47
+ SGT 7	CERT.	10.31	7.88	0.08	0.79	310	-	-	-	-
	ICP	10.55	7.72	0.08	0.79	359	180	154	61	99
x CL 127	CERT.	10.18	4.76	2.06	1.01	218	-	-	-	-
	ICP	10.02	5.03	2.07	1.04	187	1450	18	7	18
x CL 173	CERT.	11.11	3.35	2.35	1.27	352	-	-	-	0.70%
	ICP	11.46	3.41	2.26	1.28	357	222	32	300	0.69%
x CL 223	CERT.	7.95	6.72	0.69	0.47	85	-	-	-	1.79%
	ICP	7.67	7.00	0.64	0.47	105	150	15	356	1.93%

\+ Society of Glass Technology, Sheffield, UK.

x Pilkington Flat Glass Ltd., St Helens, UK.

* CERT. values are suppliers' declared concentrations.

Table 5.9

Performance of the Glass Analysis Method from

ECl.1 Control Samples

Date of Analysis	Na %	Ca %	Mg %	Al %	Fe μgg^{-1}	Ti μgg^{-1}	Mn μgg^{-1}	Sr μgg^{-1}	Ba μgg^{-1}
6/84	10.10	6.19	2.29	0.57	704	233	87	40	135
6/84	9.90	6.27	2.31	0.57	682	229	86	39	114
8/84	9.99	6.43	2.36	0.60	740	273	97	36	107
8/84	10.08	6.65	2.43	0.63	798	185	99	40	118
9/84	9.35	6.16	2.35	0.57	709	173	94	38	102
10/84	10.31	6.07	2.31	0.57	745	216	94	38	105
10/84	9.73	6.54	2.28	0.59	762	193	99	41	117
10/84	10.01	6.11	2.31	0.58	729	232	99	39	125
12/84	10.08	6.26	2.32	0.54	757	185	94	42	122
$\bar{x}$	9.95	6.32	2.33	0.58	736	213	94	39	116
s	0.274	0.226	0.046	0.025	34.956	32.003	4.950	1.787	10.517
RSD	0.0276	0.0358	0.0196	0.043	0.0475	0.1502	0.0527	0.0458	0.0907
Cert. Data	9.948	6.168	2.28	0.572	720	240	94	38	110

5.3.4.2 Discrimination of Sheet Glasses

The ability to discriminate similar glasses on the basis of multielement data is dependant to a great extent on the precision of the analytical technique. This current ICP-OES technique has demonstrated excellent precision and thus 5 sheet glasses of similar refractive indices were selected for analysis to test the potential for discrimination. The refractive indices for these samples varied from 1.51553 - 1.51563, this is similar to the range of results which can be obtained from a group of fragments derived from a typical sheet glass (216). It would therefore be difficult to discriminate these glasses on the basis of refractive index alone. The analytical results for these 5 glasses are shown in Table 5.10.

Table 5.10

Analytical Results for Five Sheet Glasses+

Element	Glass A	Glass B	Glass C	Glass D	Glass E
Na%	9.36	9.50	10.29	9.27	9.54
Ca%	5.44	5.25	4.86	5.29	5.63
Mg%	2.18	2.47	2.19	2.32	2.31
Al%	0.77	0.82	0.78	0.64	0.66
Fe μgg^{-1}	769	517	1408	1209	602
Ti μgg^{-1}	182	246	347	253	96
Mn μgg^{-1}	114	67	50	108	114
Sr μgg^{-1}	187	53	112	102	182
Ba μgg^{-1}	142	65	90	4330	138
Refractive Index	1.51553	1.51555	1.51558	1.51561	1.51563

+ All results are the means of duplicate determinations.

Considerable variations can be seen for some elements which suggested complete discrimination would be possible. The simple discrimination test employed by Hickman (222) was used and the ranges (mean ± 2 standard deviations) for each of the elements determined were compared for all samples. The samples were regarded as distinguishable if the ranges for one or more elements were separate. Using this criterion the multielement data for the 5 samples were separated into element groups and this data is shown in Table 5.11.

Table 5.11

Discrimination Test for Five Sheet Glasses‡

Element	Group Assignment for Individual Elements					Number of Element Groups
	Glass A	Glass B	Glass C	Glass D	Glass E	
Na	1	1	1	1	1	1
Ca	1	1	1	1	1	1
Mg	1	2	1	2	2	2
Al	1	1	1	2	2	2
Fe	1	2	3	4	2	4
Mn	1	2	2	1	1	2
Ti	1	1	2	1	3	3
Sr	1	2	3	4	1	4
Ba	1	2	2	3	1	3

‡ Mean ± 2 standard deviations (data from Table 5.10)

As expected, the poorest discriminatory elements are the minor constituents as these influence the refractive index of a glass. Thus, glasses of similar compositions would be expected to possess similar refractive indices. The trace elements Fe, Ti, Sr and Ba offer the

best discrimination with both Fe and Sr capable of separating 4 glasses. The elements Ti and Ba split the glasses into 3 groups while Mn is the poorest trace element for discrimination purposes.

Iron is probably the most difficult element to determine as a result of contamination. However, it has been shown that a careful analytical technique can achieve a relative standard deviation of 0.05 or better for small glass fragments. This element can distinguish 4 of the glass samples examined here, additional confidence in the discrimination can be obtained by the incorporation of data from Sr, Ti, Ba and to a lesser extent Mn. Magnesium and Al are the most useful of the minor constituents for discrimination as in each case the 5 glasses examined here could be split into 2 groups.

5.3.4.3 Forensic Glass Standards

Analysts in the Forensic Science Service rely on the rapid, non-destructive capability of x-ray techniques. To achieve accuracy for a wide variety of sample types and element concentrations, a comprehensive set of standards is required. These standards may be unique for forensic science purposes and not commercially available. The excellent accuracy of the ICP-OES glass analysis method has been demonstrated and it seemed feasible, therefore, to attempt to characterise a set of glasses for use as standards by the x-ray techniques. The glasses selected for this trial were assumed to be homogeneous on the basis of previous work with large and small samples (Table 5.7).

A set of 7 glasses was selected to cover a range of element concentrations, these had been previously analysed by neutron activation analysis (NAA) (223) and wavelength dispersive x-ray fluorescence

spectrometry (WD-XRF) (224). During the course of this work the glasses were also analysed by scanning electron microscopy with energy dispersive x-ray analysis (SEM-EDXA) (225).

The results from these analysis are shown in Table 5.12, for completeness, K was determined in these glasses by atomic absorption spectrometry. The x-ray techniques show good agreement with ICP-OES (and AAS) for typical sheet glass concentrations but the agreement is poorer for certain elements in other glass samples. This is particularly noticeable for K, Al and Mg concentrations determined by SEM-EDXA with a standard of typical sheet glass composition (EC1.1, British Glass Industry Research Association, Sheffield, UK). An x-ray spectrum of this glass is shown in Figure 5.5. It has been determined that the K deviations result from a Si "pile up" peak, Al from incomplete charge collection and Mg from inaccuracies in the computer derived background (225). These problems can be largely overcome by the use of a set of standards with varying element concentrations which ICP-OES appears capable of providing. Compared to ICP-OES, the accuracy of the NAA determinations appears variable and up to 50% of these results may be incorrect.

5.3.5 Conclusions

An ICP-OES technique has been developed which offers excellent precision and accuracy for the determination of up to 9 elements in small glass fragments.

The technique has been shown to be valuable for the discrimination of glasses of similar refractive index. A set of 5 glasses could be readily distinguished by their multielement data using a simple discriminatory test. The best discriminating elements were Fe, Sr, Ba

Figure 5.5

SEM-EDXA Spectrum of a Standard Glass

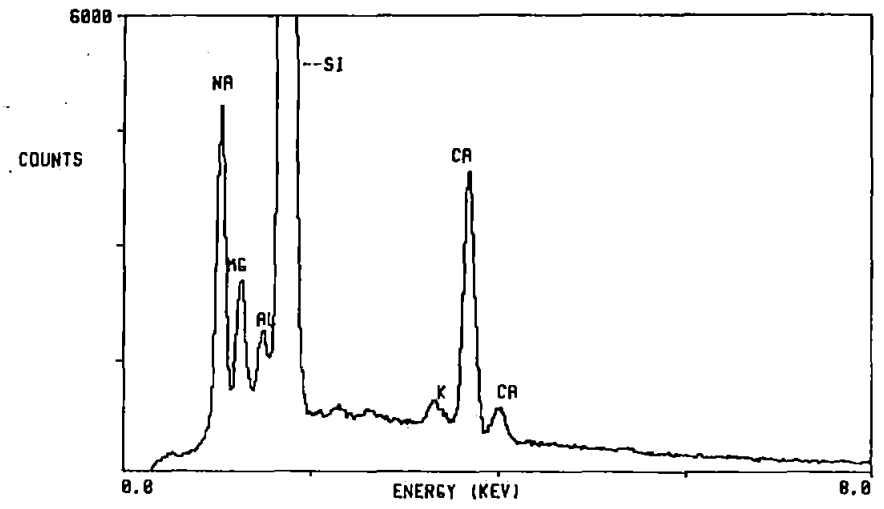

Table 5.12

Analytical Data for Potential Forensic Glass Standards

		H074	H093	H0101	H0125	H0201	H0254	H0316
Na %	NAA	7.88	9.58	9.70	10.50	9.39	9.38	10.80
	SEM	8.44	9.75	10.10	11.10	10.00	9.69	10.54
	ICP	8.70	10.22	9.86	11.31	10.25	10.56	10.63
K %	WD-XRF	-	0.66	-	0.02	0.42	0.58	0.25
	SEM	0.59	0.60	0.25	0.20	0.51	0.51	0.37
	AAS	0.60	0.64	0.12	0.06	0.40	0.58	0.23
Mg %	NAA	-	2.40	0.30	-	1.22	2.92	-
	WD-XRF	-	1.87	-	0.24	1.15	2.35	0.48
	SEM	0.11	1.88	0.21	0.25	1.05	2.39	0.37
	ICP	0.07	1.84	0.07	0.03	0.98	2.49	0.24
Al %	NAA	0.77	0.75	0.29	0.19	0.44	0.64	0.68
	SEM	0.77	0.73	0.38	0.37	0.72	0.65	0.70
	ICP	0.89	0.79	0.28	0.17	0.78	0.71	0.74
Ca %	NAA	8.62	6.59	11.90	9.57	7.36	5.70	7.44
	WD-XRF	-	6.15	-	8.65	7.08	5.65	8.44
	SEM	8.81	6.01	10.26	8.51	7.01	5.60	8.16
	ICP	8.96	6.25	10.26	8.78	6.93	6.07	8.41
Ba μgg^{-1}	NAA	201	127	122	60	1820	135	96
	ICP	175	137	43	43	1400	127	118
Fe μgg^{-1}	NAA	2030	1140	1340	675	995	1050	702
	ICP	1940	1180	1240	422	830	1075	585
Mn μgg^{-1}	NAA	65	69	66	20	57	104	36
	ICP	59	93	90	32	69	130	67
Sr μgg^{-1}	NAA	-	72	144	53	-	-	-
	ICP	76	51	234	43	70	40	68

and Ti; the most useful minor constituents were Mg and Al.

A range of well characterised glass samples has been shown to be essential for the acquisition of quantitative data by x-ray analytical techniques. The accuracy of the ICP-OES technique is sufficient to provide suitable potential standards which are not commercially available.

5.4 The Determination of Metals on Hands

5.4.1 Introduction

The analysis of hand swabs is sometimes performed in cases of suspected metal thefts. XRF is used routinely for the qualitative analysis of these swabbings and recent cases have involved the detection of Pb, Cu and Ag.

Quantitative analysis of hand swabs for Cu and Pb has been reported (226) together with qualitative detection of other metals. These workers used spark and arc spectrographic techniques and flameless AAS to determine expected levels of metal contamination amongst the general population and for specific groups of workers. The quantitative data obtained were shown to be valuable in assessing the significance of metal concentrations found on hands. The quantitative determination of Pb, Cu and Ni has also been reported using a solvent extraction technique followed by flame AAS (227).

The objective of this work was to assess the suitability of ICP-OES for the determination of Sb, Pb, Cd, Ni, Sn, Bi, Cu and Ag on hands. These elements were selected to cover a wide range of individual metals and low melting point alloys.

5.4.2 Experimental

5.4.2.1 Preparation of Swabs

Viscose swabs (~300 mg) moistened with nitric acid (1 ml, 1%) were used for this work. The swabs were placed in pre-cleaned polypropylene tubes, a nitric acid solution added (2.5 mls nitric acid

+ 6.5 mls water) and the tubes were then stoppered and shaken. The solutions were filtered before analysis. A multielement standard was prepared in the same acid concentration.

5.4.2.2 Sampling and Analysis

Metal concentrations were determined on the unwashed hands of some laboratory and workshop staff. Hands were then washed and a variety of metals briefly handled by different individuals.

5.4.3 Results and Discussion

The results obtained from five laboratory workers are shown in Table 5.13. These results indicate the low levels of detection for this technique. The extraction and analysis of these swabs was completed in 1 hour. Copper is obviously a common contaminant and probably originates from coinage, particularly when associated with Ni. Low levels of Cd were easily determined and probably arise from the surface treatment of metals. Table 5.14 shows results obtained from three staff after using workshop facilities. As expected, higher metal levels were obtained although the copper concentrations are still below the detection limit of the previously reported AAS technique (226). The high Cd concentrations obtained from B & C were traced to a tool drawer containing Cd treated components.

Table 5.13

Metals on Hands of Laboratory Workers

Worker	Sb	Pb	Cd	Ni	Sn	Bi	Cu	Ag
	(Total μg per pair of hands)							
A	<5	<3	0.3	<2	<4	<6	3	<0.4
B	<5	<3	0.4	<2	<4	<6	18	<0.4
C	<5	9	4.5	4	<4	<6	15	<0.4
D	13	<3	0.4	8	<4	<6	40	<0.4
E	<5	<3	1.7	<2	<4	<6	5	<0.4

Table 5.14

Metals on Hands of Workshop Users

Worker	Sb	Pb	Cd	Ni	Sn	Bi	Cu	Ag
	(Total μg per pair of hands)							
A	11	8	2	5	21	<6	21	<0.4
B	11	24	55	9	48	<6	5	<0.4
C	7	11	138	<2	12	<6	48	<0.4

The metals selected for the handling trial are shown in Table 5.15 and results from the brief handling of these samples are shown in Table 5.16. The low elemental concentrations found after handling the Cu rod and the counterfeit coin provide little useful information. The Ag concentration, although low in most cases, could have potential value. Lead and Sn were detected after solder was handled and Bi, Sn and Cd after handling the heat fuse. Antimony, Pb and Sn were detected following handling of the Sn based whitemetal. The data for the heat fuse and whitemetal suggest that the major constituents of an alloy may be inferred from this type of investigation.

Table 5.15

Metal Samples used for Handling Trial

Metal	Composition
Copper rod	High purity
Silver rod	High purity
Solder	70% Pb, 30% Sn
Whitemetal block	74.7% Sn, 11.5% Sb, 10.2% Pb, 3.4% Cu
Counterfeit 50p coin	63.0% Sn, 22.0% Bi, 12.7% Pb, 4.0% Sb
Centinel heat fuse	53.9% Bi, 25.9% Sn, 20.2% Cd

Table 5.16

Metals Determined in Handling Trial

Metal Handled	Sb	Pb	Cd	Ni	Sn	Bi	Cu	Ag
	(Total µg per pair of hands)							
Copper rod	<5	5	0.5	<2	< 4	<6	32	0.9
Silver rod	<5	5	0.6	<2	<4	<6	4	13
Solder	<5	20	0.4	<2	15	<6	3	<0.4
Whitemetal	65	47	15	<2	137	<6	22	<0.4
Counterfeit coin	<5	6	3	<2	10	<6	10	<0.4
Heat fuse	6	11	169	3	196	320	11	<0.4

5.4.4 Conclusions

Good detection limits have been demonstrated for the determination of eight metals on hands by ICP-OES. The method is rapid and could be readily extended to include other metals if required. The quantitative data obtained can assist the interpretation of casework results, provided suitable survey data are available.

5.5 A Proposed Method for the Quantitative Multielement Analysis of White Household Gloss Paints

5.5.1 Introduction

The evidential value of white household gloss paints has presented a perennial problem to forensic scientists because of the ubiquitous nature and similar formulations of these finishes. Forensic paint samples usually occur as chips or flakes but may be encountered as smears of fresh or dried paint. The chips or flakes can arise from force applied to a painted surface while smears are usually the result of glancing blows.

A typical brilliant white gloss paint contains 28-31% titanium dioxide pigment suspended in an oil modified alkyd resin with a white spirit solvent. The rate of drying of these paints can be modified by the addition of metal catalysts (as naphthenates or octoates) which promote the polymer crosslinking in the resin. Cobalt and manganese are "surface" or primary driers whereas secondary or "through" driers are lead, zinc, calcium and zirconium. The action of these driers does not cease when the paint film is dry and it eventually contributes to the breakdown of the film.

Both XRF and SEM-EDXA have been reported to offer good discrimination for small paint samples (70,228). Using NAA, up to 18 elements have been determined in 10 mg samples of white paints (229) but this is not a feasible casework technique because of cost and availability. Furnace AAS is reported to have given good discrimination for 2 collections of white paints following the determination of Pb and Co in 50 μg samples (230). However, this is a single element analytical technique and few forensic science laboratories possess the

facilities for this type of analysis.

The objective of this work was to re-assess the quality of information available from white household gloss paints using ICP-OES.

5.5.2 Experimental

5.5.2.1 Preparation of Dry Paint Films

The liquid paints were stirred by hand for a few minutes then painted onto pre-cleaned PTFE sheets. After a week the paint samples were peeled off and sealed in nylon bags.

5.5.2.2 Dissolution of Paint Samples

Samples of dried paint film (2 mg) were ashed in silica crucibles (500^{o}C for 1 hour). The crucibles were allowed to cool and the ashed material transferred to clean, screw capped PTFE tubes (34). A hydrofluoric/hydrochloric acid mixture (0.3 ml conc. HF + 0.2 ml conc. HCl) was pipetted onto the samples, the tubes capped then placed in an air oven at 100^{o}C for 1 hour. After cooling, distilled water (5 ml) was added, the tubes shaken then retained for analysis. All analyses were performed in triplicate using the previously stated conditions.

5.5.3 Results and Discussion

The analytical results from 3 samples of white gloss paints are shown in Table 5.17 and the results from 3 samples of brilliant white gloss paints are shown in Table 5.18.

Table 5.17

Analytical Data for White Household Gloss Paint Samples+

Element	Wavelength nm	Permoglaze	Brolac	Ripolin
Ti %	334.9	22.0	18.2	18.3
Ca %	396.9	0.29	0.18	0.74
Pb %	220.3	0.38	0.32	0.37
Zn %	213.8	0.25	0.003	0.01
Mg $\mu g g^{-1}$	285.2	745	320	3300
Co $\mu g g^{-1}$	237.8	580	450	420
Mn $\mu g g^{-1}$	257.6	< 50	< 50	< 50
Zr $\mu g g^{-1}$	343.8	630	440	650
Sr $\mu g g^{-1}$	407.7	< 50	< 50	< 50
Ba $\mu g g^{-1}$	455.4	< 50	60	50
Nb $\mu g g^{-1}$	269.7	930	< 50	350

+ Means of triplicate determinations.

Titanium dioxide concentrations are closely controlled by manufacturers for all white paints and the brilliant whites have a significantly higher concentration of this pigment. The stirring time employed in this work was obviously not sufficient to resuspend all the TiO_2 pigment (particularly as some of the paints were old), therefore the Ti concentrations cannot be used to distinguish white from brilliant white paints. However, these variations could be useful for the discrimination of these paints. The organo metallic driers Co, Ca, Pb, Zn and Zr appear useful for discrimination, in addition, the Ripolin

and Carson Hadfield paints contain high concentrations of Mg and Ba respectively. In this limited set of paint samples, additional discrimination is possible from the Nb concentrations but the trace elements Mn and Sr are of little use.

Table 5.18

Analytical Data for Brilliant White Household Gloss Paint Samples+

Element	Wavelength nm	B & Q Non drip	Macpherson	Carson Hadfields Non drip
Ti %	334.9	25.4	22.5	24.2
Ca %	396.9	0.12	0.14	0.13
Pb %	220.3	0.09	0.29	0.26
Zn $\mu g g^{-1}$	213.8	270	95	1500
Mg $\mu g g^{-1}$	285.2	205	315	270
Co $\mu g g^{-1}$	237.8	450	440	125
Mn $\mu g g^{-1}$	257.6	<50	<50	145
Zr $\mu g g^{-1}$	343.8	1600	590	815
Sr $\mu g g^{-1}$	407.7	<50	<50	120
Ba $\mu g g^{-1}$	455.4	<50	<50	6700
Nb $\mu g g^{-1}$	269.7	155	130	205

+ Means of triplicate determinations.

The sample concentration used for these analyses ($\sim$360 $\mu g\ ml^{-1}$) is higher than would normally be available from casework paint fragments. These solutions could be more dilute by a factor of 5-10 and thus some loss of element information is inevitable. However, it is unlikely that this will affect the more useful elements e.g. Ti, Ca, Zn, Pb and

the elements which have been deliberately added e.g. Nb, Mg, Zr and Ba could still be quantitatively determined.

5.5.4 Conclusions

A technique has been developed which appears capable of the quantitative multielement analysis of small fragments of white household gloss paints. The limited number of samples examined here indicate that excellent discrimination should be possible for these common finishes. However, this could only be confirmed following a survey of a large collection of samples.

Inductively coupled plasma - optical emission spectrometry is obviously a destructive analytical technique and is only suitable for the analysis of single layer paints as the separation of multiple layers is impractical for small casework fragments. The quantitative multielement capability is a valuable addition to forensic analysis either for use in selected cases or for the characterisation of a range of white paints for use as standards by the x-ray techniques.

5.6 Overall Conclusions

The sensitive, multielement nature of ICP-OES has been shown to be suitable for the analysis, classification and discrimination of a wide variety of evidential materials encountered by forensic scientists. Because of its relative freedom from interferences and extended dynamic range, ICP-OES can be used for the quantitative determination of both trace elements and major constituents with only a few simple standards being required for calibration purposes.

The destructive and time consuming nature of ICP-OES analysis

may detract from its routine use in forensic analysis. However, it is both independant of and complementary to the existing x-ray methods and can provide well characterised materials for use as standards by these techniques.

6 CONCLUSIONS AND RECOMMENDATIONS

An evaluation of ICP-OES was initiated at the Central Research Establishment of the Home Office Forensic Science Service (CRE-HOFSS) to assess the potential of the technique for forensic analysis. Preliminary studies indicated ICP-OES to be a promising multielement analytical technique for the small samples encountered in forensic science casework and thus a full evaluation was undertaken.

Simplex optimisation, using a suitable objective function, was shown to be valuable for the multielement optimisation of ICP-OES. A plasma torch fitted with a wide bore injector tube was identified as more appropriate for multielement analysis than a similar system fitted with a narrow bore injector. This was a result of its more compact analytical region. In addition, the effects of easily ionisable element (EIE) interferences were studied and the injector gas flow rate shown to be the most critical parameter for the location of an interference free zone. This zone was readily located with an interference minimisation simplex optimisation and exhibited a small degradation in detection limit performance when compared to the optimum values. Routine, interference free determinations (<2% for 0.5% Na) were shown to be critically dependant on the stability of the injector gas flowrate and nebuliser derived pressure pulses.

The application of multielement simplex optimisation to ICP-OES could be enhanced by the availability of suitable computer software. Ideally, this would be incorporated in a suite of programs supplied by the instrument manufacturer and would permit rapid data acquisition and calculation of suitable objective functions.

Two liquid sample introduction techniques were developed and evaluated for the analysis of small fragments of a variety of metal

alloys. A discrete nebulisation technique was applied to the rapid, multielement analysis of 100 µl solution droplets using polychromator detection. Although some degradation in detection limit performance was obtained compared to continuous introduction, an overall gain in performance was achieved for solid samples as a result of reduced dilution factors. The incorporation of flow injection would enable routine, automated analyses to be performed on the small solution samples studied here.

A compact, corrosion resistant recirculating nebuliser was constructed and shown to be simple to use and permit rapid sample changes with negligible contamination and dilution effects. This system was shown to be valuable for the analysis of small fragments of shotgun steels. The scanning monochromator was used for these determinations as alternative analytical lines free from Fe interference were required. The PTFE construction of this nebuliser permitted the determination of Si following hydrofluoric acid digestion and thus glasses and other refractory materials could be analysed. The performance of this nebuliser was poorer than the conventional pneumatic devices but could be improved by the incorporation of a better designed nebuliser tube. The PTFE construction precluded accurate positioning of the gas orifice and solution uptake tube as a result of the relatively soft nature of this polymer. Alternative materials may enable a more robust, precision engineered nebuliser tube to be produced which should exhibit better performance.

Inductively coupled plasma - optical emission spectrometry has been shown to be a sensitive, multielement, interference free technique for the analysis, classification and discrimination of a wide variety of evidential materials encountered by forensic scientists. The destructive and somewhat time consuming nature of the technique,

together with high equipment costs, may detract from its routine use in operational forensic science laboratories. However, operation of ICP-OES as a central service facility could improve the analytical capability of the operational laboratories by providing a variety of well characterised materials as standards to support x-ray techniques currently employed. In addition, the acquisition of quantitative survey data could assist the interpretation of casework results and the central service would be available for quantitative multielement analyses which could not be performed by existing techniques.

Appendix A

Radio Frequency Generator HFP 2500D

Supplier	Plasma Therm Inc. Kresson, N.J., USA.
Max. power output	2.5 kW
Output impedance	50 ohms
Frequency	27.12 M Hz
Frequency stability	0.05%
Auto. power control	APCS-3
Auto. impedance matching	AMNPS-1
Induction coil	3 turn copper
Cooling water	25 litres $hour^{-1}$
Gas supplies	High purity argon

Appendix B

Scanning Monochromator and Computer Control

Supplier	Bentham Inst., Reading, UK.
Model	M1000
Configuration	Symmetrical Czerny - Turner
Focal length	1 metre
Aperture	f8
Diffraction grating	90mm x 90mm plain Holographic. 1800 lines mm^{-1}.
Dispersion	0.57 nm mm^{-1}.
Spectral range	190 - 800 nm
Slit widths	20 μm entrance, 20 μm exit
Resolution (FWHM)	0.02 nm
Photomultiplier	EMI 9558 QB
EHT Supply	Bentham model 215
Amplifier	Bentham model 210E
Computer	PDP 11/03 MINC, VT 105 Terminal, RX02 Floppy Disc Drive. (Digital Equipment Corporation)
Stepping motor drive	Bentham SMD 3B controlled by MINC-11
Slewing speed	6.6 nm sec^{-1}
Data acquisition	MINC-11 via Bentham model 228 Integrating ADC
Printer	Paper Tiger IDS-440 (Integral Data Systems Inc., Natick, Mass., USA)

Appendix C

Polychromator Details

Supplier	Optical Emission Services, Milton Keynes, UK.
Model	OES 4500
Configuration	Paschen - Runge
Focal length	1 metre
Diffraction grating	Concave holographic, 1800 lines mm^{-1}
Dispersion	0.54 nm mm^{-1}
Spectral range	195 - 500 nm. (Fibre optics used for higher wavelengths e.g. for alkali metals)
Slit widths	30 μm entrance, 50 or 100 μm exit
Resolution (FWHM)	0.07 nm
Photomultipliers	Hamamatsu R750 and R763 (red)
EHT supply	Brandenburg Model 378
Computer	S100 Single Board Microcomputer containing Z80 Microprocessor. 56K memory, CP/M Operating System. (SD Systems, Dallas, Texas, USA)
Printer	Paper Tiger IDS-440. (Integral Data Systems Inc., Natick, Mass., USA)

Appendix D

Presentations and Publications

Resulting from the work reported in this thesis the following papers have been presented and published.

a. Presentations

1. R.C. Carpenter
   ICP Research at CRE. 1982, Colloquium on Multielement Analysis, Tadley, UK.
2. R.C. Carpenter
   Inductively Coupled Plasma - Optical Emission Spectrometry (ICP-OES) in Forensic Research. 1982, First Biennial Atomic Spectroscopy Symposium, Sheffield, UK.
3. R.C. Carpenter
   ICP Data Processing at CRE. 1983, Colloquium on Data Processing in ICP-OES, AWRE, Tadley, UK.
4. R.C. Carpenter
   Inductively Coupled Plasma - Optical Emission Spectrometry (ICP-OES) in Forensic Science - The analysis of Small Samples of Brasses. 1983, SAC '83, Edinburgh, UK.
5. R.C. Carpenter
   The Analysis of Evidential Materials by Inductively Coupled Plasma - Optical Emission Spectrometry. 1984, International Association of Forensic Scientists, Oxford, UK.

b. Publications

1. R.C. Carpenter and C. Till

   The Analysis of Small Samples of Brasses by Inductively Coupled Plasma - Optical Emission Spectrometry and their Classification by Two Pattern-Recognition Techniques. Analyst, 109(1984)881.

2. R.C. Carpenter

   The Analysis of Some Evidential Materials by Inductively Coupled Plasma - Optical Emission Spectrometry. Forensic Sci. Int. 27(1985)157.

3. R.C. Carpenter

   The Analysis of Casework Sized Alloy Fragments by Inductively Coupled Plasma - Optical Emission Spectrometry (ICP-OES) Using Discrete Nebulisation. Forensic Sci. Int., 27(1985)165.

4. R.C. Carpenter and L. Ebdon

   A Comparison of Inductively Coupled Plasma Torch-Sample Introduction Configurations using Simplex Optimisation. In Preparation.

Appendix E

Programme of Related Studies

a. Directed Self-learning and Guided Reading.

Dr L. Ebdon. An Introduction to Atomic Absorption Spectrometry: A Self-teaching Approach. Heyden and Son Ltd., London, (1982)

R.M. Barnes. Emission Spectroscopy. Dowden, Hutchinson and Ross, USA, (1975)

R.M. Barnes, ed. Applications of Plasma Emission Spectrochemistry. Heyden and Son Ltd., USA, (1979)

S. Kind and M. Overman. Science Against Crime. Aldus Books, London, (1972)

G.F. Kirkbright and M. Sargent. Atomic Absorption and Fluorescence Spectroscopy. Academic Press, London, (1974)

G.F. Kirkbright, ed. Keynote Lectures, XXI Colloquium Spectroscopicum Internationale, 8th International Conference on Atomic Spectroscopy. Heyden and Son Ltd., London, (1979)

C. Liteanu and I. Rica. Statistical Theory and Methodology of Trace Analysis. Ellis Horwood Ltd., Chichester, (1980)

D.L. Massart, A. Dijkstra and L. Kaufman. Evaluation and Optimisation of Laboratory Methods and Analytical Procedures. Elsevier, Amsterdam, (1978)

K. Simpson. Forensic Medicine. Edward Arnold Ltd., London, (1969)

B.L. Sharp. High Frequency Electrodeless Plasma Spectrometry. Selected Annual Reviews of the Analytical Sciences, Vol. 4. Chemical Society, London, (1976)

F. Lundquist (Vols 1 and 2) and A.S. Curry (Vols 3 and 4). Methods in Forensic Science, Vols 1-4. J. Wiley and Sons Inc., USA, (1962-1965)

J.B. Dawson, B.L. Sharp, M.S. Cresser and L. Ebdon, eds. Annual Reports on Analytical Atomic Spectroscopy. Royal Society of Chemistry. London, (1978-1982)

b. Courses, Conferences and Meetings Attended.

Quality Assurance and Atomic Spectroscopy. ARAAS Symposium. 2/4/81, Sheffield, UK.

Environmental Sciences Symposium. 23/9/81, Plymouth, UK.

Computers in Forensic Science. CRE Colloquium. 29/1/82, Tadley, UK.

Pattern Recognition: Algorithms and Applications. RSC Meeting. 10/2/82, Birmingham, UK.

Multielement Analysis. CRE Colloquium. 26/2/82, Tadley, UK.

First Biennial National Atomic Spectroscopy Symposium. 13-15/7/82, Sheffield, UK.

ICP-AES Data Processing. AWRE Colloquium. 16/2/83, Tadley, UK.

Massage is the Message - Practical Applications of Data Manipulation. RSC Meeting. 2/3/83, London, UK.

Practical Statistics for Forensic Chemists. FSTU Course. 15-17/3/83, Cardington, UK.

SAC '83. RSC International Conference. 17-23/7/83, Edinburgh, UK.

Intelligent Instruments for Analysis. RSC Meeting. 26/10/83 Loughborough, UK.

International Association of Forensic Sciences. 25/9/84, Oxford, UK.

REFERENCES

1. J.A. Evans and W.N. Waller. J. Forensic Sci. Soc., 5(1965)189
2. G.L.F. Powell and R.R. Robinson. J. Forensic Sci., 23(1978)707
3. H.J. Kobus and R.J. Decker. Forensic Sci. Int., 15(1)(1980)67
4. G.L.F. Powell, R.R. Robinson, B. Cocks and M. Wright. J. Forensic Sci., 23(1978)712
5. E.C. Blacklock and P.A. Sadler. Clin. Chim. Acta, 113(1981)87
6. E.C. Blacklock, A. Rogers, C. Wall and B.B. Wheals. Forensic Sci., 7(2)(1976)121
7. K.A. Hausknecht, E.A. Ryan and L.P. Leonard. At. Spectroscopy, 3(2)(1982)53
8. O.W. Lau and K.L. Li. Analyst, 100(1975)430
9. T.R. Ashurbekov. Sud-Med. Ekspert, 17(4)(1974)23
10. P.J. Simon, B.C. Giessen and T.R. Copeland. Anal. Chem., 49(14)(1977)2285
11. J.C. Hughes, T. Catterick and G. Southeard. Forensic Sci., 8(1976)217
12. T. Catterick and C.D. Wall. Talanta, 25(1978)573
13. C.M.Hoffman, R.L. Brunelle and K.B. Snow. J. Crim. Law Criminol. Police Sci., 60(1969)395
14. K. Chaperlin. Forensic Sci. Int., 18(1)(1981)79
15. F.F. Farris, A. Poklis and G.E. Griesman. J. Assoc. Off. Anal. Chem., 61(3)(1978)660
16. J. Locke. Anal. Chim. Acta., 104(2)(1979)225
17. L. Pickston, J.F. Lewin, J.M. Drysdale, J.M. Smith and J. Bruce. J. Anal. Toxicol., 7(1983)2
18. R.C. Carpenter. Anal. Chim. Acta., 125(1981)209
19. E.C. Blacklock and P.A. Sadler. Forensic Sci. Int., 12(1978)109
20. L.R. Bednarczyk and W. Matusiak. J. Anal. Toxicol., 6(1982)260

21. J.L. Booker, D.D. Schroeder and J.H. Prapp. J. Forensic Sci. Soc., 24(2)(1984)81

22. Y.K. Chau, P.T.S. Wong, G.A.Bengert and J.L. Dunn. Anal. Chem., 56(2)(1984)271

23. J.A. Goleb and C.R. Midkiff. Appl. Spectrosc., 29(1975)44

24. M.L. Newbury. J. Can. Soc. Forensic Sci., 13(2)(1980)19

25. J.T. Newton. J. Forensic Sci., 26(2)(1981)302

26. G.D. Renshaw, C.A. Pounds and E.F. Pearson. At. Absorp. Newsletter, 12(2)(1973)55

27. J.F. Alder, D. Alger, A.J. Samuel and T.S. West. Anal. Chim. Acta, 87(1976)301

28. J.F. Alder, A.J. Samuel and T.S. West. Anal. Chim. Acta, 87(1976)313

29. Y. Marumo. Report Nat. Res. Inst. Police Sci., 33(2)(1978)38

30. V. Hudnick, M. Marolt-Gromiscek and S. Gromiscek. Anal. Chim. Acta, 157(1984)143

31. S.L. Gaffin and H. Hornung. Clin. Toxicol., 10(3)(1977)345

32. F.E. Leung and A.R. Henderson. At. Spectosc., 4(1)(1983)1

33. K.S. Subramanian and J.C. Meranger. Analyst, 107(1982)157

34. C.R. Howden, B. German and K.W. Smalldon. J. Forensic Sci. Soc., 17(1977)153

35. J.B. Headridge and I.M. Riddington. Analyst, 109(1984)113

36. K.W. Jackson and A.P. Newman. Analyst, 108(1983)261

37. A. Roy. National Gallery Technical Bull., 3(1978)43

38. R.C. Sullivan, C. Pompa, L.V. Sabatino and J.J. Horan. J. Forensic Sci., 19(1974)486

39. G.D. Ogilvie. Anal. Proc., 18(3)(1981)117

40. M.A. Haney and J.F. Gallagher. J. Forensic Sci., 20(1975)484

41. M.A. Haney. J. Forensic Sci., 22(3)(1977)534

42. M. Desjardins and J.P. Williams. J. Am. Ceramic Soc., 51(5) (1968)296

43. B. German, D. Morgans, A. Butterworth and A. Scaplehorn. J. Forensic Sci. Soc., 18(1/2)(1978)113

44. J. Locke, D. Boase and K.W. Smalldon. J. Forensic Sci. Soc., 18(1/2)(1978)123

45. A.M. Ure and J.R. Bacon. Analyst, 103(1978)807

46. J. Locke, D.R. Boase and K.W. Smalldon. Anal. Chim. Acta, 104(2)(1979)233

47. J. Locke, D.R. Boase and K.W.Smalldon. Med. Sci. Law, 20(3)(1980) 175

48. J.R. Bacon and A.M. Ure. Analyst, 109(1984)1229

49. R. Dybczynski and K. Boboli. J. Radioanal. Chem., 31(1976)267

50. K.K.S. Pillay and R.L. Kuis. J. Radioanal. Chem., 43(1978)461

51. C.J. Mash. MSc Thesis Dept. of Forensic Sciences, University of Strathclyde, 1968.

52. T. Singh and R.B. Singh. J. Indian Acad. Forensic Sci., 17(1)(1978)25

53. R.K.H. Chan. J. Forensic Sci., 17(1)(1972)93

54. J.N. Weaver and W. B. Bowman. J. Forensic Sci., 16(4)(1971)521

55. R.J. Caldwell. J. Forensic Sci. Soc., 10(1970)69

56. N.I. Ward and D.E. Ryan. Anal. Chim. Acta, 105(1979)185

57. P. Lievens, J. Versiek, R. Cornelis and J. Hoste. J. Radioanal. Chem., 37(1)(1977)483

58. J.D. Cross, I.M. Dale and H. Smith. Proc. Analyt. Div. Chem. Soc., 12(1975)223

59. R.A. Schmitt and V. Smith. J. Forensic Sci., 15(2)(1970)253

60. R.F. Coleman and N.T. Weston. J. Forensic Sci. Soc., 8(1)(1968)32

61. S.S. Krishnan. J. Forensic Sci., 12(1)(1967)112

62. V.P. Guinn. Anal. Chem., 51(4)(1979)484A

63. V.P. Guinn. J. Radioanal. Chem., 72(1-2)(1982)645

64. M. Jauhari. T. Singh and S.M. Chatterji. Forensic Sci. Int., 19(1982)253

65. M. Jauhari, T. Singh and S.M. Chatterji. Forensic Sci. Int., 22(1983)117

66. C.R. Howden, R.J. Dudley and K.W. Smalldon. J. Forensic Sci. Soc., 18(1/2)(1978)99

67. V. Reeve, J. Mathiensen and W. Fong. J. Forensic Sci., 21(2)(1976) 291

68. V. Reeve and T. Keener. J. Forensic Sci., 21(4)(1976)883

69. L.C. Haag. J. Forensic Sci. Soc., 16(3)(1976)255

70. C.R. Howden, R.J. Dudley and K.W. Smalldon. J. Forensic Sci. Soc., 17(2/3)(1977)161

71. J.C. West. X-ray Spectrom., 4(1975)71

72. S. Seta. Int. Crim. Police Review, (1977)119

73. E.L. Covey. J. Forensic Sci., 22(2)(1977)325

74. P. Verbeke, H. Nullens and F. Adams. Proc. Anal. Div. Chem. Soc., 15(1)(1978)18

75. G.M. Wolten, R.S. Nesbitt, A.R. Calloway, G.L. Loper and P.F. Jones. J. Forensic Sci., 24(2)(1979)409

76. P.R. Oumo and E. Nieboer. Analyst, 104(1979)1037

77. L.W. Thomas and I.H. Heitur. J. Tappi, 61(5)(1978)57

78. P.J. Nolan, M. England and C. Davies. Scanning Electron Microscopy, 2(1982)599

79. J.W. Simmelink, J.W. Robinson and L.S. Staikoff. J. Forensic Sci., 26(4)(1981)686

80. S. Seta, H. Sato and M. Yoshino. Scanning Electron Microsc., 2(1979)193

81. T.Y. Toribara, D.A. Jackson, W.R. French, A.C. Thompson and J.M. Jaklevic. Anal. Chem., 54(1982)1844

82. E. Searle and C.M. Thompson. Analyst, 108(1983)254

83. I.M. Zsolnay, J.M. Brauer and S.A. Sojka. Anal. Chim. Acta, 162(1984)423

84. A. Walsh. Spectrochim. Acta, 7(1955)108

85. S. Greenfield, I.L. Jones and C.T. Berry. Analyst, 89(1964)713

86. R.H. Wendt and V.A. Fassel. Anal. Chem., 37(1965)920

87. A.F. Ward. ICP Inf. Newsl., 5(1980)448

88. R.M. Barnes. Trends Anal. Chem., 1(2)(1981)51

89. R.M. Barnes (ed.). Applications of Plasma Emission Spectrochemistry. Heyden and Son Ltd., USA, (1979)

90. R.M. Barnes (ed.). Developments in Atomic Plasma Spectrochemical Analysis. Heyden and Son Ltd., USA, (1981)

91. R.S. Houk, H.J. Svec and V.A. Fassel. Appl. Spectrosc., 35(4)(1981) 380

92. M.W. Blades. Spectrochim. Acta, 37B(10)(1982)869

93. M.W. Blades and G. Horlick. Spectrochim. Acta, 36B(9)(1981)881

94. J.A.C. Broekaert. Trends Anal. Chem., 1(1982)249

95. D.M. Lawrence. Appl. Spectrosc., 6(1)(1985)23

96. P.N. Keliher, W.J. Boyko, J.M. Patterson and J.W. Hershey. Anal. Chem., 56(5)(1984)133R

97. J. Locke. Anal. Chim. Acta, 113(1980)3

98. T. Catterick and D.A. Hickman. Analyst, 104(1979)516

99. T. Catterick and D.A. Hickman. Forensic Sci. Int., 17(1981)253

100. D.A. Hickman. Forensic Sci. Int., 17(1981)265

101. T. Catterick. Analyst, 109(1984)1465

102. R.C. Carpenter. Forensic Sci. Int., 27(1985)157

103. R.C. Carpenter and C. Till. Analyst, 109(1984)881

104. R.C.Carpenter. Forensic Sci. Int., 27(1985)165

105. G.I. Babat. J. Inst. Elec. Eng., 94(1947)27

106. T.B. Reed. J. Appl. Phys., 32(5)(1961)821

107. T.B. Reed. J. Appl. Phys., 32(12)(1961)2534

108. T.B. Reed. Int. Sci. Technol., June 1962,42

109. S. Greenfield, I.L. Jones, H.McD. McGeachin and P.B. Smith. Analyst, 89(1964)713

110. R.H. Wendt and V.A. Fassel. Anal. Chem., 37(1965)920

111. G.W. Dickinson and V.A. Fassel. Anal. Chem., 41(1969)1021

112. J.C. Souilliart and J.P. Robin. Analusis, 1(1972)413

113. P.W.J.M. Boumans and F.J. de Boer. Spectrochim. Acta, 27B(1972)391

114. R.H. Scott, V.A. Fassel, R.N. Knisely and D.E. Nixon. Anal. Chem., 46(1)(1974)75

115. Digital Equipment Corporation. Laboratory Subroutines Manual, 1978.

116. R.P.J. Duursma, H.C. Smit and F.J.M.J. Maessen. Anal. Chim. Acta, 133(1981)393

117. L.R.P. Butler. Spectrochim. Acta, 33B(5/6)(1983)913

118. H. Kaiser and A.C. Menzies. The Limit of Detection of a Complete Analytical Procedure. Adam Hilger, London(1968)

119. R.K. Winge, V.J. Peterson and V.A. Fassel. Appl. Spectrosc., 33(1979)206

120. C.E. Taylor and T.L. Floyd. Appl. Spectrosc., 34(1980)472

121. G.R. Harrison. Wavelength Tables. MIT Press, USA(1963)

122. P.W.J.M. Boumans. Line Coincidence Tables for Inductively Coupled Plasma Atomic Emission Spectrometry. Pergamon Press, Oxford(1980)

123. G.F. Larson, V.A. Fassel, R.K. Winge and R.N. Kniseley. Appl. Spectrosc., 30(4)(1976)384

124. V.A. Fassel, J.M. Katzenberger and R.K. Winge. Appl. Spectrosc., 33(1)(1979)1

125. G. Horlick and M.W. Blades. Appl. Spectrosc., 34(2)(1980)229

126. J.P. Rybarczyk, C.P. Jester, D.A. Yates and S.R. Koirtyohann. Anal. Chem., 54(1982)2162

127. R.A. Isaac and W.C. Johnson. J. Assoc. Off. Anal. Chem., 58(1975)436

128. E.I. Hamilton, M.J. Minski and J.J. Cleary. Sci. Total Environ., 1(1972/73)341

129. M.M. Platts, G.C. Goode and J.S. Hislop. Brit. Med. J., (1977)657

130. H.L. Elliot, F. Dryburgh, G.S. Fell, S. Sabet and A.I. MacDougall. Brit. Med. J., (1978)1101

131. A.C. Alfrey, G.R. Legendre and W.D. Kaehny. New England J. of Med., (1976)184

132. S. Greenfield and D. Thorburn Burns. Spectrochim. Acta, 34B(1979)423

133. S. Greenfield and D. Thorburn Burns. Anal. Chim. Acta, 113(1980)205

134. J. Kragten and A. Parczewski. Talanta, 28(1981)901

135. W. Spendley, G.R. Hext and F.R. Himsworth. Technometrics, 4(1962)441

136. D.E. Long. Anal. Chim. Acta, 46(1969)193

137. J.A. Nelder and R. Mead. Comput. J., 7(1965)308

138. S.L. Morgan and S.N. Deming. Anal. Chem., 46(9)(1974)1170

139. S.L. Morgan and S.N. Deming. J. Chromatog., 112(1975)267

140. L.A. Yarbro and S.N. Deming. Anal. Chim. Acta, 73(1974)391

141. R.G. Michel, J. Coleman and J.D. Winefordner. Spectrochim. Acta, 33B(1977)195

142. M.R. Cave, D.M. Kaminaris, L. Ebdon and D.J. Mowthorpe. Anal. Proc., (1981)12

143. L. Ebdon, M.R. Cave and D.J. Mowthorpe. Anal. Chim. Acta, 115(1980)179

144. S.P. Terblanche, K. Visser and P.B. Zeeman. Spectrochim. Acta, 36B(4)(1981)293

145. J.J. Leary, A.E. Brookes, A.F. Dorrzapf and D.W. Golightly, Appl. Spectrosc., 36(1)(1982)37

146. A.P. Wade. Anal. Proc., 20(1983)108

147. S.L. Harper, J.F. Walling, D.M. Holland and L.J. Pranger. Anal. Chem., 55(1983)1553

148. J.T. McCaffrey and R.G. Michel. Anal. Chem., 55(1983)2175

149. G.L. Moore, A.E. Watson and G.M. Russell, NIM Report 2116,(1981)

150. A. Montaser, G.R. Huse, R.A. Wax, S.K. Chan, D.W. Golightly, J.S. Kane and A.F. Dorrzapf. Anal. Chem., 56(1984)283

151. R.J. Lukasiewicz and F.G. Dewalt. ICP Inf. News, 9(11)(1984)730

152. P.B. Ryan, R.L. Barr and H.D. Todd. Anal. Chem., 52(1980)1460

153. E.R. Aberg and A.G.T. Gustavsson. Anal. Chim. Acta, 144(1982)39

154. P.F.A. Van Der Wiel, R. Maassen and G. Kateman. Anal. Chim. Acta, 153(1983)83

155. P. Norman. Private Communication

156. G.F. Wallace. Atomic Spectrosc. 4(5)(1983)188

157. P.W.J.M. Boumans and M.Ch. Lux-Steiner. Spectrochim. Acta, 37B(1982)97

158. M.W. Blades and G. Horlick. Spectrochim. Acta, 36B(9)(1981)861

159. P.W.J.M. Boumans and F.J. De Boer. Spectrochim. Acta, 30B(1975)309

160. S.S. Berman and J.W. McLaren. Appl. Spectrosc., 32(4)(1978)372

161. F.O. Bamiro, D. Littlejohn, J. Marshall and J.M. Ottaway. Anal. Proc. 20(1983)602

162. L. Ebdon. Developments in Atomic Plasma Spectrochemical Analysis (ed. R. Barnes). Heyden and Son Ltd., USA, (1981)

163. A. Montaser, V.A. Fassel and J. Zalewski. Appl. Spectrosc., 35(3)(1981)292

164. G.L. Moore, P.J. Humphries-Cuff and A.E. Watson. Spectrochim. Acta, 39B(7)(1984)915

165. H. Kawaguchi, T. Ito and A. Mizuike. Spectrochim. Acta, 36B(1981)615

166. T.E. Edmonds and G. Horlick. Appl. Spectrosc., 31(6)(1977)536

167. S.R. Koirtyohann, J.S. Jones and D.A. Yates. Spectrochim. Acta, 36B(1981)49

168. L.M. Faires, C.T. Apel and T.M. Niemczyk. Appl. Spectosc., 37(6)(1983)558

169. Y. Nojiri, K. Tanabe, H. Uchida, H. Haraguchi, K. Fuwa and J.D. Winefordner. Spectrochim. Acta, 38B(1983)61

170. B.L. Caughlin and M.W. Blades. ICP Inf. News, 10(1)(1984)17

171. G.M. Hieftje and J.W. Carr. ICP Inf. News, 10(1)(1984)19

172. G. Horlick and E.H. Choot. ICP Inf. News, 10(1)(1984)21

173. M.I. Boulos and R.M. Barnes. Developments in Atomic Plasma Spectrochemical Analysis (ed. R.M. Barnes). Heyden and Son Ltd., USA, (1981)

174. J.W. Mills and G.M. Hieftje. Spectrochim. Acta, 39B(7)(1984)859

175. M.R. Cave. PhD Thesis. CNAA, Sheffield City Polytechnic, (1980)

176. S.R. Koirtyohann, J.S. Jones and D.A. Yates. Anal. Chem., 52(1980)1966

177. H. Uchida. Spectrosc. Lett., 14(10)(1981)665

178. S.A. Myers and D.H. Tracy. ICP Inf. News., 7(4)(1981)162

179. R.L. Belchamber and G. Horlick. Spectrochim. Acta, 36B(1981)581

180. R.L. Belchamber and G. Horlick. Spectrochim. Acta, 37B(1982)1075

181. D.D. Smith and R.F. Browner. Anal. Chem., 54(1982)533

182. T. Uchida, I. Kojima and C. Iida. Anal. Chim. Acta, 116(1980)205

183. D.C. Manning. Atomic Abs. News., 14(1975)99

184. A. Eaton and E. Schiemer. Atomic Abs. News., 17(1978)113

185. P.D. Goulden. Atomic Abs. News., 16(1977)121

186. K.C. Thompson and R.G. Godden. Analyst, 101(1976)96

187. T. Catterick and C.D. Wall. Talanta, 25(1978)573

188. S. Greenfield and P.B. Smith. Anal. Chim. Acta, 59(1972)341

189. R.N. Kniseley, V.A. Fassel and C.C. Butler. Clin. Chem., 19(1973)807

190. J.A.C. Broekaert and F. Leis. Anal. Chim. Acta, 109(1979)73

191. J.A.C. Broekaert, F. Leis and K. Laqua. Fresenius Z. Anal. Chem., 301(1980)105

192. H. Uchida, Y. Nojiri, H. Haraguchi and K. Fuwa. Anal. Chim. Acta, 123(1981)57

193. A.F. Ward and L.F. Marciello. Anal. Chem., 51(1982)2264

194. J. Ruzicka and E.H. Hansen. Anal. Chim. Acta, 99(1978)37

195. S. Greenfield. Spectrochim. Acta, 38B(1983)93

196. J. Novak. Anal. Chem., 52(1980)576

197. P. Hulmston. Analyst, 108(1983)166

198. Z.Z. He and R.M. Barnes. Spectrochim. Acta, 40B(1985)11

199. P. Hulmston. Analyst, 110(1985)559

200. G.L. Moore, P.J. Humphries-Cuff and A.E. Watson. ICP Inf. News., 9(1984)763

201. O.G. Raabe. Proc. Conf. on Inhalation Carcinogenesis, Gatlinburg, Tenn., 1969

202. R.T. Drew and D.M. Bernstein. J. Toxicol. Environ. Health, 4(1978)661

203. M. Halpern, R.B. Schlesinger and M. Lippmann. Am. Ind. Hyg. Assoc. J., 41(11)(1980)843

204. V.K. Mer and R. Gruen. Trans. Faraday Soc., 48(1952)410

205. P.A.M. Ripson and L. de Galan. Anal. Chem., 55(1983)372

206. S. Greenfield, H. McD. McGeachin and P.B. Smith. Anal. Chim. Acta, 84(1976)67

207. L. Ebdon and M.R. Cave. Analyst 107(1982)172

208. S. Nukiyama and Y. Tanasawa. Trans. Soc. Mech. Eng. Jpn., 4,5,6(1938-1940)

209. D.F. Rendle. J. Forensic Sci., 26(1981)343

210. D.C. Olivier. Dept. of Psychology and Social Relations, Harvard University, Cambridge, MA, USA, 1973

211. J.W. Sammon. IEEE Trans. Comput., C-18(1969)401

212. D.F. Nelson and B.C. Revell. J. Forensic Sci. Soc., 7(1967)58

213. C.A. Pounds and K.W. Smalldon. J. Forensic Sci. Soc., 18(1978)197

214. F. Becke. Sitzung. K. Akad. Wiss. (Vien.),102(1893)358

215. J. Locke, D.G. Sanger and G.Roopnarine. Forensic Sci. Int.,20(1982)295

216. J. Locke and L.A. Rocket. Forensic Sci. Int., In press

217. J. Locke. The Microscope, 32(1984)1

218. B.R. Elliott, D.G. Goodwin, P.S. Hamer, P.M. Hayes, J. Locke and M. Underhill. Forensic Sci. Int., In press

219. D.A. Hickman, G. Harbottle and E.V. Sayre. Forensic Sci. Int., 23(1983)189

220. D.A. Hickman. Forensic Sci. Int., 23(1983)213

221. H. Uchida, T. Uchida and C. Iida. Anal. Chim. Acta, 108(1979)87

222. D.A. Hickman. Anal. Chem., 56(1984)844A

223. G.C. Goode, G.A. Wood, N.M. Brooke and R.F. Coleman. AWRE Report No. 024/71 (1971)

224. C.R. Howden, R.J. Dudley and K.W. Smalldon. Private communication.

225. D. Burt. Private communication.

226. G.D. Hudson and S.J. Butcher. J. Forensic Sci. Soc., 14(1974)9

227. I. Scott. Private communication.

228. J.M. Dubery. Private communication.

229. S.S. Krishnan. J. Forensic Sci., 21(1976)908

230. C.D. Wall. PhD Thesis (1977) University of London

231. J.A. Lambert. Private Communication.

232. J. Locke and M. Underhill. Forensic Sci. Int., 27(1985)247

Forensic Science International, 27 (1985) 165—170
Elsevier Scientific Publishers Ireland Ltd.

THE ANALYSIS OF CASEWORK SIZED ALLOY FRAGMENTS BY INDUCTIVELY COUPLED PLASMA-OPTICAL EMISSION SPECTROMETRY (ICP-OES) USING DISCRETE NEBULISATION

R.C. CARPENTER

Central Research Establishment, Home Office Forensic Science Service, Aldermaston, Reading, Berkshire RG7 4PN (U.K.)

(Received June 6, 1984)
(Revision received November 16, 1984)
(Accepted December 17, 1984)

Summary

A discrete nebulisation technique has been developed for the multi-element analysis of 100-μl solution droplets by inductively coupled plasma-optical emission spectrometry (ICP-OES). The technique increases analytical speed and uses very small solution volumes with only a slight degradation in detection limits when compared to continuous solution introduction.

To evaluate its suitability in casework, small alloy fragments were produced by cutting with a hacksaw, sample division and filing. The analysis of fragments from two different brasses indicated that quantitative data could be obtained from fragments as small as 10 μg. The accurate determination of lead, a non-homogeneous constituent of leaded brasses, required sample sizes an order of magnitude greater. Analysis of an alloy of fine grain structure (copper-nickel) demonstrated that quantitative data could be obtained from samples weighing a few micrograms or less.

Key words: Analysis; Alloy fragments; Inductively coupled plasma arc spectrometry

Introduction

Inductively coupled plasma-optical emission spectrometry (ICP-OES) has recently been used for the analysis of 100-μg samples of a collection of brass items [1]. Quantitative data from traces to major constituents were obtained following dissolution of the samples in 1 ml of acid solution. The necessity for using a minimum volume of solution of this order can lead to unacceptably large dilution factors. This can be a particular problem if samples of 10 μg or less are analysed.

An alternative technique for analysing small samples, and which has been utilised very successfully with atomic absorption spectrometry (AAS), is discrete nebulisation of small solution droplets. Discrete nebulisation/AAS has been applied to the analysis of biological materials [2], plant tissue digests [3], sediments [4], waters [5], steels [6], and glass fragments for forensic science purposes [7]. The method has normally been used either to avoid nebuliser/burner clogging when analysing solutions containing a

0379-0738/85/$03.30

high concentration of dissolved solids or for multi-element analyses on small volumes of solutions. The feasibility of the direct analysis of microsamples using a high power ICP was demonstrated as long ago as 1972 [8]. Little work has been reported with low power ICPs because the sudden entrainment of air which occurs between samples could cause plasma instability. This problem has, however, been overcome by the use of argon flushed microsampling cups [9].

More recently, a simpler system has been reported using teflon (PTFE) sampling cups and rapid manual transfer of the nebuliser tube between sample droplets and wash solutions [10].

The evaluation of ICP-OES for the analysis of evidential materials is continued in this work with the investigation of a discrete nebulisation technique for alloy fragments of the size normally encountered in casework.

Experimental

Instrumentation

An argon ICP and a 1-m polychromator [11] were used. The sample introduction system described there was modified by fitting a corrosion resistant nebuliser, spray chamber and demountable torch (Perkin Elmer Ltd, Beaconsfield, Bucks). A peristaltic pump (Buchler Instruments, NJ, U.S.A.) supplied solution to the nebuliser at a rate of 1.2 ml min^{-1}.

Discrete nebulisation

The only modifications made to the system used for continuous introduction of solution was the fitting of a narrow bore platinum-iridium tube in the end of the nebuliser tube. This facilitated its accurate positioning in the solution droplets.

Solution droplets (100 μl) were aspirated from thin PTFE tape stretched over a perspex block. The smooth PTFE surface ensured minimum contact of the solution droplets and allowed complete aspiration to be readily observed. Pre-integration and integration times (10 s and 5 s, respectively) were selected to give the best signal to background ratio and were used for all analyses. Element wavelengths and detection limits are shown in Table 1.

Sample and standards preparation

Most of the samples analysed in this work were too small for accurate weighing. Therefore, the concentration ratio technique previously used [1] was applied; this required the acquisition of only relative not absolute concentration data. Provided sufficient element coverage is available from the detection system then prior knowledge of the sampler type or elemental composition is not required.

Metal particles were degreased with 1,1,2-trichloro-1,2,2-trifluoroethane and were placed in pre-cleaned 1.5-ml polypropylene centrifuge tubes

TABLE 1

ANALYTICAL WAVELENGTHS AND DETECTION LIMITS FOR DISCRETE NEBULISATION

Element	*Wavelength (nm)*	*Detection limit*[a] *($\mu g\ ml^{-1}$)*
Zn	213.8	0.006
Pb	220.3	0.080
Ni	231.6	0.017
Mn	257.6	0.001
Fe	259.9	0.011
Cu	324.7	0.003

[a]Calculated as 3 standard deviations of the background variation (3σ).

(Hughes and Hughes Ltd, Romford, Essex). Acid cleaning was inappropriate because of selective dissolution of the major constituents. Nitric acid (120 μl, 25% by vol.) was added to each tube and the samples allowed to stand until dissolution was complete.

Multi-element standards were prepared from 1000 $\mu g\ ml^{-1}$ stock solutions (BDH Chemicals Ltd, Poole, Dorset) in the same acid concentrations as the samples.

Cutting experiments

A small hacksaw (Eclipse Junior, 6 inch blade, 32 teeth/inch) was used for cutting experiments on a previously analysed brass rod (0.25 inch diameter 60/40 brass). Four new, cleaned blades were used to cut through the rod and the fragments generated in each case were retained. Particles adhering to three of the blades were removed with a stainless steel needle. Before the remaining blade was examined for brass particles it was used to cut through a mild steel rod (0.25 inch diameter).

In a second experiment, turnings from a standard brass (BCS 385; Bureau of Analysed Samples Ltd, Middlesborough, Cleveland) were divided with a clean scalpel blade to provide a range of fragment sizes for analysis.

In a third experiment a clean, fine needle file was used to score the surface of a standard copper-nickel alloy (BCS 180/2). The file was examined under a low power binocular microscope and a collection of small alloy fragments removed for analysis.

Results and discussion

Discrete nebulisation

Detection limits obtained for the discrete nebulisation technique were up to a factor of 2 poorer than those previously obtained for continuous solution introduction using large samples [11]. This resulted from a combi-

TABLE 2

ANALYSIS OF 60/40 BRASS

Fragment weight (μg)	*Element (%)*	
	Cu	*Zn*
0.5	54.5	45.5
8.5	60.9	39.1
14.5	60.6	39.4
31.0	60.6	39.4
105[a]	60.9	39.1

[a]Analysed by continuous introduction.

nation of a slightly higher and noisier background for the plasma and a reduction in signal intensity. However, the discrete nebulisation technique gave better detection limits from small solid samples because of reduced dilution effects. In addition, sample throughput was quicker as a result of the reduction in wash time between samples.

Fragment generation and analysis

The average total weight of brass fragments removed from each of the three hacksaw blades used to cut the brass rod was found to be 3 mg. Some of these were quite firmly fixed between the teeth of the blades because of the ductility of the brass. The fragment weights varied from 0.2 μg to 200 μg with most between 5 μg and 50 μg. The remaining blade, which had subsequently cut a mild steel rod, was found to be free of brass fragments: presumably it had been effectively scoured by cutting the harder metal.

Brass fragments of varying weights, obtained from these experiments, were analysed by discrete nebulisation and the results are shown in Table 2 together with that previously obtained for the 105 μg fragment analysed by

TABLE 3

ANALYSIS OF BRASS STANDARD (BCS 385)

Fragment weight (μg)	*Element (%)*		
	Cu	*Zn*	*Pb*
10	55.7	41.0	2.85
15	58.5	38.3	2.70
20	58.9	38.6	2.40
50	58.3	38.6	2.63
70	58.6	38.5	2.43
Certified values	58.7	38.5	2.24

TABLE 4
ANALYSIS OF COPPER-NICKEL STANDARD BCS 180/2

Element	*Certified (%)*	*ICP (%)*	*Standard deviation*	*Relative standard deviation (%)*
Cu	68.12	68.72	1.99	2.9
Ni	30.35	29.07	1.57	5.4
Fe	0.68	1.26	0.35	27.8
Mn	0.75	0.94	0.19	20.2

n = 8, mean sample weight 2.7 μg, range 0.6—7.2 μg.

continuous solution introduction. It can be seen that the copper and zinc results are consistent for fragments weighing from 8.5 μg to 105 μg, suggesting that no problems arise from inhomogeneity. However, the result obtained for the 0.5 μg fragment is obviously inaccurate and indicates that samples of this size are not representative of the bulk material.

Analyses were carried out on a range of fragments taken from the standard brass (BCS 385). This material was chosen as representative of a leaded duplex brass; lead is added to improve the machining properties and is present as isolated globules in the alloy. The results of the determinations are shown in Table 3. Although the data for the major constituents are, as before, consistent down to the smaller fragments, the lead values generally increase as fragment size decreases. Lead acts as a solid lubricant in these alloys and spreads over the surface during machining. The increasing lead value is believed to result from the relative increase in surface area of fragments as their volume decreases. This reaffirms the need for careful interpretation of analytical data from small fragments of a non-homogeneous alloy.

Analytical data from eight fragments of the standard copper-nickel alloy (BCS 180/2) are shown in Table 4 together with the certified values. This material is a coinage alloy of known fine grain structure. The data for the major constituents are good for a mean sample weight of 2.7 μg and a range of 0.6—7.2 μg. The high iron value probably arises by contamination from the file; 15 ng of iron on the mean fragment weight would be sufficient to cause this elevated result. The manganese result, although high, is only one standard deviation from the certified value.

Conclusion

A discrete nebulisation technique has been developed for the multi-element analysis of 100-μl solution droplets by ICP-OES. The performance of the technique is only slightly degraded when compared to continuous solution introduction. The advantages of this technique are the increased speed of analysis, the ability to analyse small solution volumes and, hence,

the reduction of dilution factors when analysis is required on small solid samples.

In a simulated case involving cutting a brass rod with a hacksaw a relatively large number of fragments were found to be adhering to new, fine cut blades. Some of these would be expected to have long persistence times because of the firmness of their attachment. However, when one of these blades subsequently cut a mild steel rod, all evidence of the previous brass cuts was removed.

The results obtained from the materials examined here indicate the caution required in the interpretation of analytical data from small alloy fragments. It is unlikely that the analysis of fragments of non-homogeneous alloys weighing less than 100 μg will provide relevant comparative data for forensic scientists. Analytical data from fragments of homogeneous alloys weighing less than 10 μg require careful interpretation resulting from the effects of sample contamination.

References

1 R.C. Carpenter and C. Till, The analysis of small samples of brasses by inductively coupled plasma-optical emission spectrometry (ICP-OES) and their classification by two pattern recognition techniques. *Analyst*, in press.

2 T. Uchida, I. Kojima and C. Iida, Determination of metals in small samples by atomic absorption and emission spectrometry with discrete nebulisation. *Anal. Chim. Acta*, 116 (1980) 205—210.

3 D.C. Manning, Aspirating small volume samples in flame atomic absorption spectroscopy. *At. Absorpt. Newsl.*, 14 (1975) 99—102.

4 A. Eaton and E. Schiemer, A simple teflon sampling manifold for use with small injections. *At. Absorpt. Newsl.*, 17 (1978) 113—114.

5 P.D. Goulden, Controlling sample flow in flame atomic absorption spectroscopy. *At. Absorpt. Newsl.*, 16 (1977) 121—123.

6 K.C. Thompson and R.G. Godden, The application of a wide slot nitrous oxide-nitrogen-acetylene burner for the atomic absorption spectrophotometric determination of Al, As and Sn in steels by the single pulse nebuliser technique. *Analyst*, 101 (1976) 96—102.

7 T. Catterick and C.D. Wall, Rapid analysis of small glass fragments by atomic absorption spectroscopy. *Talanta*, 25 (1978) 573—577.

8 S. Greenfield and P.B. Smith, The determination of trace metals in microlitre samples by plasma torch excitation. *Anal. Chim. Acta*, 59 (1972) 341—348.

9 J.A.C. Broekaert and F. Leis, An injection method for the sequential determination of boron and several metals in waste water samples by inductively coupled plasma-atomic emission spectrometry. *Anal. Chim. Acta*, 109 (1979) 73—83.

10 H. Uchida, Y. Nojiri, H. Haraguchi and K. Fuwa, Simultaneous multielement analysis by inductively coupled plasma emission spectrometry utilising micro-sampling techniques with internal standard. *Anal. Chim. Acta*, 123 (1981) 57—63.

11 R.C. Carpenter, The analysis of some evidential materials by inductively coupled plasma-optical emission spectrometry. *Forensic Sci. Int.*, 27 (1985) 157—163.

Forensic Science International, 27 (1985) 157—163
Elsevier Scientific Publishers Ireland Ltd.

THE ANALYSIS OF SOME EVIDENTIAL MATERIALS BY INDUCTIVELY COUPLED PLASMA-OPTICAL EMISSION SPECTROMETRY

R.C. CARPENTER

Central Research Establishment, Home Office Forensic Science Service, Aldermaston, Reading, Berkshire RG7 4PN (U.K.)

(Received October 4, 1983)
(Accepted November 28, 1983)

Summary

Inductively coupled plasma-optical emission spectrometry (ICP-OES) is under evaluation at the Central Research Establishment for the analysis of evidential materials. The analysis of standard reference materials has demonstrated that quantitative multi-element data can be obtained from small samples of a variety of materials. The results of some determinations carried out in support of casework investigations are reported.

Key words: Elemental analysis; Inductively coupled plasma arc; Emission spectrometry

Introduction

The inductively coupled plasma (ICP) was developed as an excitation source for atomic spectroscopy about 20 years ago [1,2]. However, it was not until compact, high frequency, low power sources were developed in the mid 1970's that the ICP became accepted as an analytical tool. The subsequent rapid growth in commercial plasma systems results mainly from the high quality quantitative, multi-element analyses which they can perform. This increasing usage is reflected by literature publications of fundamental studies and numerous applications [e.g. 3].

Few publications have been produced by forensic scientists: Locke [4] has reported an evaluation of manufacturers' instruments for glass, steel and liver tissue analyses. At the Metropolitan Police Forensic Science Laboratory, Catterick and Hickman [5] have developed a technique for the determination of five elements in small glass fragments by inductively coupled plasma-optical emission spectrometry (ICP-OES). Their method has been applied to casework samples and data recently reported for 350 glass samples [6] have been used to formulate a glass classification system [7].

ICP-OES has been in use at the Central Research Establishment (CRE) for about 2 years and the current instrumentation has been acquired at various stages over this period. The reported ability to carry out rapid, quantitative, multi-element analyses on small samples of a wide variety of materials was the main reason for the investigation of this technique. This paper comprises a brief description of the CRE instrument and the

0379-0738/85/$03.30

TABLE 1

ICP OPERATING CONDITIONS

Forward RF power	1.0 kW
Reflected RF power	<5 W
Argon plasma gas	16 l min^{-1}
Argon auxiliary gas	0 l min^{-1}
Argon nebuliser gas	0.8 l min^{-1}
Solution uptake	1.3 ml min^{-1}
Observation height above load coil	15—20 mm

analyses of some standard reference materials and casework samples are reported.

Experimental

ICP and sample introduction

The ICP at CRE is a low power argon plasma operating at 27 MHz and supplied by Plasma Therm Inc. (Kresson, NJ, USA). The maximum power output of the radio frequency (RF) generator is 2.5 kW and the system is equipped with automatic power control and impedance matching. The torch box is remote from the generator and contains a glass, pneumatic nebuliser, a glass spray chamber and a silica plasma torch. The normal operating conditions are shown in Table 1.

Light detection and data acquisition

Light emitted from the plasma is monitored simultaneously by two spectrometers, a 1-m scanning monochromator (Bentham Inst., Reading,

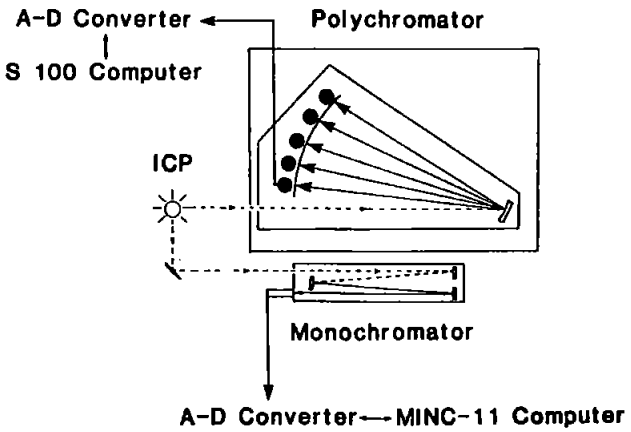

Fig. 1. The ICP-OES instrument.

TABLE 2

ANALYSIS OF REFERENCE MATERIALS

Sample material	*Analysis*	*Al*	*Ba*	*Cr*	*Cu*	*Fe*	*Pb*	*Mg*	*Mn*	*Ni*	*Sr*	*Ti*	*Zn*	*Zr*
Zn/Al Alloy	ICP%	—	—	0.15	1.33	0.25	—	2.85	0.35	—	—	0.095	5.92	0.19
BCS 300/1	Certified%	—	—	0.13	1.27	0.24	—	2.74	0.33	—	—	0.09	5.87	0.18
Nimonic 901	ICP%	0.26	—	12.66	0.032	35.0	—	—	0.08	42.1	—	3.00	—	—
BCS 387	Certified%	0.24	—	12.46	0.032	36.0	—	—	0.08	41.9	—	2.95	—	—
Mild Steel	ICP%	—	—	0.24	0.14	—	—	—	0.05	{0.10	—	—	—	—
BCS 453	Certified%	—	—	0.24	0.15	—	—	—	0.04	{0.114	—	—	—	—
High Tensile Brass	ICP%	2.28	—	—	58.3	0.99	0.39	—	0.85	0.59	—	—	35.8	—
BSC 179/2	Certified%	2.27	—	—	58.5	1.02	0.35	—	0.86	0.56	—	—	35.8	—
Human Liver Tissue	ICP ppm	—	—	—	4.9	246	—	—	1.6	—	—	—	45.5	—
CRE Analysis	AAS ppm[a]	—	—	—	4.8	240	—	—	1.4	—	—	—	44.8	—
Float Glass	ICP%	0.60	0.012	—	—	0.074	—	2.23	0.010	—	0.004	0.028	—	—
BGIRA EC1.1	Certified%	0.57	—	—	—	0.072	—	2.28	—	—	—	0.024	—	—

[a] Atomic absorption spectrometry.

UK) and a 1-m 16-channel polychromator (Optical Emission Services, Milton Keynes, UK) (Fig. 1).

Each spectrometer is interfaced to its own computer for system control and data acquisition, making each an independant analytical system. Both instruments are fitted with holographic diffraction gratings to minimise scattered light effects.

Applications studies

Five certified standards (metals and glass) and one previously examined human liver tissue ash have been analysed on the polychromator and the results are reported here. Some analyses carried out on the monochromator for casework investigations are also reported to indicate further applications.

Results and discussion

Analysis of standard reference materials (polychromator)

Six reference materials have been analysed on the polychromator: four metals (supplied by the Bureau of Analysed Samples), a sample of float glass (supplied by the British Glass Industry Research Association) and a human liver tissue (previously ashed and analysed [8]). These materials were dissolved in suitable mineral acids and the solutions diluted to contain 5% nitric acid (by vol.). Standard solutions, of matching acid concentrations, were diluted from 1000 $\mu g\ ml^{-1}$ stock solutions (BDH Chemicals Ltd., Poole, U.K.).

In order to represent the limited sample sizes commonly encountered in casework, solutions were prepared at greater dilutions than those normally used for elemental analysis by ICP-OES; the metal and glass solutions contained 100—200 $\mu g\ ml^{-1}$ of analyte and the liver solutions contained 1000 $\mu g\ ml^{-1}$ of ash. The results of the determinations are shown in Table 2.

Some spectral interferences were encountered and corrected for in the metal samples. Background correction was necessary for a number of the minor constituents in the metals. However, it was unnecessary for the tissue or glass samples. The data show very good agreement with the reference values, confirming that quantitative results from trace to major constituent can be obtained from dilute solutions of a variety of materials.

Analysis of human tissues and body fluids (monochromator)

ICP-OES has been used for the determination of toxic metals in support of casework investigations. These analyses were carried out using the normal operating conditions and the samples prepared by a combined dry ash/nitric acid oxidation procedure [9].

Water-borne aluminium has been recognised for some time as a contributory factor in the dialysis encephalopathy syndrome [10]. Patients undergoing renal dialysis in regions where tap-water concentrations of aluminium are high, are more likely to develop encephalopathy when dialysed

TABLE 3
ALUMINIUM DETERMINATIONS IN DIALYSIS DEMENTIA FATALITY

Sample	*Wet tissue concentrations (μg g^{-1})*		
	This work	*Encephalopathy fatalities*[a]	*Normal tissue*[b]
Brain-cerebral lobe	3.8	1.91 ± 0.92 (whole brain)	0.5 ± 0.1 (whole brain)
Brain-stem	3.5	1.91 ± 0.92 (whole brain)	0.5 ± 0.1 (whole brain)
Muscle-skeletal	9.7	6.44 ± 5.07	0.5 ± 0.2
Liver	139	—	2.6 ± 1.3
Rib bone	75	81.74 ± 49.83	32.4 ± 5.4

[a]Ref. [12].
[b]Ref. [13].

with softened water than when deionised water is used to prepare the dialysate [11]. Table 3 shows the aluminium concentrations obtained in tissue samples from a suspected dialysis dementia fatality. In addition, data are shown for uraemic patients following death from dialysis associated encephalopathy [12] together with aluminium concentrations reported for normal tissue [13]. The health authority concerned stated its intention to fit reverse osmosis units to all its renal dialysis machines.

Determination of boron in metallic borides (monochromator)

Following the recovery of materials believed to have been stolen from a metallurgical company, the local operational laboratory was required to analyse them to provide proof of identity and origin. ICP-OES is the most suitable technique (in the Home Office Forensic Science Service) for the quantitative determination of boron; the low atomic number precludes X-ray techniques while atomic absorption spectrometry is very insensitive. Five samples of the recovered borides were therefore submitted for analysis.

TABLE 4
DETERMINATION OF BORON IN METALLIC BORIDES

Sample	*%B ICP*	*%B Company Data*
A	17.3	17.41
B	19.3	18.28
C	17.7	17.78
D	19.7	19.42
E	18.1	17.55
BCS 373 (Certified 15.1% B)	15.2	—

A sodium carbonate/peroxide fusion, followed by dissolution of the melts in dilute hydrochloric acid, was used to prepare the borides. Analysis was carried out using the 249.77 nm line.

The results are shown in Table 4 together with data obtained by the metallurgical company using a neutron attenuation technique and from a British Chemical Standard (BCS). These boron determinations confirm the high sensitivity of ICP-OES for refractory elements and also the ability to determine quantitatively major constituents.

Other applications

ICP-OES has been used to support other casework investigations, brief details of some of these are presented here to indicate the versatility of the technique.

The determination of certain inorganic elements added in controlled quantities to specialist marker paints has been carried out. The choice of elements meant that only a quantitative atomic spectroscopic technique was capable of characterising them uniquely; ICP-OES was able to do this on casework sized fragments without problems.

Cadmium determinations were requested in a case of suspected industrial poisoning and, together with other evidence, the elevated liver and kidney concentrations were shown to be consistent with chronic cadmium poisoning.

Counterfeit coins were analysed for lead, tin, antimony and bismuth. The origin of the alloy used was then proposed by comparison of the quantitative data with the compositions of a range of low melting point alloys.

Research studies have demonstrated that quantitative determinations of up to 8 elements can be carried out on 100 μg fragments of a collection of brasses. The multi-element data can be used for classification and discrimination. This work will be reported at a later date.

Conclusions

Applications reported here have indicated the capability of ICP-OES for quantitative determinations of a range of elements in a variety of materials. Analyses of standard reference materials have demonstrated that quantitative multi-element data from trace to major constituents can be obtained on casework sized samples.

ICP-OES is, of course, a destructive analytical technique but its high sensitivity may allow small samples to be subdivided for analysis. The absolute data obtained could allow identification of manufacturing sources. In addition, the data should be useful to analysts whose techniques generate only qualitative or semi-quantitative data.

References

1 S. Greenfield, I.L. Jones and C.T. Berry, High pressure plasmas as spectroscopic emission sources. *Analyst*, 89 (1964) 713—720.

2 R.H. Wendt and V.A. Fassell, Induction coupled plasma spectrometric excitation source. *Anal. Chem.*, 37 (1965) 920—922.
3 W.J. Boyko, P.N. Keliher and J.M. Patterson, Emission spectroscopy. *Anal. Chem.*, 54 (1982) 188R—203R.
4 J. Locke, The application of plasma source atomic emission spectrometry in forensic science. *Anal. Chim. Acta*, 113 (1980) 3—12.
5 T. Catterick and D.A. Hickman, Sequential multi-element analysis of small fragments of glass by atomic emission spectrometry using an inductively coupled radiofrequency argon plasma source. *Analyst*, 104 (1979) 516—524.
6 T. Catterick and D.A. Hickman, The quantitative analysis of glass by inductively coupled plasma — atomic emission spectrometry: A five element survey. *Forensic Sci. Int.*, 17 (1981) 253—263.
7 D.A. Hickman, A classification scheme for glass. *Forensic Sci. Int.*, 17 (1981) 265—281.
8 J. Locke, The determination of eight elements in human liver tissue by flame atomic absorption spectrometry in sulphuric acid solution. *Anal. Chim. Acta*, 104 (1979) 225—231.
9 R.A. Isaac and W.C. Johnson, Collaborative study of wet and dry ashing techniques for the elemental analysis of plant tissue by atomic absorption spectrometry. *J. Assoc. Off. Anal. Chem.*, 58 (1975) 436—440.
10 M.M. Platts, G.C. Goode and J.S. Hislop, Composition of the domestic water supply and the incidence of fractures and encephalopathy in patients on home dialysis. *Br. Med. J.*, 2 (1977) 657—660.
11 H.L. Elliot, F. Dryburgh, G.S. Fell, S. Sabet and A.I. MacDougall, Aluminium toxicity during regular haemodialysis. *Br. Med. J.*, 1 (1978) 1101—1103.
12 A.C. Alfrey, G.R. Legendre and W.D. Kaehny, The dialysis encephalopathy syndrome, *New Engl. J. Med.*, 94 (1976) 184—188.
13 E.I. Hamilton, M.J. Minski and J.J. Cleary, The concentration and distribution of some stable elements in healthy human tissues from the United Kingdom. *Sci. Total Environ.*, 1 (1972/73) 341—374.

Analysis of Small Samples of Brasses by Inductively Coupled Plasma - Optical Emission Spectrometry and their Classification by Two Pattern-recognition Techniques*

Robert C. Carpenter and Clare Till
Central Research Establishment, Home Office Forensic Science Service, Aldermaston, Reading, Berkshire, RG7 4PN, UK

As part of its evaluation in the analysis of evidential materials, inductively coupled plasma - optical emission spectrometry (ICP-OES) has been used to obtain quantitative data for up to eight elements in 100-μg samples of a collection of brasses. The precision and accuracy of the method were monitored by repeat analyses of a certified brass standard. The quantitative data from the 37 brasses form a reference collection that will assist forensic scientists in the interpretation of certain alloy analyses. Methods for the objective classification of the samples were investigated by applying hierarchic clustering and non-linear mapping techniques to the data set.

Keywords: *Inductively coupled plasma - optical emission spectrometry; pattern-recognition techniques; brass analysis*

The major task of forensic science laboratories is the examination of materials associated with criminal activity. A frequent requirement is to establish whether or not a suspect can be linked with a particular crime scene. This may involve the examination of materials such as body fluids, hair, soils, paint, fibres, glass and metals. For example, metal swarf or particulates are often recovered in forensic science casework from the clothing, shoes, vehicles or tools of suspects in cases of theft or illegal entry of industrial premises.

The techniques normally employed for alloy analysis in UK forensic science laboratories are X-ray fluorescence (XRF), electron probe microanalysis (EPMA) and X-ray diffraction (XRD). XRF would not normally be used for quantitative analyses of the sample sizes considered in this work. XRD is a valuable technique but its usefulness is limited to the identification of phases and the estimation of copper to zinc ratios in certain brasses.[1] EPMA is the most popular technique for small samples but to obtain quantitative data closely matched standards are required. Problems can also be encountered from surface smearing of the lead in leaded brasses.

Inductively coupled plasma - optical emission spectrometry (ICP-OES) is under evaluation at the Central Research Establishment for the analysis of evidential materials.[2] This evaluation is continued with an investigation into its use for the quantitative analysis of *ca.* 100-μg samples of a collection of 37 brass items.

Experimental

Instrumentation

The determinations were carried out with an argon ICP (Plasma Therm Inc., Kresson, NJ, USA) fitted with a concentric glass nebuliser (Type TR-30-A3; J. E. Meinhard Associates, Santa Ana, CA, USA), glass spray chamber[3] and all-silica torch. Signal detection was by means of a 1-m 16-channel polychromator (Optical Emission Services, Milton Keynes, Buckinghamshire, UK) fitted with a holographic diffraction grating. Full details of this instrument are published elsewhere.[2] The normal operating conditions were as follows: forward RF power, 1.0 kW; reflected RF power, < 5 W; argon plasma gas, 16 l min^{-1}; argon auxiliary gas, 0 l min^{-1}; argon nebuliser gas, 0.8 l min^{-1}; solution uptake, 1.3 ml min^{-1}; and observation height above load coil, 15–20 mm.

Sample Preparation

The surface of each brass item was de-greased using 1,1,2-trichloro-1,2,2-trifluoroethane, the sampling area cleaned with fine silicon carbide paper (600 grit), rinsed with distilled water and dried. Samples were taken by drilling with a cleaned No. 50 drill (1.8 mm, high-speed steel), and the drillings were then placed in a cleaned polythene container.

Nominal 100-μg samples (approximately 80–120 μg) were taken from the drillings of each item and placed in acid-cleaned polythene snap-top containers (1.5 ml). Duplicate samples were taken from all items. Nitric acid (50%, 0.5 ml) was pipetted on to each sample, 30 min was allowed for dissolution, distilled water (0.5 ml) was then added and the containers were capped and shaken.

To assess the accuracy and precision of the analyses, duplicate samples of a standard, high-tensile brass (BCS 179/2; Bureau of Analysed Samples Ltd., Middlesbrough, Cleveland, UK) were prepared in a similar fashion. In addition, a bulk solution of this standard was prepared at a concentration of 100 μg ml^{-1}.

Choice of Elements and Standard Preparation

The element set was chosen by considering the major elements, alloying additions and other minor constituents. Following preliminary experiments the set was reduced to 8 elements, unavailable element lines being arsenic (generally <0.05%) and silicon (1% in silicon brasses). The elements and their wavelengths are shown in Table 1, together with practical determination limits in the solid samples, based on 100 μg of sample in 1 ml of solution.

Multi-element standards were prepared from 1 000 μg ml^{-1} stock solutions (BDH Chemicals Ltd., Poole, Dorset, UK) in nitric acid (25%, *V/V*). Grade A calibrated glassware was used at all times and the final standard solutions were stored in pre-cleaned polythene bottles.

Interferences

Zinc and lead were shown to be subject to spectral interferences. The zinc wavelength was interfered with to a small

* Presented at SAC 83, the 6th SAC International Conference on Analytical Chemistry, Edinburgh, UK, 17–23 July 1983.

Table 1. Element data

Element	Wavelength/ nm	Limit of determination,* %
Zn	213.8	Major constituent
Pb	220.3	0.20
Ni	231.6	0.07
Mn	257.6	0.004
Fe	259.9	0.02
Sn	284.0	0.25
Cu	327.4	Major constituent
Al	396.1	0.03

* Calculated as 10σ (10 standard deviations of the background variation) applied to the solid sample (100 μg in 1 ml).

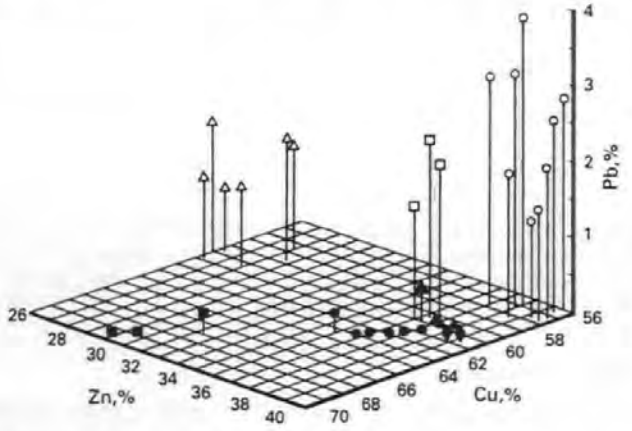

Fig. 1. Three-dimensional plot of brass samples. ■, Cartridge brass (2); △, nickel silver (3); ●, common brass (4); □, leaded alpha brass (5); ▲, naval brass (6); ◆, lead-free duplex brass (7); and ○, leaded duplex brass (8)

extent by the copper 213.6-nm line, lead interference was caused by both copper and zinc and appeared to result from a change in the spectral background intensity owing to scattered light. Interference corrections were determined with each batch of samples and applied prior to the calculation of final concentrations. The lead correction was the more significant, particularly at low lead concentrations.

Calculation

Time-consuming weighing of samples was minimised and weighing errors associated with small samples were eliminated by the use of a concentration ratio technique that required the acquisition of only relative not absolute solution concentrations.[4] Concentration ratios of all elements to the major constituent were determined from intensity ratios. The concentration of the major constituent could then be determined and hence the individual element concentrations. For this calculation to be valid it is necessary to measure the concentration of all elements present in significant amounts and to ensure that all determinations are carried out within the linear calibration range of the instrument.

Results and Discussion

Accuracy and Precision of the Analysis

Controls were included with each batch of samples in the form of aliquots of bulk solution, prepared from the brass standard BCS 179/2, and those prepared on each occasion from the solid standard. The sample analyses were carried out over five weeks during which seven duplicate results were obtained for the controls. The results, shown in Table 2, are considered to

Table 2. Accuracy and precision of brass analyses. Each result is the mean of duplicate determinations

Sample	Element, % Zn			Pb			Ni			Mn			Fe			Sn			Cu			Al		
	Amount	SD*	RSD†	Amount	SD	RSD	Amount	SD	RSD	Amount	SD	RSD	Amount	SD	RSD	Amount	SD	RSD	Amount	SD	RSD	Amount	SD	RSD
BCS 179/2 (certified data)	35.8			0.35			0.56			0.86			1.02			0.70			58.5			2.22		
Solution samples ..	35.9	0.40	0.011	0.36	0.08	0.214	0.59	0.02	0.027	0.86	0.01	0.013	1.01	0.03	0.026	0.72	0.03	0.309	58.3	0.29	0.005	2.22	0.05	0.024
Solid samples	36.3	0.59	0.016	0.41	0.12	0.297	0.61	0.04	0.070	0.85	0.04	0.044	1.04	0.06	0.062	0.67	0.05	0.078	57.9	0.39	0.007	2.17	0.11	0.052

* SD, standard deviation; $n = 7$.
† RSD, relative standard deviation.

Table 3. Data for grouped brasses

	Element, *%								Sample
	Zn	Pb	Ni	Mn	Fe	Sn	Cu	Al	No.
Group 1—alpha brass									
Nickel brass blank	19.9	—†	1.07	—	0.07	—	78.8	—	4
Group 2—alpha brass (cartridge)									
Cartridge case, 0.22	29.6	—	—	—	0.03	—	70.3	—	13
Tube, ¼ in, BS2871	30.1	—	—	—	—	—	69.9	—	30
Continental mains plug	32.0	0.21	—	—	—	—	67.7	—	3
Group 3—nickel silver									
Dominion key	25.9	1.67	11.0	0.23	0.06	—	61.1	—	12
Betakey	27.7	1.02	9.8	0.11	0.14	—	61.2	—	19
Union padlock key	26.2	0.98	11.1	0.05	0.14	—	61.6	—	33
Union key	26.4	1.35	11.0	0.18	—	—	60.9	—	35
Union key	28.6	1.46	10.3	0.23	0.15	—	59.3	—	36
Yale key	27.8	1.34	11.3	0.34	0.20	—	58.3	0.03	37
Group 4—alpha brass (common)									
Gauze, 1 mm mesh	35.8	—	—	—	—	—	64.1	—	20
Washer, ½ in	36.1	—	—	—	0.02	—	63.9	—	21
Car thermostat	36.5	—	—	—	—	—	63.5	—	24
Identity disc	36.9	—	—	—	0.02	—	63.1	—	14
Cup hook	37.3	—	—	—	0.03	—	62.7	—	18
Wood screw	37.9	—	—	—	0.02	—	62.0	—	17
Group 5—leaded alpha brass									
13-A mains plug	37.1	2.34	—	—	0.05	—	60.5	—	2
35-mm pipe olive	37.4	1.47	—	—	—	—	61.1	—	8
Yale key	37.8	1.95	—	—	0.03	—	60.2	—	11
Group 6—naval brass									
Vacuum coupling	37.4	0.47	—	—	0.24	1.32	60.6	—	23
Rod, 1 in, BS2874	38.7	—	—	—	0.06	1.01	60.2	—	29
Rod, ½ in, BS2874	37.6	—	—	—	0.05	1.37	61.0	—	31
Rod, ¼ in, BS2874	37.9	—	—	—	0.09	1.37	60.7	—	32
Group 7—lead-free duplex brass									
Screw, 0 BA	38.8	—	—	—	0.02	—	61.1	—	16
Flat bar, BS1949	39.2	—	—	—	—	—	60.7	—	27
Group 8—leaded duplex brass									
15-mm pipe fitting	40.7	1.98	0.10	—	0.10	—	57.2	—	5
6-mm pipe fitting	39.5	2.63	0.13	—	0.10	—	57.6	—	6
6-mm pipe fitting	39.0	2.98	0.14	0.007	0.19	—	57.7	—	7
6-mm pipe fitting	39.2	3.77	—	0.01	0.12	—	57.0	—	9
6-mm pipe fitting	39.5	2.61	0.11	0.004	0.15	—	57.6	—	10
5-A mains plug	39.1	3.14	0.09	0.02	0.33	—	57.4	—	1
Hinge, 1 in	40.4	2.51	0.08	0.01	0.17	—	56.5	0.35	15
Wing nut	40.7	1.36	—	—	0.11	—	57.8	—	22
Angle, ½ in	40.7	2.79	—	—	0.19	—	56.0	0.26	28
Pipe clamp	39.6	1.94	0.12	0.005	0.16	—	58.2	—	25
Door chain block	40.5	1.33	—	0.02	0.11	—	57.8	0.18	26
Union padlock	39.3	3.01	—	—	0.19	—	57.5	—	34

* Means of duplicate determinations.
† Limits of determination as shown in Table 1.

be a realistic estimate of the long-term precision and accuracy of the method.

The over-all accuracy of the determinations is excellent and the degradation in precision from solution to solid samples reflects the problems of manipulating and preparing very small samples, but, except for lead, the precision is more than adequate for classification. The variation in the lead results arises from the poor detection limit for this element; however, the lead content of this standard is artificially low for a leaded brass and more precise results can be expected from samples likely to be encountered in forensic science casework.

Analysis and Classification of the Sample Set

Quantitative results for up to eight elements were obtained from duplicate 100-μg samples of the set of 37 brasses. Because brasses cover a wide range of copper- and zinc-containing alloys it was decided to attempt a simple classification to aid the presentation and interpretation of the data. Fig. 1 shows a three-dimensional plot of the data using zinc, copper and lead contents for the axes. A few samples have been omitted from this plot either because of their similarity to others or, for one sample, a considerably different composition. The major alloy types are distinguished in the legend.

The samples of nickel (or German) silver are characterised by their approximately 10% nickel content and the naval brasses by their tin content (*ca.* 1%). The leaded alpha brasses form a compact group as do the leaded duplex brasses. The lead-free brasses cover a wide concentration range and can be split into at least two sub-groups. Table 3 shows a group classification based on the determination of the major and alloying constituents; the complete data for these groups are also shown. Although the sample numbers in some of the groups are obviously limited, the sample of nickel brass in group 1 is clearly distinguished as are the three samples of cartridge and leaded alpha brass. The samples that are most difficult to separate are the common alpha and lead-free duplex brasses in groups 4 and 7. The only feature that distinguishes between these is the threshold concentration of 38% zinc for duplex brass.

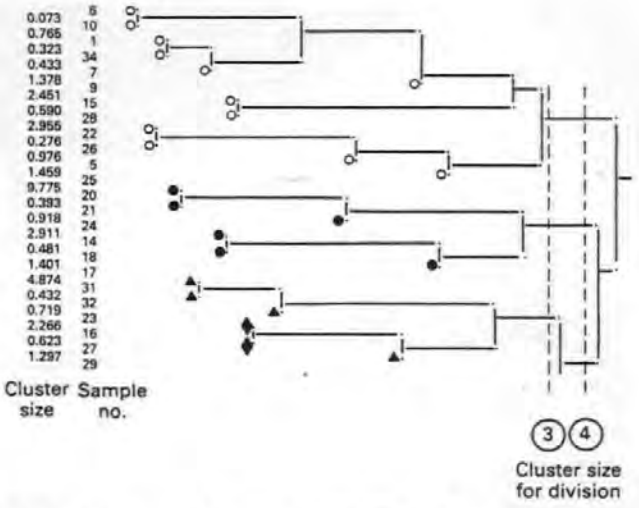

Fig. 2. Dendrogram of some brass samples. ●, Common brass (4); ▲, naval brass (6); ◆, lead-free duplex brass (7); and ○, leaded duplex brass (8)

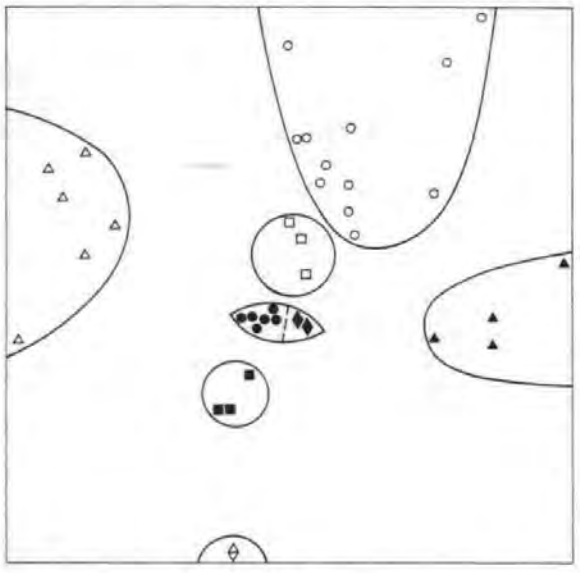

Fig. 3. Scattergram of brass samples. ◇, Nickel brass; ■, cartridge brass; △, nickel silver; ●, common brass; □, leaded alpha brass; ▲, naval brass; ◆, lead-free duplex brass; and ○, leaded duplex brass

Pattern Recognition

Two clustering techniques available on our Prime 550 minicomputer were applied to data on the brasses in an attempt to achieve a more objective means of classification.

The hierarchic clustering program AGCLUS[5] was used to identify homogeneous groups or clusters in the data set using the farthest neighbour criterion applied to normalised data. Cluster analysis is conventionally displayed in the form of a dendrogram in which the individual samples and clusters are joined at nodes. Fig. 2 shows part of the dendrogram obtained from these samples. The main features of cluster size, sample number and group identity can be clearly seen. By consulting the dendrogram a choice has to be made on the number of groups into which the sample set can be split, in this instance cluster sizes of three and four were chosen for sub-division. The cluster size of four gave six groups (similar to the earlier assignment except that groups 5, 6 and 7 were combined into one). Division at a cluster size of three gave nine groups, where groups 6 and 7 were combined and 2 and 3 were split.

A non-linear mapping technique[6] was then applied to the samples in an attempt to identify their inter-relationships. Fig. 3 shows a scattergram produced by the program from normalised data. The original groups can clearly be identified (arbitrary boundaries) and except for groups 4 and 7 (as previously discussed) they are well separated. A second printout from this program identifies the individual samples.

Conclusions

The determination of up to 8 elements in 100-μg samples of 37 brass items has been reported. The analyses carried out by ICP-OES included elements from trace to major constituents. The accuracy and precision of the method has been shown to be good from repeat analyses of a brass standard. The quantitative data are of potential use to forensic scientists as a reference collection and to assist the interpretation of alloy analyses.

Although the samples could be easily split into at least seven groups by considering their alloying constituents, a more objective classification was achieved by pattern-recognition techniques. Non-linear mapping was shown to be the more suitable method in this study as the scattergram can be easily evaluated and the algorithm preserves the structural relationship between samples. The hierarchic clustering technique appears to be more useful for larger data sets where bigger clusters could perhaps be divided with greater confidence.

References

1. Rendle, D. F., *J. Forensic Sci.*, 1981, **26**, 343.
2. Carpenter, R. C., *Forensic Sci. Int.*, in the press.
3. Scott, R. H., Fassel, V. A., Kniseley, R. N., and Nixon, D. E., *Anal. Chem.*, 1974, **46**, 75.
4. Ward, A. F., and Marciello, L. F., *Anal. Chem.*, 1979, **51**, 2264.
5. Olivier, D. C., "AGGLUS, An Agregative Hierarchical Clustering Program," Dept. of Psychology and Social Relations, Harvard University, Cambridge, MA, USA, 1973.
6. Sammon, J. W., *IEEE Trans. Comput.*, 1969, **C-18**, 401.

Paper A3/428
Received December 5th, 1983
Accepted February 20th, 1984